

INTEGRATED OPERATION OF MEMBRANE BIOREACTORS: SIMULATION AND EXPERIMENTAL STUDIES

Montserrat Dalmau Figueras

Dipòsit legal: Gi. 2032-2014
<http://hdl.handle.net/10803/284740>

ADVERTIMENT. L'accés als continguts d'aquesta tesi doctoral i la seva utilització ha de respectar els drets de la persona autora. Pot ser utilitzada per a consulta o estudi personal, així com en activitats o materials d'investigació i docència en els termes establerts a l'art. 32 del Text Refós de la Llei de Propietat Intel·lectual (RDL 1/1996). Per altres utilitzacions es requereix l'autorització prèvia i expressa de la persona autora. En qualsevol cas, en la utilització dels seus continguts caldrà indicar de forma clara el nom i cognoms de la persona autora i el títol de la tesi doctoral. No s'autoritza la seva reproducció o altres formes d'explotació efectuades amb finalitats de lucre ni la seva comunicació pública des d'un lloc aliè al servei TDX. Tampoc s'autoritza la presentació del seu contingut en una finestra o marc aliè a TDX (framing). Aquesta reserva de drets afecta tant als continguts de la tesi com als seus resums i índexs.

ADVERTENCIA. El acceso a los contenidos de esta tesis doctoral y su utilización debe respetar los derechos de la persona autora. Puede ser utilizada para consulta o estudio personal, así como en actividades o materiales de investigación y docencia en los términos establecidos en el art. 32 del Texto Refundido de la Ley de Propiedad Intelectual (RDL 1/1996). Para otros usos se requiere la autorización previa y expresa de la persona autora. En cualquier caso, en la utilización de sus contenidos se deberá indicar de forma clara el nombre y apellidos de la persona autora y el título de la tesis doctoral. No se autoriza su reproducción u otras formas de explotación efectuadas con fines lucrativos ni su comunicación pública desde un sitio ajeno al servicio TDR. Tampoco se autoriza la presentación de su contenido en una ventana o marco ajeno a TDR (framing). Esta reserva de derechos afecta tanto al contenido de la tesis como a sus resúmenes e índices.

WARNING. Access to the contents of this doctoral thesis and its use must respect the rights of the author. It can be used for reference or private study, as well as research and learning activities or materials in the terms established by the 32nd article of the Spanish Consolidated Copyright Act (RDL 1/1996). Express and previous authorization of the author is required for any other uses. In any case, when using its content, full name of the author and title of the thesis must be clearly indicated. Reproduction or other forms of for profit use or public communication from outside TDX service is not allowed. Presentation of its content in a window or frame external to TDX (framing) is not authorized either. These rights affect both the content of the thesis and its abstracts and indexes.



Universitat de Girona

Doctoral Thesis
**INTEGRATED OPERATION
OF MEMBRANE BIOREACTORS:
SIMULATION AND EXPERIMENTAL STUDIES**

Montserrat Dalmau Figueras
2014



Doctoral Thesis

INTEGRATED OPERATION
OF MEMBRANE BIOREACTORS:
SIMULATION AND EXPERIMENTAL STUDIES

Montserrat Dalmau Figueras

2014

Supervisors: Dr. Joaquim Comas Matas, Ignasi Rodriguez-Roda, Eduardo Ayesa Iturrate

Thesis submitted in fulfillment of the requirements for the degree of Doctor from the University of Girona (Experimental Science and Sustainability Doctoral programme).

JOAQUIM COMAS MATAS

Professor del Departament de Química, Agrària i Tecnologia Agroalimentària i membre de l'Institut de Medi Ambient (Universitat de Girona)

IGNASI RODRIGUEZ-RODA

Professor del Departament de Química, Agrària i Tecnologia Agroalimentària i membre de l'Institut de Medi Ambient (Universitat de Girona) i cap de l'àrea de Tecnologies i Avaluació de l'Institut Català de l'Aigua (ICRA, Girona)

EDUARDO AYESA ITURRATE

Professor de TECNUN, Escuela de Ingenieros (Universidad de Navarra, Sant Sebastià) i cap de l'àrea d'Enginyeria Ambiental del CEIT (Centro de Estudios e Investigaciones Técnicas, Sant Sebastià)

Certifiquen:

Que aquest treball titulat "*Integrated operation of membrane bioreactors: simulation and experimental studies*", que presenta la llicenciada en química Montserrat Dalmau Figueras, per a l'obtenció del títol de doctora, ha estat realitzat sota la nostra direcció i que compleix els requeriments per poder optar a Menció Europea.

I per a que en prengueu coneixement i tingui els efectes que corresponguin, presentem davant la Facultat de Ciències de la Universitat de Girona l'esmentada Tesi, signant aquesta certificació.

Dr. Joaquim Comas Matas

Dr. Ignasi Rodriguez-Roda Layret

Dr. Eduardo Ayesa Iturrate

This research was financially supported by AGAUR (2010 VALOR 00170), the Spanish Ministry of Economy and Competitiveness (CTM2012-38314-C02-01, CTM2009-14742-C02-01, PCIN-2013-074, CONSOLIDER-CSD2007-00055), Water_2020 (Action COST ES 1202), and from the People Programme (Marie Curie Actions) of the European Union's Seventh Framework Programme FP7/2007-2013, under REA agreement 289193 (SANITAS). The author was awarded by the Spanish Ministry of Economy and Competitiveness (BES-2010-033288). Moreover, this research was conducted thanks to the staff of the WWTP of La Bisbal d'Empordà and Castell d'Aro.

“ We are all very ignorant, but not all ignorant of the same things ”

▣ Albert Einstein

Als meus pares,
a la Nuri
i a l'Albert

AGRAÏMENTS / ACKNOWLEDGEMENTS

Aquell dia, quan en una optativa de Reactors en Manel Poch va oferir unes pràctiques per fer en un grup d'investigació de la Universitat de Girona, no m'imaginava fins a quin punt m'estava endinsant en el món de la recerca. Va ser llavors quan em vaig trobar a l'Ignasi (que es recordava de mi de segon de Química: Hola Dalmau!), explicant-me la importància de la depuració d'aigües residuals i com una tecnologia anomenada bioreactors de membranes podien ser-ne d'útils. Interessant. Per què no provar-ho... I seguidament vaig conèixer en Quim, que amb optimisme de seguida em va suggerir i motivar a fer el màster en Ciència i Tecnologia de l'Aigua. I així, com qui no vol la cosa, començar el doctorat. I fins ara han estat els dos principals punters de la tesi. Animant-me en els moments crítics i amb afers de superació en tot moment. Complementant-se i motivant-me, i ajudant-me a créixer com a científica. Moltes gràcies per a confiar en mi, i oferir-me l'oportunitat de formar part del vostre equip.

Además, también quiero agradecer a Eduardo Ayesa, que aunque supervisándolo des de la distancia siempre me ha ayudado a salir adelante, ofreciéndome consejos y aportando un toque de calidad que siempre se agradece. Gracias también al resto del grupo del CEIT para acogerme tan bien durante mis visitas.

Aquest camí ha estat molt més planer gràcies a dos persones inqüestionables. La Sara i l'Hèctor. L'Hèctor i la Sara. La millor companya de treball que podria haver trobat, i millor amiga. I el millor amic que pots tenir en una feina, i millor company. Gràcies per ser-hi en tot moment. I tampoc puc oblidar-me de la resta d'equip MBR que ha contribuït indiscutiblement a optimitzar el meu treball. En primer lloc els consells de la Mariona, el suport d'en Jordi, l'incondicional Ivan o el punt crític de la Giuliana, sense oblidar l'ajut informàtic de l'Afra i l'Anna. I en segon lloc, però no menys important, en Sergi, disposat a ajudar-te quan i pel que faci falta, la Marta, la millor companya que podria tenir en una planta pilot, juntament amb en Michele. And at the end of this long way Julian arrived, who has become irreplaceable and necessary in our team. I els MBR adoptats, en Serni, que tot i no ser MBR i d'Almenar, sempre ha tingut un moment per donar-te

TABLE OF CONTENTS

| | |
|--|-----------|
| TABLE OF CONTENTS | I |
| LIST OF TABLES | V |
| LIST OF FIGURES | VI |
| NOMENCLATURE | IX |
| RESUM..... | XI |
| RESUMEN | XIII |
| SUMMARY..... | XV |
| LIST OF PUBLICATIONS..... | XVII |
| 1 INTRODUCTION | 1 |
| 1.1 BACKGROUND..... | 2 |
| 1.2 MEMBRANE BIOREACTOR TECHNOLOGY | 3 |
| 1.2.1 <i>Advantages and Drawbacks</i> | 3 |
| 1.2.2 <i>Type of membranes</i> | 5 |
| 1.2.3 <i>MBR configurations</i> | 5 |
| 1.2.4 <i>Filtration process: Design and operating parameters</i> | 6 |
| 1.2.5 <i>Fouling phenomena</i> | 7 |
| 1.3 MODELS FOR MEMBRANES BIOREACTORS | 11 |
| 1.3.1 <i>The current status of MBRs in literature, with special focus on modelling</i> | 12 |
| 1.3.2 <i>MBR modelling: State of the art</i> | 14 |
| 1.4 CONTROL AND OPTIMISATION: STATE OF THE ART | 20 |
| 1.4.1 <i>Empirical studies</i> | 21 |
| 1.4.2 <i>Modelling studies</i> | 24 |
| 1.5 ANTECEDENTS..... | 26 |
| 2 OBJECTIVES..... | 27 |
| 3 METHODOLOGY..... | 31 |

| | | |
|----------|--|-----------|
| 3.1 | EXPERIMENTAL SYSTEMS | 32 |
| 3.1.1 | <i>Pilot-plant MBR</i> | 32 |
| 3.1.2 | <i>Full-scale MBR</i> | 35 |
| 3.2 | ANALYTICAL METHODS..... | 36 |
| 3.2.1 | <i>Influent and effluent analysis</i> | 36 |
| 3.2.2 | <i>Sludge samples</i> | 37 |
| 3.3 | MODELLING SOFTWARE TOOLS | 38 |
| 3.3.1 | <i>West by mike DHI</i> | 38 |
| 3.3.2 | <i>Weka</i> | 38 |
| 3.3.3 | <i>Risk assessment</i> | 38 |
| 4 | RESULTS I: DEVELOPMENT OF A DECISION TREE FOR THE INTEGRATED OPERATION OF NUTRIENT REMOVAL MBRS BASED ON SIMULATION STUDIES AND EXPERT KNOWLEDGE..... | 41 |
| 4.1 | OVERVIEW..... | 42 |
| 4.2 | MATERIALS AND METHODS | 44 |
| 4.2.1 | <i>Experimental system</i> | 44 |
| 4.2.2 | <i>Model-based methodology for the development of operational decision trees</i> | 45 |
| 4.2.3 | <i>Model development</i> | 46 |
| 4.2.4 | <i>System analysis tools</i> | 50 |
| 4.3 | RESULTS AND DISCUSSION | 51 |
| 4.3.1 | <i>Model calibration and validation</i> | 51 |
| 4.3.2 | <i>Local sensitivity analysis (LSA)</i> | 53 |
| 4.3.3 | <i>Scenario analysis</i> | 55 |
| 4.3.4 | <i>Operational decision tree for the integrated operation of MBRS</i> | 58 |
| 4.4 | CONCLUSIONS | 61 |
| 5 | RESULTS II: MODEL-BASED OPTIMISATION OF A FULL-SCALE HYBRID MBR..... | 63 |
| 5.1 | OVERVIEW..... | 64 |
| 5.2 | MATERIAL AND METHODS..... | 65 |
| 5.2.1 | <i>Simulation procedure and evaluation</i> | 69 |
| 5.3 | RESULTS AND DISCUSSION | 70 |
| 5.3.1 | <i>Secondary settler calibration</i> | 70 |
| 5.3.2 | <i>Steady state simulation</i> | 72 |
| 5.3.3 | <i>Dynamic simulation</i> | 73 |

| | | |
|----------|---|------------|
| 5.3.4 | Scenario analysis..... | 76 |
| 5.4 | CONCLUSIONS..... | 78 |
| 6 | RESULTS III: MODELLING MBR FOULING WITH DETERMINISTIC AND DATA-DRIVEN MODELS... | 79 |
| 6.1 | OVERVIEW | 80 |
| 6.2 | MATERIALS AND METHODS..... | 81 |
| 6.2.1 | <i>Experimental system</i> | 81 |
| 6.2.2 | <i>Model development and evaluation</i> | 82 |
| 6.2.3 | <i>Data collection and processing</i> | 83 |
| 6.2.4 | <i>Model set up</i> | 84 |
| 6.3 | RESULTS AND DISCUSSION | 89 |
| 6.3.1 | <i>Model set-up, calibration and validation</i> | 89 |
| 6.3.2 | <i>Model evaluation</i> | 91 |
| 6.4 | CONCLUSIONS..... | 97 |
| 6.5 | ANNEX | 98 |
| 7 | RESULTS IV: TOWARDS INTEGRATED OPERATION OF MBRS: EFFECTS OF AERATION ON BIOLOGICAL AND FILTRATION PERFORMANCE | 101 |
| 7.1 | OVERVIEW | 102 |
| 7.2 | MATERIALS AND METHODS..... | 103 |
| 7.2.1 | <i>UCT-MBR pilot plant</i> | 103 |
| 7.2.2 | <i>Experimental procedure</i> | 105 |
| 7.2.3 | <i>Experimental monitoring</i> | 105 |
| 7.3 | RESULTS | 108 |
| 7.3.1 | <i>Experiment A: Modification of the DO set-point in the aerobic compartment</i> | 108 |
| 7.3.2 | <i>Experiment B: Modification of the air-scouring flow in the membrane compartment</i> | 113 |
| 7.4 | DISCUSSION..... | 118 |
| 7.4.1 | <i>Biological nutrient removal</i> | 118 |
| 7.4.2 | <i>Sludge characteristics</i> | 119 |
| 7.4.3 | <i>Filtration performance</i> | 120 |
| 7.4.4 | <i>Energy efficiencies</i> | 121 |
| 7.5 | CONCLUSIONS..... | 121 |

| | | |
|-----------|---|------------|
| 8 | RESULTS V: FULL-SCALE VALIDATION OF A CONTROL SYSTEM FOR ENERGY SAVING IN MEMBRANE BIOREACTORS FOR WASTEWATER TREATMENT..... | 123 |
| 8.1 | OVERVIEW..... | 124 |
| 8.2 | MATERIALS AND METHODS | 125 |
| 8.2.1 | <i>La Bisbal d’Empordà WWTP.....</i> | <i>125</i> |
| 8.2.2 | <i>Air-scouring control system: Smart Air MBR®</i> | <i>127</i> |
| 8.3 | RESULTS AND DISCUSSION | 129 |
| 8.3.1 | <i>Phase 1: Data gathering and calibration of the control system</i> | <i>129</i> |
| 8.3.2 | <i>Phase 2: Validation.....</i> | <i>132</i> |
| 8.4 | CONCLUSIONS | 136 |
| 9 | DISCUSSION | 137 |
| 10 | CONCLUSIONS..... | 147 |
| 11 | BIBLIOGRAPHY..... | 151 |

LIST OF TABLES

| | |
|--|-----|
| Table 3.1 Description of the methodologies described in chapters, indicating type, year and scale of performance. | 32 |
| Table 3.2 Analytical methods used for the determination of the influent and effluent concentrations. | 36 |
| Table 4.1 Initial (reference) operational conditions of the pilot plant..... | 47 |
| Table 4.2 Average characteristics of the UCT-MBR pilot plant influent during the experimental campaign (after primary settler; daily samples during a week)..... | 47 |
| Table 4.3 Steady state simulated values versus the experimental values. | 52 |
| Table 4.4 Scenario analysis grid, showing the studied set-points for each sensitive parameter..... | 55 |
| Table 4.5 The best 10 operational parameters set obtained with the Pareto front and the screening over the SCA, allowing minor TMP, EQ and OCI, all of them fulfilling the EU Directive (91/271/CEE)..... | 56 |
| Table 4.6 Global sensitivity analysis results.. | 57 |
| Table 5.1 Plant, effluent and influent details. | 66 |
| Table 5.2 Initial values and optimal values of the estimated parameters of the settling functions.... | 71 |
| Table 5.3 Optimal parameter values for the model of Bürger et al. (2011)..... | 71 |
| Table 5.4 Calibrated model parameters for steady-state and dynamic simulations. | 72 |
| Table 6.1 Operating conditions of the different periods used for simulation..... | 85 |
| Table 6.2 Influent and effluent characteristics along the different periods (units: mg·L ⁻¹)..... | 86 |
| Table 6.3 RMSE for each period for both models. The lowest value for each period is in bold..... | 92 |
| Table 6.4 . List of all linear models developed by the data driven model..... | 98 |
| Table 7.1 Design and operating parameters. | 104 |
| Table 7.2 Influent characteristics. | 106 |
| Table 7.3 AOB, NOB, PAOS and DPAOS in Experiment A. | 109 |
| Table 7.4 AOB, NOB, PAOS and DPAOS activities in Experiment B..... | 113 |
| Table 8.1 Membrane characteristics at <i>La Bisbal d'Empordà</i> WWTP..... | 126 |
| Table 8.2 Control system actions..... | 131 |
| Table 8.3 Activated sludge properties and biological nutrient removal over the last three years.... | 134 |

LIST OF FIGURES

| | |
|---|----|
| Figure 1.1 MBR process configurations, (a) side-stream MBR, with the membrane located next to the bioreactor and (b) submerged or immersed MBR, with the membranes inside the bioreactor, from Judd (2011). | 5 |
| Figure 1.2 Various membrane configurations: Flat sheet membrane (a), tubular membranes (b) and hollow fiber membranes (c), from Judd (2011). | 6 |
| Figure 1.3 Schematic procedure of the fouling mechanisms: reversible fouling, irreversible fouling and irrecoverable fouling (adapted from Meng et al., (2009) and Judd (2011)). | 8 |
| Figure 1.4 Inter-relationships between engineering decisions and permeability loss. | 9 |
| Figure 1.5 Operational cost distribution for a stand-alone MBRs..... | 12 |
| Figure 1.6 Number of publications and patents related to MBRs in the last 20 years..... | 12 |
| Figure 1.7 MBR publications in the last 20 years and sorted by type. | 13 |
| Figure 1.8 Graphical representation of the main keywords appearing in MBR modelling publications (April 2014) | 13 |
| Figure 1.9 Different model-based methodologies to describe the permeability loss in membranes. | 16 |
| Figure 1.10 Empirical and model-based strategies based on filtration, biological, costs, hydrodynamics or integrated processes in MBR. Superscript numbers in the figure stand for a related publication | 21 |
| Figure 2.1 Outline of the thesis..... | 28 |
| Figure 3.1 Detailed pictures of the pilot-scale plant located in Castell-Platja d'Aro. | 34 |
| Figure 3.2 Overview of the SCADA system installed in the pilot plant..... | 34 |
| Figure 3.3 Overview of the WWTP of La Bisbal d'Empordà..... | 35 |
| Figure 3.4 Simplified scheme of the full-scale facility. | 35 |
| Figure 3.5 Relationship between the mechanistic model and the fuzzy knowledge base to estimate risk of microbiology-related solids separation problems..... | 39 |
| Figure 4.1 Schematic overview of the UCT–MBR pilot plant showing the different compartments, flow directions and main instruments and equipment. | 45 |
| Figure 4.2 Methodology for the development of operational decision trees. | 45 |
| Figure 4.3 Relation between the dynamic simulation results and the experimental results | 52 |

Figure 4.4 | Results obtained from the LSA, showing the most sensitive parameters related to the filtration process based on TMP (a) and effluent quality (b). 54

Figure 4.5 | Outputs of the scenario analysis in terms of operational costs (OCI), effluent quality and TMP: (a) represents all the set-point combinations (only strategies using relaxation time equal to 0), highlighting Pareto results; (b) only the 48 solutions corresponding to the Pareto front; and (c) the 10 best configurations after the screening method. 56

Figure 4.6 | Decision tree for selecting good operational strategies for MBRs. 60

Figure 5.1 | Hybrid MBR Flow scheme. Dashed lines indicate occasional flow. 65

Figure 5.2 | Model implementation of the hybrid MBR plant layout 69

Figure 5.3 | Batch settling curves for different initial solids concentrations with sludge from the WWTP of La Bisbal d’Empordà. 70

Figure 5.4 | Simulated and recorded sludge and effluent results for the calibrated steady-state model. 73

Figure 5.5 | Simulated and recorded effluent results for the calibrated dynamic model for nitrogen and phosphorous 74

Figure 5.6 | Simulated and recorded effluent results for 365 days, where A represents de influent flow, B the ammonia concentration, C the nitrates and nitrites concentration and D phosphates concentration 75

Figure 5.7 | Simulated pumping energy, aeration energy and effluent quality index results for the scenario analysis with the calibrated dynamic model. 77

Figure 5.8 | Simulated effluent results for the scenario analysis with the calibrated dynamic model. 77

Figure 6.1 | Schematic of the configuration of the MBR pilot-scale plant. 82

Figure 6.2 | Regression model tree developed for the TMP prediction, with subdomains and multivariable linear models (LM). Five main subdomains are numbered, representing different typical values of TMP (coloured in different grey tones)..... 91

Figure 6.3 | Measured TMP and simulated TMP values using both data-driven and deterministic models versus time 92

Figure 6.4 | Sensitivity of different parameters in the deterministic TMP model 93

Figure 6.5 | Experimental influence of TMP vs. the permeate flux increase (a) and SMP increase and temperature decrease (b)..... 94

Figure 7.1 | Pilot plant diagram. 104

Figure 7.2 | Evolution of nutrient concentrations in the effluent and influent grab samples along the aerobic DO set-point modification. 109

| | |
|---|-----|
| Figure 7.3 Sludge characteristics evolution in Experiment A..... | 110 |
| Figure 7.4 Evolution of the TMP and the fouling rates during the aerobic DO set-point modification in Experiment A. A.1, A.2 and A.3 illustrate the evolution of the TMP and the fouling rates three experimental cycles operating at 1.5, 0.5 and 0 mg O ₂ · L ⁻¹ , respectively..... | 112 |
| Figure 7.5 Evolution of the nutrient concentrations in the effluent and influent grab samples during the membrane air-scouring flow rate modification of Experiment B. | 114 |
| Figure 7.6 Sludge characteristics evolution in Experiment B. | 115 |
| Figure 7.7 The evolution of the TMP and the fouling rates during the membrane air-scouring flow modification in Experiment B. B.1, B.2 and B.3 illustrate the evolution of the TMP and the fouling rate of three specific filtration cycles working at different SAD _m values (1.25, 0.75 and 1.25 mbar·s ⁻¹) on day 1, 8 and 14, respectively. | 117 |
| Figure 8.1 Flow diagram of LBE water line. | 125 |
| Figure 8.2 Different relationships between LT and ST permeability. | 127 |
| Figure 8.3 Schematic diagram of the control system of the LBE WWTP. | 129 |
| Figure 8.4 Fouling evolution (permeability) during 4 months previous of the control system activation. | 130 |
| Figure 8.5 SR percentage of occurrence. A) Probability B) Accumulated probability. | 130 |
| Figure 8.6 Fouling evolution in the La Bisbal d’Empordà WWTP: K(A) with Smart Air MBR and K(B) without Smart Air MBR. | 132 |
| Figure 8.7 Permeability slope per each permeate cycle: MBR-A with Smart Air MBR and MBR-B without Smart Air MBR. | 133 |
| Figure 8.8 Energy consumption evolution with Smart Air MBR..... | 135 |
| Figure 9.1 A knowledge-based DSS for the integrated operation of MBR..... | 141 |
| Figure 9.2 Effects of operating conditions on filtration performance, sludge and biological processes. | 145 |

NOMENCLATURE

ACRONYMS

| | | | |
|--------------|--|--------------|---|
| AE | AERATION ENERGY | MSRE | MEAN SQUARE RELATIVE ERROR |
| AOB | AMMONIUM OXIDISING BACTERIA | MT | MODEL TREE |
| ASM | ACTIVATED SLUDGE MODEL | NOB | NITRITE OXIDISING BACTERIA |
| BOD | BIOCHEMICAL OXYGEN DEMAND | OCI | OPERATIONAL COST INDEX |
| BRN | BIOLOGICAL NUTRIENT REMOVAL | OPEX | OPERATING COSTS |
| BSM | BENCHMARK SIMULATION MODEL | ORP | OXYDATION/REDUCTION POTENTIAL |
| CAPEX | CAPITAL COSTS | PAO | PHOSPHORUS ACCUMULATING ORGANISMS |
| CAS | CONVENTIONAL ACTIVATED SLUDGE | PE | PUMPING ENERGY |
| CEB | CHEMICALLY ENHANCED BACKFLUSHES | PLC | POWER LINE COMMUNICATION |
| CFD | COMPUTATIONAL FLUID DYNAMICS | PSD | PARTICLE SIZE DISTRIBUTION |
| COD | CHEMICAL OXYGEN DEMAND | RMSE | ROOT MEAN SQUARE ERROR |
| CST | CAPILARITY SUCTION TIME | RSF | RELATIVE SENSITIVITY FUNCTION |
| CSTR | CONTINUOUS STIRRED TANK REACTORS | SADm | SPECIFIC AERATION DEMAND PER MEMBRANE AREA |
| DO | DISSOLVED OXYGEN | SADp | SPECIFIC AERATION DEMAND PER PERMEATE VOLUME UNIT |
| DPAO | DENITRIFYING PHOSPHORUS ACCUMULATING ORGANISMS | SCA | SCENARIO ANALYSIS |
| DSVI | DILUTED SLUDGE VOLUM INDEX | SCADA | SUPERVISORY CONTROL AND DATA ACQUISITION |
| EC | EXTERNAL CARBON ADDITION | SF | SENSITIVITY FUNCTION |
| EPS | EXTRACELLULAR POLYMERIC SUBSTANCES | SMP | SOLUBLE MICROBIAL PRODUCTS |
| EQI | EFFLUENT QUALITY INDEX | SNdN | SIMULTANEOUS NITRIFICATION/DENITRIFICATION |
| FI | FILAMENTOUS INDEX | SP | SLUDGE PRODUCTION |
| FR | FOULING RATE | SRC | STANDARD REGRESSION OF COEFFICIENTS |
| FS | FLAT SHEET | SRT | SLUDGE RETENTION TIME |
| HF | HOLLOW FIBRE | ST | SHORT TERM |
| HRT | HYDRAULIC RETENTION TIME | SVI | SLUDGE VOLUM INDEX |
| IWA | INTERNATIONAL WATER ASSOCIATION | TKN | TOTAL KJELDAHL NITROGEN |
| LM | LINEAR MODEL | TMP | TRANSMEMBRANE PRESSURE |
| LSA | LOCAL SENSITIVITY ANALYSIS | TN | TOTAL NITROGEN |
| LT | LONG TERM | TP | TOTAL PHOSPHORUS |
| MBR | MEMBRANE BIOREACTORS | TSS | TOTAL SUSPENDED SOLIDS |
| ME | MIXING ENERGY | UCT | UNIVERSITY CAPE TOWN |
| MLSS | MIXED LIQUOR SUSPENDED SOLIDS | WWTP | WASTEWATER TREATMENT PLANT |

LIST OF SYMBOLS

| | |
|--------------------------|---|
| A | AREA |
| A0 | INITIAL AREA |
| b_PAO | VELOCITY DECAY OF PAO |
| Ccrit | CONCENTRATION BELOW WHICH THE SETTLING VELOCITY BECOMES 0 |
| d_{comp} | COMPRESSION FUNCTION |
| d_{disp} | DISPERSION FUNCTION |
| J | FLUX |
| K_O | HALF SATURATION COEFFICIENTS FOR OXYGEN |
| K_{O_AUT} | HALF SATURATION COEFFICIENTS FOR OXYGEN FOR AUTOTROPHS |
| K_{La} | OXYGEN MASS TRANSPORT COEFFICIENT |
| K_{NH4} | NITROGEN HALF SATURATION COEFFICIENT FOR AUTOTROPHS |
| η | VISCOSITY |
| η_{NO3-H} | REDUCTION FACTOR FOR DENITRIFICATION |
| R_b | THE RESISTANCE OF THE BIOFILM |
| R_c | CAKE LAYER RESISTANCE |
| R_{cp} | CONCENTRATION POLARIZATION |
| r_H | SETTLING CHARACTERISTIC OF THE HINDERED SETTLING ZONE |
| R_m | CONSTANT RESISTANCE OF THE CLEAN MEMBRANE |
| R_m | CLEAN MEMBRANE RESISTANCE |
| R_p | RESISTANCE DUE TO PORE BLOCKING |
| r_p | SETTLING CHARACTERISTIC OF LOW SOLIDS CONCENTRATION |
| R_{sc} | CONCENTRATION OF SCALING |
| r_v | SETTLING MODEL PARAMETER |
| S_A | VOLATILE FATTY ACIDS (INFLUENT FRACTIONATION) |
| S_F | FERMENTABLE ORGANIC MATTER (INFLUENT FRACTIONATION) |
| S_{NH4} | AMMONIUM PLUS AMMONIA NITROGEN (INFLUENT FRACTIONATION) |
| S_{NO} | NITRATE PLUS NITRITE NITROGEN (INFLUENT FRACTIONATION) |
| S_{PO4} | PHOSPHATES (INFLUENT FRACTIONATION) |
| SO2 | DISSOLVED OXYGEN (INFLUENT FRACTIONATION) |
| v₀ | MAXIMUM SETTLING VELOCITY |
| v_s | HINDERED SETTLING VELOCITY FUNCTION |
| w | CAKE MASS |
| X_I | SOLUBLE UNDEGRADABLE ORGANICS (INFLUENT FRACTIONATION) |
| X_S | SLOWLY BIODEGRADABLE SUBSTRATES (INFLUENT FRACTIONATION) |
| X_{TSS} | TOTAL SUSPENDED SOLID (INFLUENT FRACTIONATION) |
| y | PROCESS VARIABLE |
| α | SPECIFIC CAKE RESISTANCE |
| θ_j | OPERATIONAL PARAMETER |
| ξ | PERTURBATION FACTOR |

RESUM

Els bioreactors de membranes (BRM) són una combinació dels reactors convencionals i una unitat de filtració que reté la biomassa, de manera que presenten com a gran avantatge una qualitat de sortida amb estàndards de reutilització, i molt poca necessitat d'espai. Amb la creixent demanda d'aigua, els rigorosos requeriments de qualitat i l'increment de zones propenses a l'escassetat d'aigua, la tecnologia BRM ha esdevingut una opció molt prometedora en les estacions depuradores d'aigües residuals. Tot i que l'embrutiment de les membranes i els costos associats per la seva neteja són els principals inconvenients, no s'han identificat encara les estratègies d'operació òptima per millorar l'eficiència dels processos que tenen lloc en els BRM d'una forma integrada, és a dir, optimitzar al mateix temps els processos biològics d'eliminació de contaminants i els físics de filtració, per tal de minimitzar l'embrutiment i, si és possible, reduir els costos d'operació.

Aquesta tesi presenta un pas endavant cap a l'operació integrada dels BRM mitjançant estudis experimentals i de modelització. Les interaccions entre els processos biològics (eliminació de nutrients i característiques de la biomassa) i físics (hidrodinàmica i filtració) que tenen lloc als BRM s'han estudiat, amb l'objectiu final de millorar-ne la seva operació i el control integrat.

Primerament, es van identificar les condicions òptimes d'operació per l'eliminació de nutrients mitjançant un model aplicat a una planta pilot. Gràcies a una anàlisi de sensibilitat es van trobar quins van ser els paràmetres més sensibles respecte a l'operació integrada dels processos d'eliminació de nutrients i filtració. La recirculació aeròbia, el cabal aire en el tanc de membranes i en el compartiment aerobi i el cabal de purga van ser identificats com a paràmetres més determinants per l'eliminació de nutrients, mentre que el temps de relaxació i el cabal de filtració van ser els més sensibles respecte a la filtració. Aquesta informació complementada amb coneixement expert, va permetre la creació d'un arbre de decisió pel control integrat dels processos de filtració i eliminació de nutrients.

Respecte la hidrodinàmica, es va optimitzar una planta híbrida a escala real tenint en compte la qualitat de l'efluent i els costos operacionals mitjançant estudis de modelització i simulació, considerant el tractament de l'aigua a través de les membranes, el decantador secundari o una combinació d'ambdós. Això també va permetre l'estudi de la hidrodinàmica del carrousel mitjançant diferents tancs en sèrie i dividint cada tanc en dos capes horitzontals. L'operació amb membranes implicà uns costos més elevats deguts a l'aire subministrat a aquestes, però es va demostrar la capacitat de l'aeració de bombolla gruixuda per finalitzar la nitrificació en el tanc de membranes. D'altra banda, l'operació amb el decantador secundari representà més temps

anòxic, resultant amb menors nitrats i costos associats però empitjorant la qualitat global de l'efluent de la planta.

Tenint en compte el fenomen de l'embrutiment, es van utilitzar dos models diferents (determinístic i basat en dades) per descriure la pressió transmembrana (PTM) en una planta pilot que va treballar sota diferents modes operacionals al llarg d'un any i mig. Concretament, el model determinístic va permetre la descripció de la PTM en condicions d'estat estacionari o amb canvis de flux, mentre que el model basat en dades captà millor les dinàmiques canviants del sistema. Així el model basat en dades anà un pas més enllà en la predicció de la PTM, mentre que el determinístic no va ser suficientment detallat, sobretot amb majors dinàmiques causades per les pertorbacions. En qualsevol cas, els models de filtració necessiten també incorporar models determinístics de llots actius per poder descriure els processos biològics i tenir una descripció completa dels processos que es duen a terme en els BRM.

D'altra banda, els estudis experimentals van permetre superar les limitacions dels models. Les relacions entre els processos biològics d'eliminació de nutrients, els processos de filtració i les característiques dels fangs determinaren les estratègies pel control integrat de dos dels paràmetres operacionals més importants en els BRM: l'aeració biològica i de membranes. En aquest sentit, es demostrà com l'aeració d'una planta pilot no només influenciava a l'eliminació de nutrients, sinó també afectava a les propietats dels fangs i això afectà a l'embrutiment. La reducció de l'aeració de membranes afectà dràsticament el procés de filtració, sense mostrar recuperació després de restablir les condicions d'aire inicials i empitjorant la qualitat de l'efluent i les propietats de la biomassa. Aquest estudi va permetre identificar les condicions d'operació òptimes dels BRM, amb una reducció del 42% en el cabal d'aire total, aconseguint un 75% d'estalvi energètic respecte a l'operació inicial.

Un sistema innovador de control d'aire focalitzat en l'aeració de membranes, va ser validat amb èxit durant 320 dies en una planta BRM a escala real. La mitjana de reducció de cabal va ser del 13%, amb un màxim d'estalvi limitat per l'usuari al 20%, sense afectar a les característiques del fang ni la qualitat de l'efluent. Aquesta reducció del cabal es va traduir en una disminució mitjana del 14% en el consum energètic de l'aeració de membranes, aconseguint-se estalvis màxims del 22%.

Els resultats obtinguts en aquesta tesi permetran millorar l'operació i el control automàtic dels processos biològics i de filtració d'una forma integrada, reduir també els costos energètics i contribuir d'aquesta manera a la millora de la competitivitat de la tecnologia BRM, especialment com a solució per a problemes d'escassetat d'aigua.

RESUMEN

Los bioreactores de membrana (BRM) son una combinación de reactores convencionales seguidos por una unidad de filtración que retiene la biomasa, de forma que presentan como gran ventaja una calidad de agua de salida con estándares de reutilización y requiriendo poco espacio. Con la creciente demanda de agua, los rigurosos requisitos de calidad y el incremento de zonas propensas a la escasez de agua, la tecnología BRM se ha convertido en una opción muy prometedora en estaciones depuradoras de aguas residuales. Conociéndose que el ensuciamiento y sus costes asociados son los principales inconvenientes, no se ha encontrado aún cuál es la operación óptima para mejorar la eficacia de los BRM de forma integrada. Es decir, optimizar al mismo tiempo los procesos biológicos de eliminación de contaminantes y los procesos físicos de filtración con el fin de minimizar el ensuciamiento, y si es posible, los costes de operación.

Esta tesis presenta un paso adelante hacia la operación integrada de los BRM mediante estudios experimentales y de modelización. Las interacciones entre los procesos biológicos (eliminación de nutrientes y características de biomasa) y físicos (hidrodinámica y filtración) que tienen lugar en los BRM se han estudiado, con el objetivo final de mejorarse su operación y control integrado.

En primer lugar, se identificaron las condiciones óptimas de operación para la eliminación de nutrientes mediante un modelo aplicado a la planta piloto. Gracias a un análisis de sensibilidad se hallaron los parámetros más sensibles respecto a la operación integrada de los procesos de eliminación de nutrientes y filtración. La recirculación aerobia, el caudal aire en el tanque de membranas y en compartimento aerobio y el caudal de purga fueron identificados como parámetros más determinantes para la eliminación de nutrientes, mientras que el tiempo de relajación y el caudal de filtración son los más sensibles respecto a la filtración. Complementado con conocimiento experto, se creó un árbol de decisión para el control integrado de los procesos de filtración y eliminación de nutrientes.

Respecto a la hidrodinámica, se optimizó una planta híbrida a escala real con respeto a la calidad del efluente y los costes operacionales mediante estudios de modelización y simulación, considerando el tratamiento de agua a través de las membranas, el decantador secundario o una combinación de ambos. También se estudió la hidrodinámica en el carrusel mediante diferentes tanques en serie y dividiendo cada tanque en dos capas horizontales. La operación con membranas implicó unos costes más elevados debido al aire suministrado a éstas, pero se demostró la capacidad de la aeración con burbuja gruesa de finalizar la nitrificación en el tanque de membranas. Por otra parte, la operación con el decantador secundario representó más

tiempo anóxico, resultando con menos nitratos y menores costes asociados por deterioro de la calidad global del efluente de la planta.

Teniendo en cuenta el fenómeno del ensuciamiento, dos modelos distintos (determinístico y basado en datos) se utilizaron para describir la presión transmembrana (PTM) en una planta piloto trabajando con diferentes modos de operación a lo largo de un año y medio. Concretamente, el modelo determinístico permitió la descripción de la PTM en condiciones de estado estacionario o con cambios de flujo, mientras que el modelo basado en datos reprodujo mejor las dinámicas cambiantes del sistema. De esta forma, el modelo basado en datos permitió dar un paso adelante en la predicción de la PTM, mientras que el determinístico no fue suficientemente detallado, sobre todo cuando con mayores dinámicas debido a las perturbaciones. En cualquier caso, los modelos de filtración necesitan incorporar modelos determinísticos de hongos activos para describir los procesos biológicos y tener una descripción completa de los procesos que se llevan a cabo en los BRM.

Por otra parte, los estudios experimentales permitieron superar las limitaciones de los modelos. Las relaciones entre los procesos biológicos de eliminación de nutrientes, los procesos de filtración y las características de la biomasa determinan las estrategias para el control integrado de dos de los parámetros operacionales más importantes en los BRM: la aeración biológica y de membranas. En este sentido, se demostró como la aeración de una planta piloto no solo influenciaba a la eliminación de nutrientes, sino que también afectaba a las propiedades de los lodos y eso afectó al ensuciamiento. La reducción de la aeración de membranas afectó drásticamente al proceso de filtración, sin mostrar recuperación después de restablecer las condiciones de aire iniciales, empeorándose también la calidad del efluente y las propiedades de la biomasa. Este estudio permitió identificar las condiciones de operación óptimas con una reducción del 14% en el caudal de aire total, lográndose un 75% de ahorro energético respecto la operación inicial.

Un sistema innovador de control automático de aire focalizado en la aeración de membranas, fue validado con éxito a lo largo de 320 días en una planta BRM a escala real. La media de reducción de caudal de aire fue del 13%, con un ahorro máximo limitado por parte del usuario al 20% sin afectar a las características de la biomasa ni a la calidad del efluente. Esta reducción del caudal de aire se tradujo en una disminución media del 14% en el consumo energético de la aeración de membranas, consiguiéndose ahorros máximos del 22%.

Los resultados obtenidos en esta tesis permitirán mejorar la operación y el control automático de los procesos biológicos y de filtración de una forma integrada, reducir los costes energéticos y contribuir a la mejora de la competitividad de la tecnología BRM, especialmente como a solución para problemas de escasez de agua.

SUMMARY

Membrane bioreactors (MBR) are a combination of common bioreactors and membrane filtration units for biomass retention, presenting unique advantages like high effluent quality and a smaller footprint than that one by conventional wastertreatment plants. Due to the growing demand for fresh water, ncreasingly stringent environmental water quality requirements and the increase of areas prone to water scarcity, MBR technology has become a competitive alternative for municipal wastewater treatment plants (WWTP) or their upgrades. Although fouling and its associated operational costs have been known to be a key issue in MBRs, the optimal operation to enhance MBR efficiency regarding biological and physical processes is still lacking. For this reason, the research developed in the framework of this thesis has been focused on the identification of the optimal operational strategies to improve the efficiency of the processes taking place in the MBR in an integrated way, optimizing simultaneously biological and physical processes to minimize fouling and, if possible, operational costs.

This thesis presents a step towards the integrated operation of MBRs through experimental and model-based studies. Interactions between the biological (nutrient removal and sludge characteristics) and physical (hydrodynamics and filtration) processes in MBRs were studied, with the final aim being to improve their integrated operation and control.

Firstly, the optimal operating conditions for proper nutrient removal were identified through a model-based approach in a pilot-scale MBR plant. Sensitivity analysis enabled the identification of the most sensitive parameters of the integrated operation of nutrient removal and filtration process. Aerobic recirculation, aeration in the membrane and in the aerobic tank and waste flow rate were determinant for the nutrient removal process, whereas relaxation time and the filtration flux were the most sensitive parameters affecting the filtration performance. Complemented with expert knowledge, a decision tree has been developed for the integrated operation of biological nutrient removal and filtration processes.

A hydraulic model optimised a hybrid full-scale MBR with respect to effluent quality and operational costs, depending on the treatment of wastewater flux through membranes, secondary settler or through a combination of both. It also allowed the study of the hydraulics of the oxidation ditch by means of several in-series tanks and dividing each tank in two horizontal layers. Membrane operation implied higher energy costs due to the membrane aeration, but the capability of the coarse-bubble aeration to finish the nitrification step in the membrane tank was demonstrated. On the other hand, the operation of the plant with the secondary settler caused

higher anoxic times, resulting in lower nitrates concentration in the effluent and lower associated costs but lower effluent quality.

Regarding the fouling phenomenon, two different model approaches were used to describe this phenomenon transmembrane pressure (TMP) in an MBR pilot plant under different operating modes along one year and a half. Concretely, the deterministic model enabled the prediction of the TMP under steady-state operation or flux changes, while the data-driven model coped with all the other dynamics of the system. Thus the data-driven model went one step further in the prediction of TMP whereas deterministic models were not detailed enough, especially when variables changed due to perturbations. In any case, filtration models need to be integrated with the deterministic activated sludge models in order to describe the biological processes and to have a complete description of the MBR systems.

Additionally, the experimental studies overcame the modelling studies gaps. Interrelations between biological nutrient removal processes, filtration processes and sludge characteristics determined the strategies for the integrated control of the two most important operating parameters in MBR: biological and membrane aeration. In that sense, it was demonstrated how the biological aeration of a pilot-scale plant not only influenced the biological nutrient removal, but also caused the deterioration of the sludge characteristics and thus affecting the fouling propensity. The reduction of the membrane aeration influenced drastically the filtration performance, with no recovery after achieving the initial aeration conditions and worsening the effluent quality and the sludge properties. The identification of the optimal aeration conditions led to an airflow rate reduction of 42%, representing an energy saving of 75% compared to the initial operating conditions.

Regarding membrane aeration, the novel air-scouring control system was successfully validated for 320 days in a full-scale MBR. The average reduction of the air-scouring flow rate was 13%, with the maximum reduction being limited to 20%, without compromising sludge characteristics and effluent quality. The control actions led to an average decrease in the energy consumption for membranes aeration of 14% and reaching a maximum of 22%.

The results obtained as part of this thesis will improve the integrated operation and the automatic control of the biological and filtration processes simultaneously. Moreover, the reduced energy costs and the better understanding of MBR operation may contribute to making MBR systems a more competitive technology to deal with water scarcity problems.

LIST OF PUBLICATIONS

The following list contains the journal publications resulting from this doctoral thesis:

Dalmau, M., Rodriguez-Roda, I., Ayesa, E., Odriozola, J., Sancho, L., Comas, J. (2013)
Development of a decision tree for the integrated operation of nutrient removal MBRs based on simulation studies and expert knowledge.

Chemical Engineering Journal 217, 174-18.

Author's contribution: All the experimental study, development of the simulation work, with help from the other authors in the calibration issues (E. Ayesa, J. Odriozola, L. Sancho). Writing the chapter, with contribution from the other authors.

Dalmau M., Maere, T., Nopens, I., Rodriguez-Roda, I., Comas, J.

Model-based optimisation of a full-scale hybrid MBR.

Submitted.

Author's contribution: All the experimental study and influent characterization. Simulation work, with help from the other authors in the calibration and development of the model (T. Maere). Writing the chapter, with contribution from the other authors.

Dalmau M., Atanasova N., Gabarrón S., Rodriguez-Roda I., Comas J.

Modelling MBR fouling with deterministic and data-driven models.

Chemical Engineering Journal, accepted for publication.

Author's contribution: All the experimental study, monitoring the pilot plant and data analysis. Writing the chapter, with contribution from the other authors.

Dalmau, M. , Monclús, H., Gabarrón, S., Rodriguez-Roda, I., Comas, J.

Towards integrated operation of MBRs: effects on aeration on biological and filtration performance. Bioresource Technology, accepted for publication.

Author's contribution: All the experimental study, monitoring the pilot plant and data analysis. Writing the chapter, with contribution from the other authors.

Monclús, H., **Dalmau, M.**, Ferrero, G., Gabarron,S., Comas, J, Rodriguez-Roda, I.

Full-scale validation of a control system for energy saving in membrane bioreactors for wastewater treatment.

Submitted.

Author's contribution: Experimental analysis. Data collection was performed by H. Monclús, and control strategies assisted by H. Monclús and Ferrero. G. Writing the chapter, with contribution from the other authors.

1

INTRODUCTION

1.1 BACKGROUND

Pollution is related to human civilization and its actions. As industrialization and urbanization have steadily increased, this has been accompanied by a corresponding increase in the demand for water along with a rise in waste production; a significant part of which will end up as waste water (Foster 2003).

In recent decades, improvements in water quality in the waste water treatment field have been made in the most developed countries. Over the years, defining and removing those constituents that may cause long-term effects and environmental impacts have played an important role in the water treatment field. As a result, the degree to which the water is treated has increased considerably (Henze et al. 2008). It is not only important to fulfil water quality objectives and meet the standards required by each country, but it is also important to meet the demand for water whilst taking into account the scarcity of this resource.

There are a number of technologies which, by means of activated sludge, facilitate the removal of any organic matter and/or nutrient present in the wastewater. Most of the wastewater treatment plants (WWTPs) are designed as conventional activated sludge (CAS) systems. CAS systems are a combination of physical, chemical and biological processes composed of different grades of treatment; preliminary, primary, secondary, and tertiary and/or advanced wastewater treatment (Tchobanoglous et al. 2003). However, the main limitation of CAS technology is the space required to run the entire treatment line. In addition, the secondary settlers used in CAS present some limitations related to activated sludge settling problems, thus causing the deterioration of effluent quality due to problems separating microbiology-related solids. For instance, some of the most common problems are filamentous bulking, foaming, rising and deflocculation (Comas et al. 2008). As a result, variations and new technologies, such as membrane bioreactors (MBRs), are being developed to deal with waste water treatment.

In Europe, the first full-scale MBRs plant treating municipal wastewater and with a capacity of 3800 p.e. was built in 1998 in Porlock (UK). Subsequent waste water treatment plants were implemented with this technology in Germany (1999, Büchel -1000 p.e.- and Rödigen -3000 p.e.) and France (Perthes-en-Gâtinais, 4500 p.e.). Later on other MBRs lines were put into service such as the MBR line in Brescia, Italy which treats 42,000m³/d or the one constructed in Kaarst, Germany to serve a population of 80000 p.e and which treats 45000 m³/d (Kraume and Drews

2010). In Catalonia, the first waste water treatment plant using MBR technology was commissioned in La Bisbal d'Empordà (2003) as a hybrid MBR plant. Nowadays, seven full-scale MBR to treat municipal wastewater have been installed in Catalonia (Gabarrón et al. 2014).

1.2 MEMBRANE BIOREACTOR TECHNOLOGY

Membrane bioreactors (MBRs) refer to a technology which combines a membrane process (microfiltration or ultrafiltration) with a suspended growth bioreactor (Judd 2011).

MBRs are characterized by a small footprint, easy retrofit and high effluent quality. MBRs not only replace the secondary settler, diminishing considerably the space, but also achieve high quality effluent comparable to tertiary treatments. This technology is the proper one selected for upgrading existing WWTPs with limited space and/or for water reuse applications (Brepols et al. 2008). In that sense, MBRs are becoming increasingly popular for waste water treatment, not only being noticed in the global market growth but also with higher public acceptance of water reuse. More stringent environmental regulations and more investments on cost-effective MBRs make them the first choice for WWTPs.

1.2.1 ADVANTAGES AND DRAWBACKS

MBR processes present unique advantages compared to other technologies and these are widely recognized. Some of these are listed below:

MBRs can produce a high quality, clarified and largely disinfected permeate in a single step. Depending on the pore size of the membranes, significantly smaller pathogenic bacteria and viruses from the sludge can be retained on the membrane surface (Marti et al. 2011).

In CAS systems, solids separation is done in the secondary settler. The particle size should be big enough to ensure proper sedimentation, thus demanding a minimum hydraulic retention time (HRT) for growth. In this sense, MBRs present an independent control of HRT and sludge retention time (SRT) (Judd 2008), as the particles, bigger than the membrane pore size, will be retained within the system. In addition, MBRs also avoid any rising problems, (present in the secondary settler), which occur when the compacted settled sludge starts to rise to the surface usually due to denitrification, or anaerobic biological activity that produces carbon dioxide or

methane (Tchobanoglous et al. 2003). Other settling problems of a microbiological origin are issues such as 1) bulking, when the density of the sludge tends to decrease as a consequence of an overabundance of filamentous microorganisms, 2) foaming, which is a variant of filamentous bulking propagated by growth of a certain bacteria causing foam on the settler sludge surface, or 3) sludge deflocculation, all of which lead to a deterioration of the effluent quality which can actually be avoided with membrane filtration. Thus, MBRs can also ensure higher effluent qualities and avoid having particles in the effluent.

The ability of MBRs to work at higher mixed liquor suspended solids (MLSS) concentrations, thus higher SRT, not only reduces the required space of the reactors, but also reproduces the conditions of specific nitrifying bacteria able to enhance ammonia removal. In addition, more solids are retained in the membrane tank, thereby reducing solid production and waste flow (Judd 2011).

However, MBRs systems do have some constraints. To ensure longer membrane life and to avoid membrane flow channels, initial screening should be more effective than in CAS so as to limit the entry of large particles (>1-3 mm in size) (Judd 2008). Along with this, MBRs require added procedures and operational protocols for membrane maintenance and cleanings, thereby adding complexity to their operation.

When MBR technology is compared to CAS, cost is still the main drawback as MBR installation requires a higher capital expenditure (CAPEX) on equipment and entails greater operating costs (OPEX) (Judd 2008). However, a CAS process with tertiary treatment has a higher CAPEX than an MBR achieving comparable effluent quality (Brepols et al. 2010). While membrane module prices may have decreased in recent years leading to a reduction in CAPEX, the MBR elevated energy demands to cope with fouling have become the main factor in OPEX; with membrane aeration being the biggest contributor to the overall operating costs (Fenu et al. 2010b, Gabarrón et al. 2014, Verrecht et al. 2010b). In this sense, it could be understood that the high operational costs are directly related to fouling abatement. Therefore, fouling and cost mitigation have become the key issues in this field.

1.2.2 TYPE OF MEMBRANES

The most commonly used membranes in the separation process are microfiltration (100-1000 nm) and ultrafiltration (5 – 100 nm).

The most commonly employed materials in membrane manufacture are polymers and ceramics, i.e. celluloses, polyamides, polysulphones and other polymeric materials with high chemical and physical resistance. In addition, it is desirable to have hydrophilic membranes to prevent fouling, due to the hydrophobic characteristics of the foulants.

1.2.3 MBR CONFIGURATIONS

Conventionally, two different configurations can be distinguished; (a) side-stream MBR, with membranes located next to the bioreactor and separation being done by pressure-driven filtration, or (b) submerged or immersed MBR, where vacuum-driven membranes are submerged in the bioreactor and filtration is operated in the dead-end mode (Figure 1.1). In both configurations, shear is necessary to prevent fouling. In side-stream MBRs this is achieved through pumping, whereas in immersed MBRs aeration provides the shear. In waste water treatment, where energy requirements are relatively lower, immersed membranes are the most widely used.

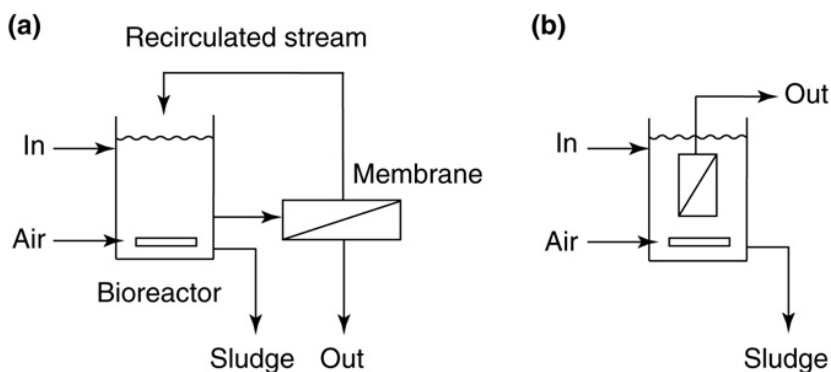


Figure 1.1 | MBR process configurations, (a) side-stream MBR, with the membrane located next to the bioreactor and (b) submerged or immersed MBR, with the membranes inside the bioreactor, from Judd (2011).

While there are different modules used in membrane bioreactors, the most common are flat sheet membranes (FS) or hollow fibre (HF) when working in submerged MBR. By applying negative pressure, water can pass through the membrane. Aeration is usually placed at the bottom of the bioreactor to ensure a homogeneous mixture. On the other hand, multi-tube membranes are the most commonly used in side-stream MBR which pump the sludge into the membrane compartment located next to the bioreactor (Figure 1.2).

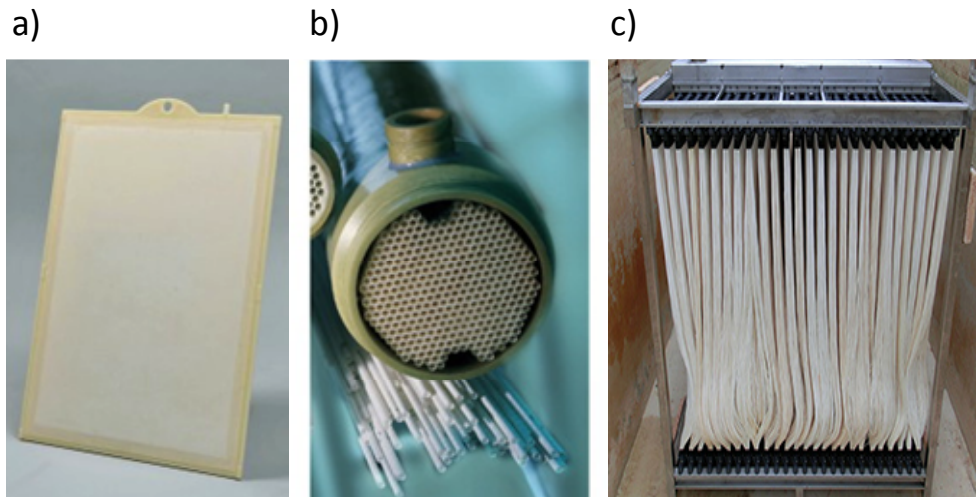


Figure 1.2 | Various membrane configurations: Flat sheet membrane (a), tubular membranes (b) and hollow fiber membranes (c), from Judd (2011).

1.2.4 FILTRATION PROCESS: DESIGN AND OPERATING PARAMETERS

Membrane filtration involves the flow of water-containing pollutants across a membrane. The water passing through the membrane is called the permeate, whereas the water with a higher concentration of materials is known as the concentrate.

The key parameters to monitor the membranes are:

- Transmembrane pressure (TMP): the driving force for the process. This is the energy required to filter at a constant flux. When the flux passes through the membranes there is a pressure drop called transmembrane pressure which is normally expressed in bar or mbars.
- Flux (normally denoted J): the quantity of permeate able to cross a unit area of membrane per unit time. Commonly, it is expressed as $L \cdot m^{-2} \cdot h^{-1}$ (LMH), but it takes the SI

units of $\text{m}^3 \cdot \text{m}^{-2} \text{s}^{-1}$, or simply m/s. MBRs generally operate at fluxes between 10 and 150 LMH; the flux relates directly to the driving force (i.e. the transmembrane pressure, or TMP, for conventional MBRs) and the total hydraulic resistance offered by the membrane and the interfacial region adjacent to it. It is influenced by the TMP, viscosity of the medium (μ) and the total resistance (R_{tot}), as the sum of the intrinsic membrane resistance and the bulk of the membrane surface.

$$J = \frac{\Delta TMP}{\mu \cdot R_{tot}} \quad (\text{Eq. 1.1})$$

- Permeability (normally denoted K): is the ratio of the flux and TMP, is highly dependent on temperature and normally takes the units of $\text{L} \cdot \text{m}^{-2} \cdot \text{h}^{-1} \cdot \text{bar}^{-1}$. At constant flux, permeability is proportional to TMP values. In that sense, K could be used to test the membrane state and the effectiveness of the physical/chemical cleanings performed.

$$K = \frac{J}{\Delta TMP} = \frac{1}{\mu \cdot R_{tot}} \quad (\text{Eq. 1.2})$$

- Specific aeration demand (SAD) is the air flow per membrane area ($\text{SAD}_m, \text{m} \cdot \text{h}^{-1}$) or per permeate volume unit (SAD_p).

$$\text{SAD}_m = \frac{\text{air flow}}{\text{membrane surface}} \quad (\text{Eq. 1.3})$$

$$\text{SAD}_p = \frac{\text{air flow}}{\text{permeate flow}} \quad (\text{Eq. 1.4})$$

1.2.5 FOULING PHENOMENA

A permeate flux decrease or TMP increase during a membrane process is recognized as “fouling”. Membrane fouling is the main drawback associated to this technology. As described by Drews (2010), *fouling in its strict form is the coverage of the membrane surface (external and internal) by deposits which adsorb or simply accumulate during operation*. As a consequence, there is a loss in permeability, an increase in resistance, and a reduction of the effective membrane area requiring an increase of the transmembrane pressure (when working at constant flux) or

decrease of permeate production (when working at constant pressure). At the end, this results in higher energy expenses and the need to chemically clean the membranes.

As a measure of fouling, permeability can be used as an indicator. Since flux is influenced by the TMP, viscosity and the total resistance, K is inversely proportional to the total resistance of the membrane.

The different types of fouling can be characterized as reversible, irreversible or irrecoverable fouling. Reversible (also called removable) fouling can be easily removed with a physical cleaning (backwashing or relaxation), whereas irreversible fouling needs to be chemically cleaned to be eliminated. In general, reversible fouling can be recognised by the cake formation on the membrane surface while irreversible fouling is observed through pore blocking and highly attached foulants during the filtration. Irrecoverable fouling, which also can be classified as clogging, is a permanent fouling and there are no possible courses of action to recover the membrane (Figure 1.3).

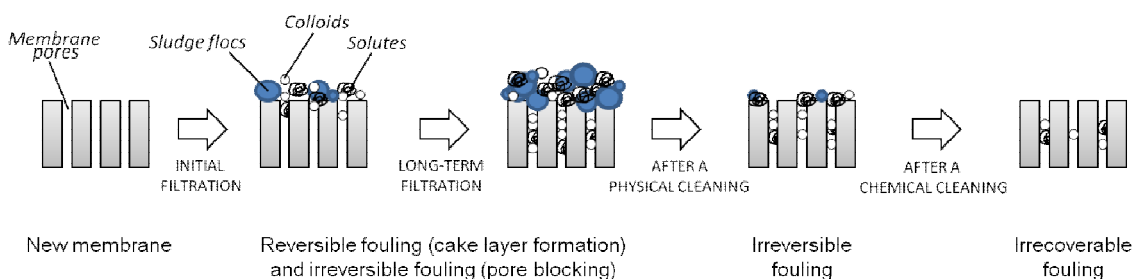


Figure 1.3] Schematic procedure of the fouling mechanisms: reversible fouling, irreversible fouling and irrecoverable fouling (adapted from Meng et al., (2009) and Judd (2011)).

There are many factors affecting fouling and this makes it difficult to characterize properly; despite the large body of research available on this subject (e.g. (Bouhabila et al. 2001, Drews 2010, Le-Clech et al. 2006)). According to Drews (2010), the three main reasons regarding the contradictory results and non-unravelling phenomena rely on:

- i) The complexity of the phenomena. This encourages researchers to jump to foregone conclusions when observing any relationship at all. Thus, neither is it possible to cope with a model able to explain the entire variables related to the fouling process (Naessens et al. 2012a). There are substantial interactions among operating conditions with membrane characteristics, biomass characteristics and feed

characteristics being the main factors in the fouling process reflected in the loss of permeability (Figure 1.4).

- ii) The lack of standard protocols for analysing fouling. Fouling analysis has increased in recent years to deal with fouling mechanisms and predict fouling behaviour. However, there are neither unique methodologies being used nor standard protocols. Apart from that, there is still the question about how useful they are in terms of fouling prediction, for instance, the analysis of exopolymeric substances (EPS). It is difficult to compare published results due to the differences (scale, materials, feed characteristics, and operating conditions) among the plants studied as well as the analytical differences; for example sample preparation.
- iii) Clearer explanations should be used in terminological terms. For instance, soluble microbial product (SMP) is a blanket term used to refer to a group of compounds despite having been analysed by diverse means. This in turn leads to confusing results and hampers the interpretation of the results obtained by different investigations.

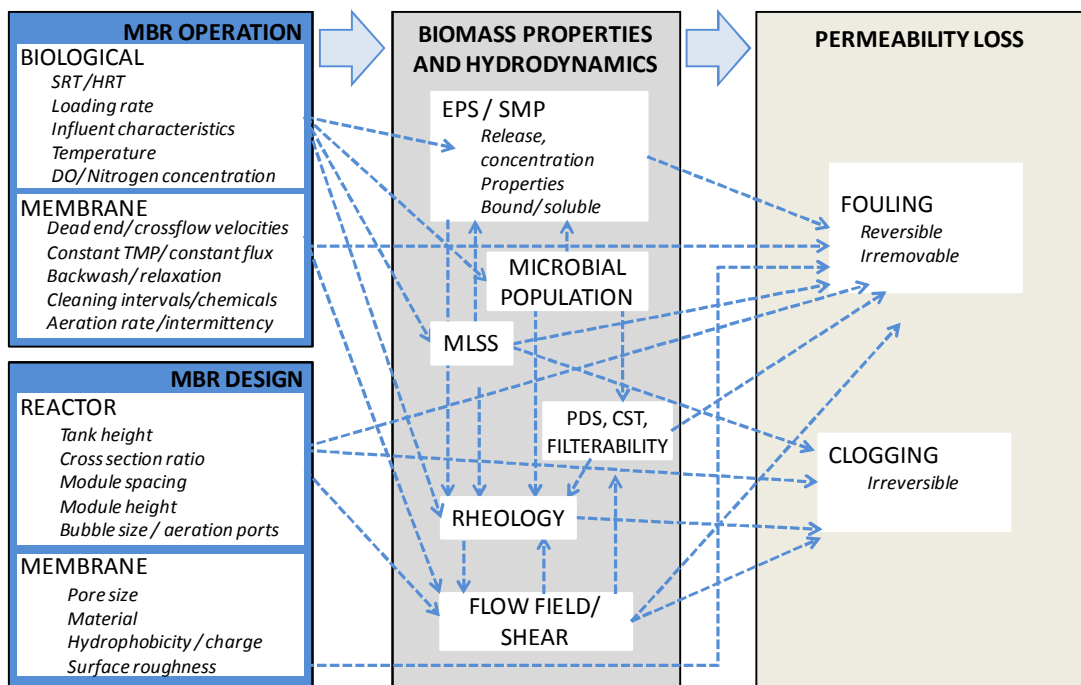


Figure 1.4 | Inter-relationships between engineering decisions and permeability loss (adapted from Drews (2010)), where CST: capillarity suction time; DO: dissolved oxygen concentration; EPS: extracellular polymeric substances; HRT: hydraulic retention time; MLSS: mixed liquor suspended solids; PSD: particle size distribution; SMP: soluble microbial products; SRT: sludge age.

As shown in Figure 1.4, there are a vast number of factors influencing fouling mechanisms.

However, the main factors affecting fouling can be divided into four groups: (i) operating parameters, (ii) design, (iii) feed characteristics and (iv) biomass properties and dynamics.

i) **Operating parameters.** Operating parameters have a significant influence on fouling. As an example, temperature clearly shows an effect on the TMP, namely the higher the temperatures, the less propensity to fouling there is (Al-Amri et al. 2010, Ma et al. 2013).

Moreover, aeration plays an important role, not only in providing oxygen to the biomass (Braak et al. 2011, Germain et al. 2007, Verrecht et al. 2008), but also in avoiding particle deposit on the membrane surface. Several control strategies related to aeration have been studied, some of these have been reviewed by Ferrero et al. (2012).

Sludge retention time (SRT) is the average time the activated-sludge solids are in the system. The SRT is an important design and operating parameter for the activated-sludge process and is usually expressed in days (Tchobanoglous et al. 2003). MLSS are directly related to SRT. In the literature, it is found that low SRT involves higher fouling propensity (Van den Broeck et al. 2012), while some correlations have been found with SRT and microbial communities (Grelier et al. 2006) and sludge filterability (Sabia et al. 2013).

Parameters related to membrane filtration are also affecting the fouling phenomena, for instance chemical cleanings affect the permeability loss by aging the membrane or working at high permeate flux, leads to a steep rise in TMP (in other words, operating over the so-called critical flux). Proper relaxation or backwashing periods can be useful to improve the increase of fouling (Mannina and Cosenza 2013).

ii) **Membrane design** is subject to its pore size and configuration. On the one hand, membrane pore size affects membrane fouling. On the other hand, membrane orientation (in relation to the flow of water or the position in the containers taking into account packing density or aeration) can negatively influence fouling. Membrane material (type, hydrophobicity, roughness) also influences fouling. In addition, the design of the reactor (height, module spacing or type of air-scouring) can affect the fouling propensity.

iii) Although **influent characteristics** do not form part of the most important interactions in MBR fouling, some alterations in the feed can affect it. Some authors reported how salinity is damaging the biomass and directly affecting membrane fouling (Di Bella et al. 2013), or how differences in temperature are affecting the

TMP behaviour (Krzeminski et al. 2012a). Van den Broeck et al. (2010) also noticed, by changing the ratio of monovalent over polyvalent cations in the influent, differences in sludge flocculation thus affecting fouling.

- iv) Focusing more on **biomass properties**, some of the most commonly encountered parameters related to fouling are listed below:

Extracellular polymeric substances (EPS), including proteins, polysaccharides, humic acids, etc., are considered the main cause of fouling. They are classified as (a) bound EPS or (b) soluble EPS or soluble microbial products (SMP). Bound EPS are located at the cell surface and bound to the sludge flocs. On the other hand, soluble EPS or SMP are defined as compounds released by the microorganisms into the solution. If they are released during substrate metabolism, they can be defined as substrate-utilization-associated-products (UAP), whereas they are biomass-associated-products if they are formed during biomass decay (Meng et al. 2009). Several mathematical models have been developed to attempt to describe the relationship of EPS on fouling (Jiang et al. 2008, Mannina et al. 2011, Menniti and Morgenroth 2010b, Tian et al. 2011a, Zuthi et al. 2012). In relation to fouling, proteins and polysaccharides fractions are considered the main contributors. However, the role of EPS has not yet been revealed, with many controversial results (Bugge et al. 2013, Drews et al. 2006b, Monclús et al. 2011, Wang et al. 2009), extended to other biopolymers (transparent exopolymer particles or biopolymers clusters).

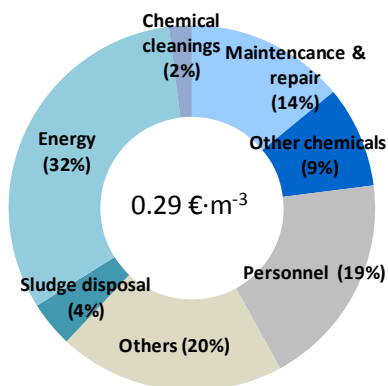
Biomass concentration, also known as mixed liquor suspended solid (MLSS) concentration, is a necessary and easy parameter to follow. The stand-alone use of MLSS as a fouling indicator is insufficient (Le-Clech et al. 2006). However, optimal MLSS concentration ranges are recommended in Lousada-Ferreira (2010).

Particle size distribution (PSD), viscosity, sludge hydrophobicity and microscopic images can help us to determine the state of the biomass and find relationships with fouling (Van den Broeck et al. 2011). In addition, filterability of the sludge and capillarity suction time (CST) are also indicators of the sludge quality for membrane filtration.

1.3 MODELS FOR MEMBRANES BIOREACTORS

Fouling is one of the main drawbacks of this technology alongside large energy consumption compared to conventional activated sludge technologies. Most of these systems are working in a conservative way; in other words with significant room for optimization. The usual safeguard operation consists of a fixed approach to remedy fouling with membrane aeration, backwashing

and chemical cleaning. These strategies neither take into account influent changes nor fouling causes, which results in higher energy and chemical (Figure 1.5).



Therefore, there is a significant potential for improving cost efficiency in dynamic and online control and modelling (Drews 2010). The use of models in these systems can be a really valuable tool to optimize this technology.

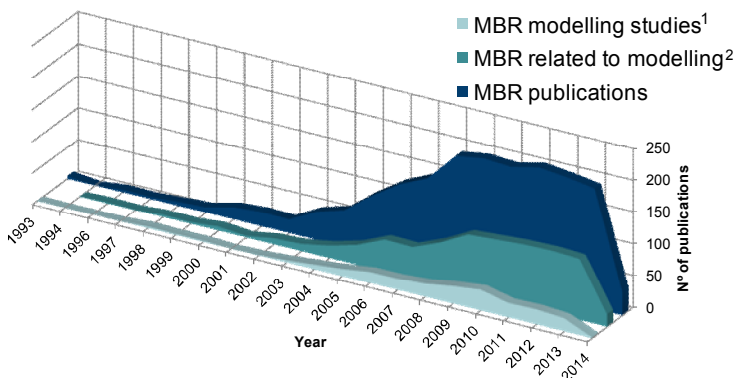
Figure 1.5 | Operational cost distribution for a stand-alone MBRs, adapted from Krzeminski et al. (2012b).

1.3.1 THE CURRENT STATUS OF MBRs IN LITERATURE, WITH SPECIAL FOCUS ON MODELLING

In the last 20 years, an increase in the number of publications related to MBRs has been noted (~2000), concurring with the implementation of this technology in WWTPs. In particular, there was a surge of publications from 2003 onwards which eventually levelled off in 2009 and since then has maintained the same rate until present-day (Figure 1.6).

As expected, this growth has been accompanied by publications on modelling, with a total number of 675 publications related to modelling and 221 were modelling studies.

Figure 1.6 | Number of publications and patents related to MBRs in the last 20 years. ¹MBR publications focused on modelling studies; ²MBR publications not strictly dedicated to models. Keywords search: “MBR AND membrane AND water” in the abstract, title and keywords, with extension of *modelling* in the full text (²) or in the abstract, title and keywords (¹). Source: Scopus™ and Wipo™ data bases (April 2014).



1.3.2 MBR MODELLING: STATE OF THE ART

Mathematical modelling has become a useful tool to design plants, operating and optimization practices so as to limit environmental pollution and costs. As the application of MBRs in WWTPs has significantly increased, MBR models for optimization experienced a significant growth. There is significant room for improvement in that field, especially in the reduction of energy consumption, bearing in mind that most of the full-scale MBRs are working in a conservative manner. However, the filtration element in MBR models implies additional complexity in comparison to CAS.

BIOLOGICAL NUTRIENT REMOVAL MODELLING IN MBRs

The existing family of activated sludge models (ASM) to describe the biological nutrient removal in CAS are well known (Henze et al. 2000). ASM are divided into three main groups: ASM1, for carbon and nitrogen removal, ASM2/ASM2d, for phosphorous removal and ASM3, a more detailed model, for N and carbon removal.

To describe the biological reactions taking place in MBRs, the models can be used directly or adapted based on any membrane specificities that may differ from the standard values used in CAS (Fenu et al. 2010a, Naessens et al. 2012a, Zuthi et al. 2012). Basically, and mainly due to membrane cycles, kinetic differences are because of the high retention times of the systems, high biomass concentrations and hydrodynamics. Taking those specifications into account, the unmodified ASM to model MBRs facilitates the description of good BNR and its effluent quality production. The sludge production and balances on the system are also collated by MBR-ASM models. In that sense, several authors using AMS models describe optimization studies for BNR and costs in benchmark plants (Maere et al. 2011, Odriozola et al. 2013), pilot plants (Mannina et al. 2011) and full-scale plants (Verrecht et al. 2010a). Nonetheless, special attention should be paid to several areas, starting with influent fractionation. Since MBRs are highly susceptible because of their complete retention and high SRT, influent fractionation (particularly on the inert fractions) plays an important role in the proper model description and calibration. Taking into consideration the nitrification and denitrification kinetics, parameters related to this process (namely, half-saturation coefficients) could change in the MBR models found in literature. Results indicate the need to increase half-saturation constants to allow adequate model predictions in

simultaneous nitrification and denitrification (SNdN), especially at high MLSS (Insel et al. 2011) to be run. Specific operating conditions required dissolved oxygen and nitrogen half-saturation coefficients to be calibrated so as to accurately model system SNdN performance; the higher the MLSS concentrations are, the higher the mass transfer limitations will be, as explained by the higher half-saturation constant in switch functions (Sarioglu et al. 2008, 2009). In addition, floc size, sludge morphology, filamentous bacteria and their kinetics, and the higher viscosity and EPS are other factors suspected of contributing to the behaviour of MBR systems and affecting mass transfer limitations.

However, since separation mechanisms are the main difference between CAS (using secondary settlers) and MBR systems (with membrane filtration), conventional ASM do not take into account the rheological and morphological characteristics of the MBR sludge, i.e. floc size, viscosity and EPS effects. For this reason, the modified ASM models appeared to describe or incorporate the EPS/SMP production and degradation. During the filtration, flocs, bacteria, polymeric substances (proteins and polysaccharides) and colloids are retained in the system and are all highly susceptible to biodegradation. Those fractions are not considered in the general ASM models but can have a high metabolic impact on MBR systems. Along these lines, Rittmann and co-workers developed a model that describes the interaction between heterotrophic and nitrifying bacteria in biological treatment processes, with regards to membrane retaining biomass characteristics (Laspidou and Rittmann 2002a, b). In the model, SMP are divided into two groups: utilization-associated products (UAPs), which are produced by biomass growth, and biomass-associated products (BAPS), which arise from biological decay. Fenu et al. (2010) reviewed the main model equations and mechanisms to describe the formation of EPS and SMP, and some of them have been used to upgrade a number of ASM models, as explained by Lu et al. (2001) and Ahn et al. (2006). In addition, Naessens et al. (2012a) classified the existing biokinetic models applied to MBRs.

FILTRATION PROCESS MODELLING IN MBRs

The most difficult and most important part of modelling MBRs is the long term decline of flux (more precisely: permeability) that occurs during operation as a result of the fouling phenomena. In addition, proper characterization of the fouling phenomena through modelling can help to develop control strategies to save costs. There is room for improvement in the areas of operating

and capital costs, i.e. upgrading filtration cycles, aeration, and chemical cleanings or increasing membrane life-time. Thus, a proper filtration model can help to develop adequate conditions for improving energy, efficiency, and the use of chemicals, as well as reducing membrane ageing and avoiding fouling.

A filtration model aims to describe the behaviour of the flux going through the membrane, how it becomes fouled and the TMP performance. However, simplified models have been used without taking into account the fouling phenomena. When the aim of the study veers away from studying filtration performance, an ideal filtration can be used with an ideal settler, thus omitting the TMP and the filtration cycles.

Different modelling techniques have been used to describe filtration performance. To provide an overview, two large groups can be distinguished: mechanistic or deterministic models and data-driven models. Deterministic models used to describe filtration can be divided into resistance-in-series models and mass-transport models. For data-driven models, statistical models and artificial intelligence models can be distinguished (Figure 1.9).

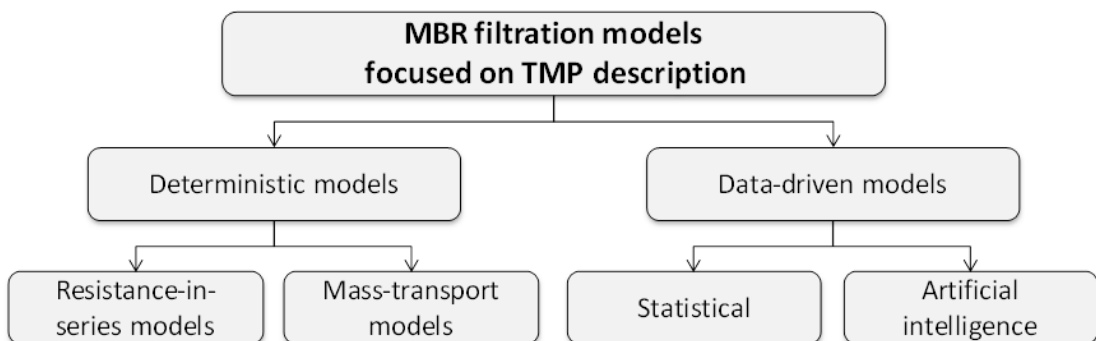


Figure 1.9 | Different model-based methodologies to describe the permeability loss in membranes.

RESISTANCE-IN-SERIES MODELS

The accumulation of material on the membrane surface over time provokes an increase in hydraulic resistance. This hydraulic resistance can be explained as a sum of different resistances (i.e. different fouling mechanisms) related to filtration flow (working at constant pressure) or TMP decrease (when working at constant flux). The equation relating flux to a difference in TMP

is described by Darcy's law (Aimar et al. 1989) in the previous equation 1.1. In order to describe the aforementioned hydraulic resistance, the most widely extended and commonly used equation was proposed by Busch et al. (2007):

$$\mathbf{R}_{total}(t, x) = \mathbf{R}_m(x) + \mathbf{R}_c(t, x) + \mathbf{R}_p(t, x) + \mathbf{R}_b(t, x) + \mathbf{R}_{cp}(t, x) + \mathbf{R}_{sc}(t, x) \quad (\text{Eq. 1.5})$$

where R_m is the constant resistance of the clean membrane, R_c is the cake layer resistance, R_p is the resistance due to pore blocking, and R_b is the resistance of the biofilm. The resistances due to concentration polarization R_{cp} and due to scaling R_{sc} are considered. Note that except for the clean membrane resistance R_m all resistances are time-dependent.

An advantage of using a resistance-in-series model is the ability to discern the components clogging the membrane and their sensitivity to the membrane resistance. The different components describing hydraulic resistance differ depending on the model. Jeong et al. (2007) identified the main individual resistances affecting the fouling by means of accumulating solids and particles in and onto the membrane and removing them with physical and chemical cleanings. Other models went into more detail about the filtration cycles; determining the amount of particles deposited on the membrane and the reduction of the compression after cleaning periods (Jiang et al. 2008, Li and Wang 2006).

On the other hand, extended mathematical deductions on the individual resistances of the membrane to model fouling have appeared. These kinds of integrated models which combine biological and biomass kinetic models are known as hybrid MBR models, where the physical MBR element is almost always described by resistances-in-series models. The connection between biological-physical and fouling processes have been carefully described in the model developed by Zarragoita-González et al. (2008), although it does not enable a complete and correct COD balance and presents a high number of SMP related parameters. Following the same tendencies, Di Bella et al. (2008) proposed an integrated model which takes into account the effect of cake layer on COD removal, however, fouling deposition was not fully integrated. The

physical processes, SMP formation and degradation, cake layer attachment–detachment and its influences on fouling development and TMP were improved in Mannina’s et al. (2011) model. However, despite the complexity of the hybrid models, to date there is no consensus on the use of a single model which would enable the description of the fouling phenomena.

MASS-TRANSPORT MODELS

Mass transfer models describe the net movement of substance from one location (usually a stream) phase, fraction or component, to another. It is well known that the sludge flow is, in terms of heat and mass transfer enhancement, significant in two-phase flow regimes. Fouling phenomena can be described as mass-transport by means of the precipitation of the dissolved material in water, where the Brownian diffusion is the main physical phenomenon. Therefore, these models are really valuable for describing the physical reactions, focused on the particles pathway in the fluid and their effects on the filtration performance, taking place during the filtration process. However, their implementation is not easy owing to the complexity of the sludge behaviour. In the last decade there have been many reports on the hydrodynamics, based on computational fluid dynamics (CFD). Brannock et al. (2010) used a CFD model for a flat sheet and hollow fibre MBRs accounting for aeration, sludge rheology and geometry and demonstrated that the effect of sludge settling and rheology had minimal impact on bulk mixing. Ndinisa et al. (2006a), studied the hydrodynamic factors such as airflow rate, nozzle size, intermittent filtration, channel gap width, feed concentration, imposed flux, and the use of membrane baffle and its effects on fouling phenomena, or by identifying the most effective flow profiles for fouling minimization (Ndinisa et al. 2006b). Other CFD results showed a high correlation with resistance data, and how a specific baffle angle had a significant impact on shear stress (Khalili-Garakani et al. 2011).

DATA-DRIVEN MODELS: STATISTICAL AND ARTIFICIAL INTELLIGENCE MODELS

Other attempts to model fouling move from mechanistic models and some researchers leapt to explore the capabilities of empirical modelling using data-driven models. Data-driven is the computational process of discovering patterns in large data sets involving methods at the intersection of artificial intelligence and statistics. In recent years, there have been various

attempts to advance the use of artificial intelligence as a viable approach to develop data-driven models to describe the performance of membrane processes. The advantages of using neural network models is that there is neither a need to separate biological and filtration processes, nor is any process knowledge required. These types of black box models enable the estimation of filtration performance using influent, effluent or operational parameters, without paying too much attention to the biological processes describing the flux decline (Chellam 2005, Liu et al. 2009, Pendashteh et al. 2011, Soleimani et al. 2013). As an example, Chellam (2005) modelled the membrane fouling induced by polydisperse feed, demonstrating that the permeate flux is the most important operational variable. Liu et al. (2009) predicted fouling in microfiltration membranes, using just 5 inputs, demonstrating that turbidity, flux and backwashing time are equally important parameters. However, the main drawback in all cases is the need to do intensive and empirical calibrations and so to acquire reliable models a very large amount of data is mandatory.

Other chemometric studies have been used to understand the fouling phenomena as well. Maere et al. (2012), described the fouling behaviour through principal component analysis, where it was possible to determine the severity or reversibility of fouling qualitatively in an automated manner without the need for additional sensors or tests. Galhina et al. (2011, 2012) used a statistically-based approach to monitor and control the key performance parameters of membrane bioreactors, by means of fluorescence analysis and minor analytical requirements. Similarly, MBR parameters such as water quality variables and operating conditions were used in this model by Kaneko and Funatsu (2013) to predict TMP in long-term operation, or by Philippe et al. (2013) for long-term permeability evolution through operating conditions (SRT, temperature, MLSS, F:M ratio, iron dosing and membrane flux. Focussing more closely on sludge characteristics, statistical analysis such as multi-component analysis has been carried out to correlate the characteristics of activated sludge (i.e. biomass concentration, relative hydrophobicity, sludge morphology, EPS, surface charge and total organic carbon) with sludge filterability. Results determined that there is no correlation to a first classification of filterability between single sludge parameters and fouling. But sludge morphology and relative hydrophobicity can classify the sludge in two categories, i.e., bad and poor to good, implying that deflocculation and a low relative hydrophobicity have a negative impact on activated sludge filterability (Van den Broeck et al. 2011). Recent studies suggest a combination of both

deterministic and black box models to determine biological and filtration descriptions, respectively (Galinha et al. 2013).

1.4 CONTROL AND OPTIMISATION: STATE OF THE ART

MBR models can be a helpful tool to optimise operation and control of biological or filtration processes in MBR systems. However, experimental studies are necessary to improve the present deterministic or data-driven models and to study processes or associations that current models do not cover.

In general, most of the optimisation studies, either modelling or experimental, are focused on a specific process (e.g. biological processes or filtration processes) disregarding the effect of other processes in an integrated way. A large number of contributions in the literature have dealt with filtration processes, or have focused on fouling phenomena or on understanding the increase in TMP because of membrane aeration intensity (air-scouring) or look at the permeate flux cycle (e.g. backwashing/relaxation periods and duration or flux). On the other hand, achieving good BNR in an MBR or proper MLSS concentrations for filtration have been also fundamental objectives. Most of the strategies for optimal operation resulted in an increase of energy and costs and so in recent years far more attention has been paid to energy-saving strategies. Moreover, studies on the hydrodynamics are also relevant in MBR due to the high shear provoked by aeration and hydraulic load variations. Despite a significant potential for improvement, the integration of all the above-mentioned objectives (improvement in filtration, cost reduction in biological and hydrodynamic processes etc.) have seldom been studied. There have also been a few studies, mainly empirical, focused on improving automatic controls of biological or filtration processes.

Figure 1.10 assembles the most significant studies related to these objectives, and divides them into empirical and model-based studies, while also distinguishing those studies involving an improvement in control of each element.

| | STRATEGIES | EMPIRICAL | MODEL-BASED |
|---|---|--|--|
|  Lower occurrence | OBJECTIVES | | |
| | FILTRATION PROCESSES (fouling, TMP) | <i>Air-scour</i> ^{1,2,3,4,5,6,7} <i>Flux</i> ^{4,8,9,10,11,12} | <i>Permeability description</i> ^{30,31,32,33,34,44,51} |
| | BIOLOGICAL PROCESSES | <i>BNR</i> ^{13,14,15,16,17,18} <i>MLSS</i> ¹⁹ | <i>BNR</i> ^{39,40,43,44,45,52} <i>MLSS</i> ⁴¹ |
| | COSTS | <i>Energy-saving strategies</i> ^{3,6,7,24,25,26,27,28,29} | <i>Cost-optimisation</i> ^{41,42,43,44,45} |
| | HYDRODYNAMICS | <i>Shear and hydraulic studies</i> ^{20,21,22,23} | <i>Shear and hydraulic studies</i> ^{44,45,46,47,48} |
| INTEGRATED OPERATION | <i>Filtration, sludge characteristics and BNR</i> ¹⁷ | <i>Hybrid models: biological and fouling models</i> ^{45,49,50,51} | |

Figure 1.10 | Empirical and model-based strategies based on filtration, biological, costs, hydrodynamics or integrated processes in MBR. Superscript numbers in the figure stand for a related publication. Control studies marked in blue. ¹ (Germain et al. 2007), ² (Germain et al. 2005), ³ (Hong et al. 2007), ⁴ (Howell et al. 2004), ⁵ (Ferrero et al. 2011a), ⁶ (Ferrero et al. 2011b), ⁷ (Ferrero et al. 2011), ⁸ (Field et al. 1995), ⁹ (Le-lech et al. 2003), ¹⁰ (Bacchin et al. 2006), ¹¹ (Tiranuntakul et al. 2011), ¹² (Zsirai et al. 2013), ¹³ (Monti et al. 2006), ¹⁴ (Monclús et al. 2010), ¹⁵ (Fu et al. 2008), ¹⁶ (Choi et al. 2009), ¹⁷ (Fatone et al. 2008), ¹⁸ (Kim et al. 2008), ¹⁹ (Monclús et al. 2011), ²⁰ (Menniti et al. 2009), ²¹ (Stricot et al. 2010), ²² (Braak et al. 2011), ²⁴ (Brepols et al. 2010), ²⁵ (Gabarrón et al. 2014), ²⁶ (Krzeminski et al. 2012c), ²⁷ (Ginzburg et al. 2008), ²⁸ (Busch and Marquardt, 2009), ²⁹ (Ferrero et al. 2012), ³⁰ (Busch et al. 2007), ³¹ (Drews et al. 2009), ³² (Jiang et al. 2008), ³³ (Liu et al. 2009), ³⁴ (Maere et al. 2012), ³⁵ (Galinha et al. 2013), ³⁶ (Maere et al. 2012), ³⁷ (Philippe et al. 2013), ³⁸ (Zuthi et al. 2013), ³⁹ (Cosenza et al. 2013), ⁴⁰ (Odriozola et al. 2013), ⁴¹ (Beltrán et al. 2009), ⁴² (Fenu et al. (2010b)), ⁴³ (Verrecht et al. 2010b), ⁴⁴ (Maere et al. 2011), ⁴⁵ (Mannina and Cosenza 2013), ⁴⁶ (Verrecht et al. 2010a), ⁴⁷ (Brannock et al. 2010), ⁴⁸ (Khalili-Garakani 2011), ⁴⁹ (Mannina et al. 2011), ⁵⁰ (Tian et al. 2011), ⁵¹ (Zarragoitia-González et al. 2008), ⁵² (Galinha et al. 2011), ⁵³ (Galinha et al. 2013).

1.4.1 EMPIRICAL STUDIES

To date, most of the MBR research has been focused on empirical studies to comprehend and evaluate the MBR process. Along these lines, several studies have been focused on membrane aeration and its effects on the TMP. Germain et al. (2007, 2005) studied relationships between oxygen transfer and biomass characteristics in the membrane tank, while others were more focused on mitigating fouling through intermittent aeration (Hong et al. 2007) or by membrane aeration changes to manipulate the critical flux (Howell et al. 2004). The use of control strategies focused on membrane aeration were studied by Ferrero et al. (2011a, 2011c, 2011d), with the

aim of identifying the best filtration performance by reducing air-scouring and saving costs. With regards to the filtration processes, membrane flux has also been extensively studied and starting with the so-called critical flux concept, i.e. flux below which a decline of flux with time does not occur (Field et al. 1995). Le-Clech et al. (2003) compared data derived from different flux-step analyses to determine the critical flux, with the best practice for its determination appearing to be small flux intervals coupled with moderate filtration time. Critical flux was also reviewed by Bacchin et al. (2006), who pointed out the different flux-step methodologies used and the influence of membrane and suspension properties on the critical flux. Later on, further studies were carried out to compare the critical flux values obtained from various determination methods. These studies recommended smaller step heights while the step length had no effect on critical flux, regardless of the determination methods employed (Tiranuntakul et al. 2011). Zsirai et al. (2013) pointed out the limitations of the flux step test and the difficulty of obtaining precise fouling rate data in full-scale MBR in complex hydrodynamic systems.

With biological processes, the effect of mixed liquor/permeate recirculation on carbon and nutrient removal was studied by Monti et al. (2006), achieving higher BNR rates than with conventional activated sludge systems with a higher loading rate and better effluent quality. This was again demonstrated by Monclús et al. (2010a) during 210 days of operation in an MBR pilot plant. The influence of influent chemical oxygen demand and nitrogen ratio was also studied in an MBR, demonstrating a total N removal efficiency decrease as the COD/N decreased (Fu et al. 2008). Choi et al. (2009) used oxidation reduction potential to improve nitrogen removal through the on/off control of an aerator. Fatone et al. (2008) validated, on both pilot and full scale level, an online control system for intermittent biological aeration in MBR to improve nitrogen removal. Kim et al. (2008) carried out a fouling control system by changing membrane depth, and consequently achieved better nitrogen removal. However, in the case of sludge characteristics, MLSS was the only monitored parameter. As for the biological characteristics of the sludge, the optimization of start-up procedures in MBR with low initial solids concentrations was achieved with a knowledge-based control module, which also saved time and preserved the membrane integrity (Monclús 2012).

On the other hand, there are several empirical studies on the topic of how hydrodynamics affect the filtration process, e.g., how shear can affect the production of SMP in an MBR system

(Menniti et al. 2009) or how the effluent quality and fouling are affected by the hydrodynamic stress (Stricot et al. 2010). Braak et al. (2011) deal with hydrodynamics in MBRs, studying aeration parameters and their impact on filtration performance or novel air-scouring membrane systems in the filtration processes. To control fouling, the study of continuous and non-continuous membrane operation on permeate flux decline was examined (Hong et al. 2002). It was determined that intermittent suction operation resulted in slower flux decline due to an enhanced removal of foulants accumulated on the membrane surface.

Most of the strategies to avoid fouling consist of membrane aeration, backwashing and chemical cleaning in conjunction with routine analyses on membranes, thus resulting in an increase in energy demand, chemicals and a reduction in the life-time of the membrane. Hence, empirical optimizations and assessments in full-scale MBRs have been applied with the aim of reducing costs. Brepols et al. (2010) compared the specific energy demand of MBRs and conventional WWTP, where the small and medium sized MBRs do not have a disadvantage in actual energy consumption compared to similar-sized CAS with tertiary treatment. Gabarrón et al. (2014) assessed seven full-scale MBRs and achieved a 34% energy reduction through optimization strategies, thus demonstrating that hydraulic load was the main determining factor in energy consumption. In addition, operation at optimal flow conditions was demonstrated to result in low specific energy consumption and in an energy efficient process (Krzeminski et al. 2012c). Ginzburg et al. (2008) studied how to control fouling through different operating modes to uncover energy saving strategies. This emphasizes the idea that predetermined schemes are never optimal, and flexible operations become the solution to dealing with changing influent, biological and membrane conditions. As reported by Busch and Marquardt (2009) significant potential for improving cost efficiency is available in the area of dynamic and online control. Ferrero et al. (2012) reviewed the most important control strategies applied to MBR systems. The very few literature contributions coping with dynamic and online fouling control and the absence of full-scale control implementations were identified. Thus, fully-integrated control or optimization of MBRs, regarding biological processes and filtration, are practically non-existent. In addition, the few optimization and control strategies applied until now present conservative operational solutions owing to the restricted operating conditions recommended by the manufacturer to preserve the guarantee.

1.4.2 MODELLING STUDIES

Modelling studies have been carried out that can help the development of possible optimal strategies for MBRs operation. Focusing on the filtration process, modelling studies based on permeability loss are the most frequent. Their common aim is to determine the best operational strategies for reducing or predicting fouling. Most of them are through deterministic models (Busch et al. 2007, Drews et al. 2009, Jiang et al. 2008, Liu et al. 2009, Maere et al. 2012) or data-driven models (Galinha et al. 2013, Maere et al. 2012, Philippe et al. 2013, Zuthi et al. 2013). In spite of these modelling approaches, a general and widely accepted validated model still does not exist. In fact, not only have model-based biological nutrient removal studies for improving the process efficiency through simulation also been carried out (Cosenza et al. 2013, Odriozola et al. 2013), but heuristic models have been used to describe the gradient of solids among the reactors as well (Beltrán et al. 2009). With model-based costs studies, Fenu et al. (2010b) evaluated the cost of an MBR plant and other WWTPs using ASM models, determining higher consumption for MBRs in comparison with a WWTP treatment resulting in similar effluent quality. Similarly, a cost analysis of the impact of representative dynamic flow and load conditions using ASM1 was evaluated in an MBR, which determined sludge production and the application of buffer tanks as the most appropriate for diminishing operational costs (Verrecht et al. 2010b). Other studies improved BNR together with a cost reduction using ASM2d as the biological model. For example, Maere et al. (2011), at an MBR-benchmark plant, took into consideration the shear by coarse-bubble aeration where membrane aeration was simulated; Mannina and Cosenza (2013) studied diverse operational strategies, such as aeration, hydraulic filtration/backwashing cycles or membrane cleanings to improve BNR and reduce costs. A small-decentralised MBR was able to be optimised by up to 23%, with respect to energy consumption, and without compromising effluent quality (Verrecht et al. 2010a). More focused on hydrodynamics, Brannock et al. (2010) optimized a full-scale MBR in terms of aeration, sludge rheology and geometry by using CFD. Similarly, Khalili-Garakani (2011) evaluated fouling on the membrane surface and determined a minimal effect of rheology on the bulk mixing. Although it is essential to integrate fouling and biological models, only very few authors in specific studies have done so (Mannina et al. 2011, Tian et al. 2011a, Zarragoitia-González et al. 2008). In addition, the use of models to develop control strategies to improve the filtration process, i.e. real-time calculation of fouling indicators for control (Galinha et al. 2011) or the use of biological models to

improve the system in real time (Galinha et al. 2013), can also be a useful tool for operators to facilitate the MBR process. In that sense, hybrid models for real-time control are a promising tool with significant potential for application.

There is a lack of good modelling practice in MBRs on the subject of data collection and its relationship to the influent fractionation, calibration and validation. In all the studies reviewed, it is important to note the importance of model validation. In that sense, most of the models require further insight into the validation steps. Furthermore, most of the MBR models are based on theoretical studies, and few of them are based on laboratory and pilot-scale plant results. In this sense, there is a noticeable absence of applying these models to full-scale municipal or industrial MBRs, so as to evaluate the different control strategies in terms of energy, time savings and water quality.

Hence, to overcome the limitations of the current models, it is indispensable to combine them with experimental studies. Thus, experimental studies can help to fill the gaps where modelling tools are not able to describe the entire system. Although some variables are clearly correlated with fouling, for other variables it is not that clear at all because of their dynamic nature. In fact, there are a lot of variables interacting in an MBR, for instance TMP, thus MBR filtration really becomes a very complex problem to describe with deterministic models. The integration of empirical studies with modelling and control approaches is still lacking in the literature, and it should be further investigated. Empirical and model-based studies are complementary tools which are useful for improving, optimising and understanding the MBR process in terms of BNR, sludge characteristics, hydrodynamics, costs and filtration performance.

This thesis has contributed in the water/wastewater engineering field in the following way: first a methodology for generate decision trees combining systems analysis and expert knowledge. Secondly with a model based evaluation study of an MBR-CAS hybrid system. Thirdly, the improvement of fouling predictions combining mechanistic and data-driven models has been done. Fourthly, experimental relations of the aeration (biological and from the membrane compartment) have been identified. And finally, a control system to reduce the energy cost of the aeration in MBRs was validated in a full-scale MBR plant.

1.5 ANTECEDENTS

To date, the research of the group has aimed for a better understanding of MBR processes and operation, i.e. biological and filtration processes. This has been achieved through basic research and experimentation with different membrane configurations in pilot and full-scale facilities. With a total funding of approximately 2 million euros, this research has been carried out within the framework of several public research projects that have been operating since 2006 (Colmatar, Colmatar+, Waterfate, demEAUmed, MBR2, AtWat), public-private schemes (MMA and CDTI with INIMA) and contracts with government administrations (ACA, ACCIO). Preceding works include three doctoral theses (Ferrero 2011, Gabarrón 2014, Monclús 2011), several MSc, around 30 scientific publications and a patent approved by the Spanish Intellectual Property Authority on October 22nd 2010 (ES 2333837 (Rodriguez-Roda et al. 2011)).

An innovative air-scouring control system was developed and optimized by Ferrero (2011). This control system has been implemented, adapted and validated on a pilot scale. It has achieved energy savings of up to 20% (with respect to the minimum aeration recommended by the membrane suppliers), without any fouling interferences and with good BNR efficiency. This study led to the above-mentioned patent application (ES 2333837(Rodriguez-Roda et al. 2011)).

Monclús (2011) defined and extended a knowledge-based decision support system for biological nutrient removal in municipal MBR. The system achieves good efficiency in both the start-up and steady-state periods. Fouling indicators have been identified, resulting in the proposal of a new method for monitoring and estimating membrane fouling in an MBR. In addition, operational strategies to speed up the start-up process in MBRs were proposed.

in addition, recently a state of the art study of the design, operation and diagnosis of the municipal MBRs in Catalonia was carried out (Gabarrón, 2014) with the main operational problems being identified and several optimization strategies presented to improve the operation of this technology and its costs.

This thesis will attempt to fill the gaps of previous works, such as the integrated operations and controls for biological nutrient removal, filtration and sludge properties, and the validation of the air-scouring system in a full-scale MBRs. Integrated optimization strategies will be tested by means of modelling and experimental studies on both pilot and full scale levels.

OBJECTIVES

The principal objective of this thesis is to study the interactions between the biological (nutrient removal and sludge characteristics) and physical (hydrodynamics and filtration) processes in MBRs to improve their integration operation and control. In order to achieve it, several sub-objectives were established:

- To optimise biological nutrient removal in MBRs through a model-based approach.
- To improve the description of system hydrodynamics and optimise hydraulic management of MBRs in terms of process efficiency and economy by means of modelling.
- To improve the description of the filtration performance (i.e. TMP evolution) through both data driven and deterministic modelling approaches.
- To understand the effects of the aerobic and membrane aeration regulation on the nutrient removal and filtration processes, as well as to sludge characteristics.
- To validate the effectiveness of an innovative automatic control system for membrane aeration at full scale.

The attainment of the previous sub-objectives has led to the following thesis outline (Figure 2.1).

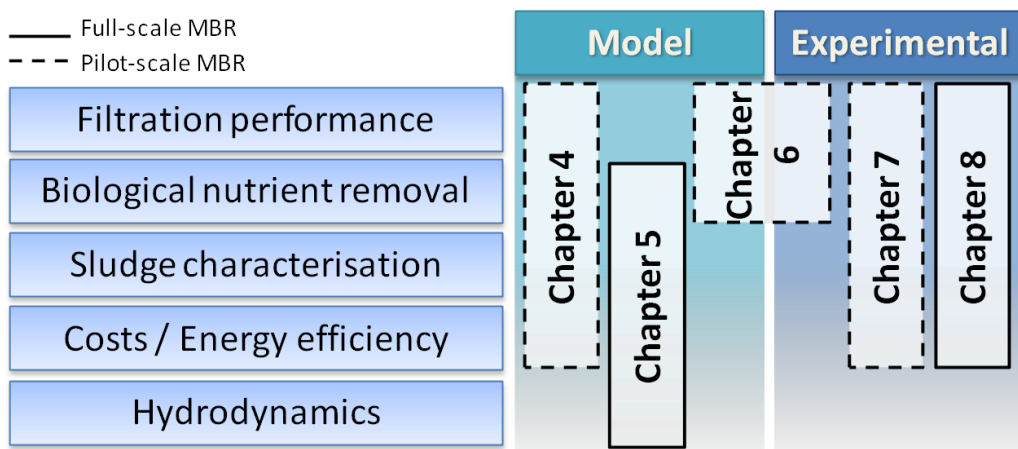


Figure 2.1 | Outline of the thesis. Note that for the calibration/validation of the models in Chapter 4 and Chapter 5 experimental results were used.

Chapter 4 identifies the most sensitive operating parameters for a UCT-MBR pilot plant. A model-based study (ASM) together with a sensitivity and scenario analysis are used in the optimization of process set-points, and an operational decision tree for the integrated operation of MBRs for nutrient removal is developed based on modelling results and expert knowledge.

Hydrodynamics of a full-scale hybrid wastewater treatment is investigated in **Chapter 5**. The selection of appropriate plant operational conditions (effluent treated by membranes or secondary settler) through deterministic biological modelling (ASM) and solids separation risk model is assessed for this complex system.

Chapter 6 gives a comparison of deterministic and data-driven models to describe the evolution of TMP in a pilot-scale MBR giving a reliable description of membrane fouling.

Chapter 7 presents the changes in filtration processes, nutrient removal processes and the biomass characteristics by modifications of biological and membrane aeration.

Chapter 8 illustrates how modifications to membrane aeration can achieve energy saving (with no negative impact on biological processes and filtration) at a full-scale MBR through the validation of the air-scouring control system *Smart Air MBR*[®].

METHODOLOGY

This chapter describes the research methodology followed in this thesis. Simulation and model-based studies were complemented and validated by experimental work carried out in pilot- and full-scale MBRs (Table 3.1).

Chapters 4, 5 and 6 were simulation-based studies each utilizing a deterministic model. In Chapter 6 a data-driven model for the filtration processes was also used to complement the deterministic model. Experimental characterisation of the influent, the effluent and sludge characteristics were carried out for each of the models developed. On-line parameters were also monitored. The modelling study in Chapter 6 utilized experimental data from 1.5 years of operation.

Chapters 7 and 8 were entirely experimental. The results from these two chapters reinforce the findings from the models described in the previous chapters. Additional data was obtained from an MBR pilot plant which was operated for 3 years and a full-scale MBR plant monitored for 2 years.

Table 3.1 | Description of the methodologies described in chapters, indicating type, year and scale of performance.

| Chapter | Type of experiment | | Scale |
|-----------|------------------------|-----------|-------------|
| | Experimental | Modelling | |
| Chapter 4 | 2010 ¹ | 2011 | Pilot-plant |
| Chapter 5 | 2011-2012 ¹ | 2012-2014 | Full-scale |
| Chapter 6 | 2011-2013 | 2013-2014 | Pilot-plant |
| Chapter 7 | 2013 | | Pilot-plant |
| Chapter 8 | 2012-2013 | | Full-scale |

¹ Experimental work for the calibration and validation of the modelling studies

3.1 EXPERIMENTAL SYSTEMS

3.1.1 PILOT-PLANT MBR

The pilot plant is located at the Castell-Platja d'Aro WWTP, Catalonia, North-East of Spain (Figure 3.1). The pilot plant treats municipal wastewater with an average ratio of nutrients (C:N:P) of 100:11:0.8. The characteristics of the raw wastewater fed to the pilot plant MBR are detailed in each chapter. The pilot plant comprises of a pre-screening system (0.25 m³, with 1 cm screen), a

bioreactor with UCT configuration (total volume of 2.26 m³), i.e. anaerobic (14% of the total volume), anoxic (14%) and aerobic (23%) reactor compartments, that are ultimately followed by a compartment (49%) with submerged flat sheet membranes with a nominal pore size of 0.4 µm (Kubota). The total membrane area is 8 m². Total suspended solids (TSS) sensors (Solitax; Hach Lange, *Düsseldorf, Germany*) are installed in the anaerobic and membrane compartments. The anoxic reactor is equipped with an ORP (oxidation reduction potential) sensor (Alldos, *Reinach, Switzerland*). All compartments are equipped with a mixer. In the aerobic and membrane reactor compartments two DO-temperature sensors (Crison, *Alella, Barcelona, Spain*) are installed. Furthermore, in the aerobic bioreactor compartment and in the membrane compartment a pH sensor (ProMinent, *Heidelberg, Germany*) are installed respectively. An on-line ammonia analyser (Amtax, Hach Lange, Germany), nitrate sensor (Nitratax, Hach Lange, Germany) and phosphate analyser (Phosphax, Hach Lange, Germany) are installed in the membrane compartment. Downstream of the sensor and analyser units, a filtering unit is installed to filter the samples at 0.2 µm (Filtratax, Hach Lange, Germany).

The raw wastewater is collected directly from the sewer entering the full-scale WWTP, after passing the bars for gross solids. The wastewater is pumped to the pilot plant using a peristaltic pump (Bredel SPX25, *Watson Marlow, USA*) and then passes through a second 1 cm screen located in a primary settler. The water is then pumped through a 1 mm pore size filter and stored in a mixed 500 L buffer tank. From this buffer tank the wastewater is pumped to the anaerobic reactor compartment with a positive displacement pump (Seepex, *Bottrop, Germany*) passing through a second filter with a pore size of 0.6 mm to prevent large solids from entering the bioreactor and damaging the membranes. The permeate is obtained by applying a vacuum pressure drop over the membranes using a second positive displacement pump, which is controlled by pressure transducers that measure the transmembrane pressure (TMP). Treated effluent is collected in the permeate tank and discharged from the pilot plant to the WWTP sewer.



Figure 3.1| Detailed pictures of the pilot-scale plant located in Castell-Platja d'Aro.

In the aerobic reactor a PID controller maintains the dissolved oxygen at the desired set-point, using two membrane air diffusers. The bioreactor is operated with three different recirculation flows proportional to the inflow, transferring the sludge from the membrane bioreactor to the anoxic compartment (external recirculation), from the aerobic to the anoxic compartment (anoxic recirculation) and from the anoxic to the anaerobic compartment (anaerobic recirculation).

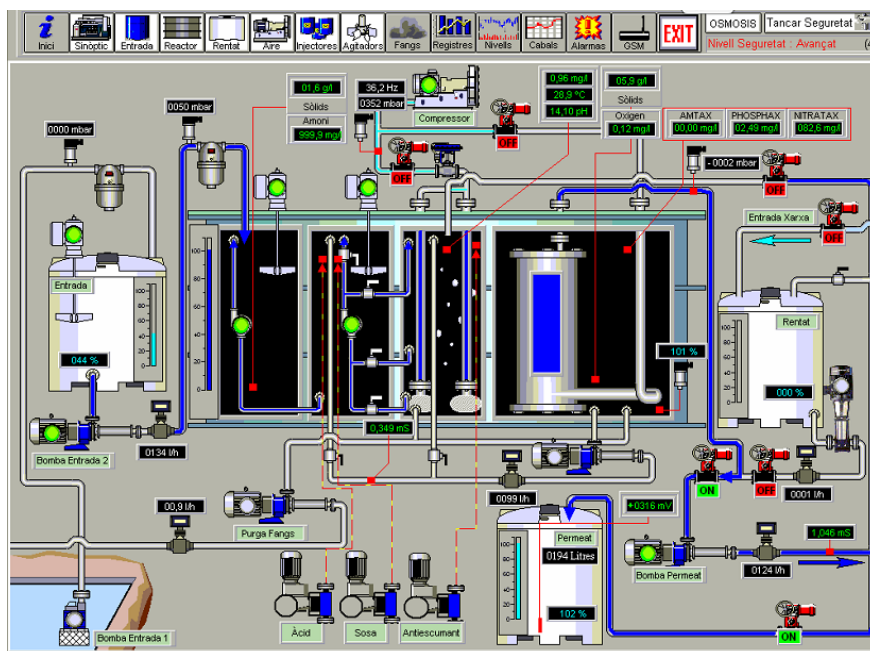


Figure 3.2| Overview of the SCADA system installed in the pilot plant.

The pilot plant is equipped with a programmable logic controller (PLC) and supervisory control and data acquisition (SCADA) system that acquires digital and analogical data and controls all the automatic control loops of the plant: aeration, permeate fluxes, hydraulic retention time (HRT), SRT and mixed liquor suspended solids (MLSS) concentration and recycles.

3.1.2 FULL-SCALE MBR

A full-scale MBR facility treating municipal wastewater and located in La Bisbal d'Empordà (Girona, Spain) was evaluated. This WWTP has a hybrid configuration, combining membrane treatment and secondary sedimentation.

The primary treatment is composed of coarse screen (8 cm), a fine screen (1 mm), a grit chamber, a lamination tank (1112 m³) with prolonged aeration to prevent the sedimentation and maintaining the water in mixed conditions, and finally a sieve.

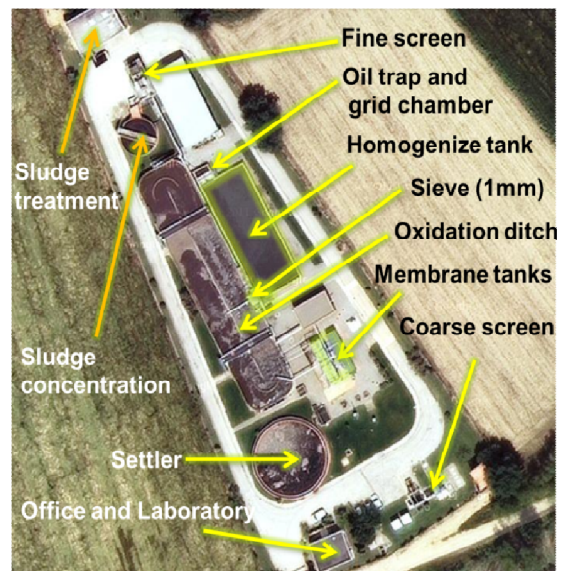


Figure 3.3 | Overview of the WWTP of La Bisbal d'Empordà.

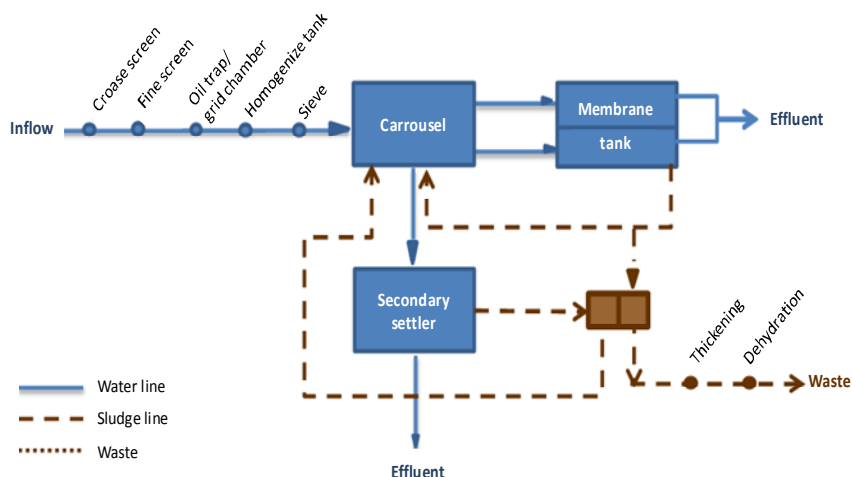


Figure 3.4 | Simplified scheme of the full-scale facility.

The secondary treatment is composed of biological reactor with an approximate volume of 4000 m³ (oxidation ditch type) with four surface aerators, two of which have a variable speed. Water is then pumped to two MBR tanks (A and B, 30 m² each) where Zenon 500c hollow fibre membranes are installed, with a total membrane area of 5808 m² and a specific aeration demand (SADm) of 0.405 m³·h⁻¹. Permeate flux is 27±1 L·m⁻²·h⁻¹ (LMH), with 10 minutes of filtration and 40 seconds of backpulse, adding 6.3 mg ·L⁻¹ of NaClO. The facility treats a maximum daily flow of 3225 m³·day⁻¹ by membrane ultrafiltration. When the influent flow rate is higher than 3225 m³·day⁻¹, the excess flow is treated with the secondary settler (925 m³, and a surface of 314 m²). All the underflow sludge from the secondary sedimentation tank is returned to the oxidation ditch, and there is an external recirculation from the membranes to the oxidation ditch. The average SRT is of 19±2 days, wasting the sludge from the membrane recirculation. The effluent flow rate and the TMP were respectively monitored by a flowmeter and a pressure gauge, and all data is stored in a SCADA system.

3.2 ANALYTICAL METHODS

3.2.1 INFLUENT AND EFFLUENT ANALYSIS

Several analytical methods have been used to determine the concentration of nutrients, organic matter and suspended solids in the influent and effluent of the WWTP. A description of the analytical methods used is detailed in 3.2.

Table 3.2 | Analytical methods used for the determination of the influent and effluent concentrations.

| Analysis | Reference (APHA 2005) |
|--|--|
| Total suspended solids (TSS) | APHA standard method 2540D |
| Volatile suspended solids (VSS) | APHA standard method 2540C |
| Chemical oxygen demand (COD) | APHA standard method 5220B |
| Biochemical oxygen demand (BOD) | APHA standard method 5210D |
| Total Kjeldahl Nitrogen (TKN-N) | APHA standard method 4500-Norg B. using boric acid and destillator Büchi (Postfach, Switzerland) |
| Ammonium (NH ₄ ⁺ -N) | APHA standard method B324, using boric acid and destillator Büchi (Postfach, Switzerland) |
| Nitrates, nitrites and phosphates (NO ₃ ⁻ -N, NO ₂ ⁻ -N, PO ₄ ³⁻ -P) | APHA standard method 4110B, using ionic chromatography (Metrohm 761-Compact) |

3.2.2 SLUDGE SAMPLES

To determine the sludge properties, different analyses have been carried out.

The concentration of **solids** in the sludge compartments was determined according to APHA standard method 2540D. **Sludge volume index (SVI)** was determined according to Metcalf and Eddy (2002), using 1 L of membrane tank' sludge and settling 30 minutes. Due to the high concentration of solids in the pilot plant, the **diluted sludge volumetric index (DSVI)** was used.

The dewaterability of the different mixed liquor samples was evaluated by measuring the **capillary suction time** (Triton electronics Ltd., type 304 B) with CST papers and the 6 mL of sludge sample. **Filterability** was determined using the protocol described by Kubota (R) through 50 ml of sample through a 2-4 μm pore disc filter (ALPL1244185) under gravity during 5 minutes.

Particle size distribution (PSD) was measured with a particle size analyzer (Beckman Coulter LS 13 320) using the Universal Liquid Module and including a polarization intensity differential scattering technology to measure the small particles.

Filtered supernatant was analysed for **soluble microbial products (SMP)**. Extraction of bound EPS from the sludge samples was made through the cationic exchange resin method of Froelund et al. (1996). Protein concentration was measured spectrophotometrically using Lowry method (Lowry et al. 1951) as modified by Peterson (1979). **Polysaccharides** content was analysed using Dubois method (Dubois et al. 1956) by using 5% phenol concentration (Raunkjaer et al. 1994).

Microscopic examinations were done using a Nikon model Eclipse E200 microscope and the microscope pictures were recorded using the Zeiss KS100.3 software. **Filamentous index (FI)** was determined based on the subjective method for filamentous bacteria abundance scoring suggested by Eikelboom et al. 2002.

For the determination of the **hydrophobicity**, sludge samples were diluted to 1 g MLSS/L. This dilution sample is measured as the initial value at 650 nm (Absi) in a spectrophotometer (DR5000, Hach Lange) with the filtrate from this sample as a blank. 3 mL of this dilution sample is shaken vigorously with an equal amount of n-hexadecane for 2 min. After that, the sample is allowed to separate again for 5 min. The absorbance in the aqueous phase is then measured at

650 nm (Abs_f) and compared to the absorbance of the dilution sample (blank). Hydrophobicity can then be calculated as follows:

$$\text{Hydrophobicity} = \left(1 - \frac{\text{Abs}_f}{\text{Abs}_i}\right) \cdot 100 \quad (\text{Eq. 3.1})$$

3.3 MODELLING SOFTWARE TOOLS

3.3.1 WEST BY MIKE DHI

WEST™ (mikebydhi.com) is a powerful tool for dynamic modelling and simulation of WWTPs. The extensive deterministic models and process library of WEST (e.g. ASM model family) allows the possibility to model and evaluate almost any kind of WWTP. The tool allows the simulation of scenarios with dynamic flow rate profiles and the evaluation of possible control systems.

This was used to describe the biological (ASM2d, Henze et al. 1999) and the membrane filtration process behavior (resistance-in-series model) in Chapters 4 and 6 or coarse bubble aeration (Maere et al. 2011) in Chapter 5.

3.3.2 WEKA

Weka™ is a collection of machine learning algorithms for data mining tasks. The algorithms can either be applied directly to a dataset or called from your own Java code. Weka contains tools for data pre-processing, classification, regression, clustering, association rules, and visualization. It is also well-suited for developing new machine learning schemes. It was used for the description of the TMP in Chapter 5 by means of a data-driven model. Further details of the models used are available in Chapter 5.

3.3.3 RISK ASSESSMENT

The presence of heuristics and qualitative knowledge on complex phenomena such as filamentous bulking, foaming and rising sludge stands in sharp contrast with the lack of basic

mechanistic knowledge on the population dynamics of the microorganisms causing these phenomena. Benchmark system applies a risk assessment model, which integrates empirical knowledge with the mechanisms of standard deterministic models to infer solids separation problems of microbiological origin (Comas et al., 2008), applied in Chapter 5. The intention is to propose a risk assessment model for microbiology-related problems using only information available in the simulation outputs, either directly or after simple data processing. The reader is referred to the detailed technical reports for a full description of all three risk models (Comas et al., 2008).

The mathematical representation of the decision tree is captured using the principles of fuzzy decision theory (Figure 3.5).

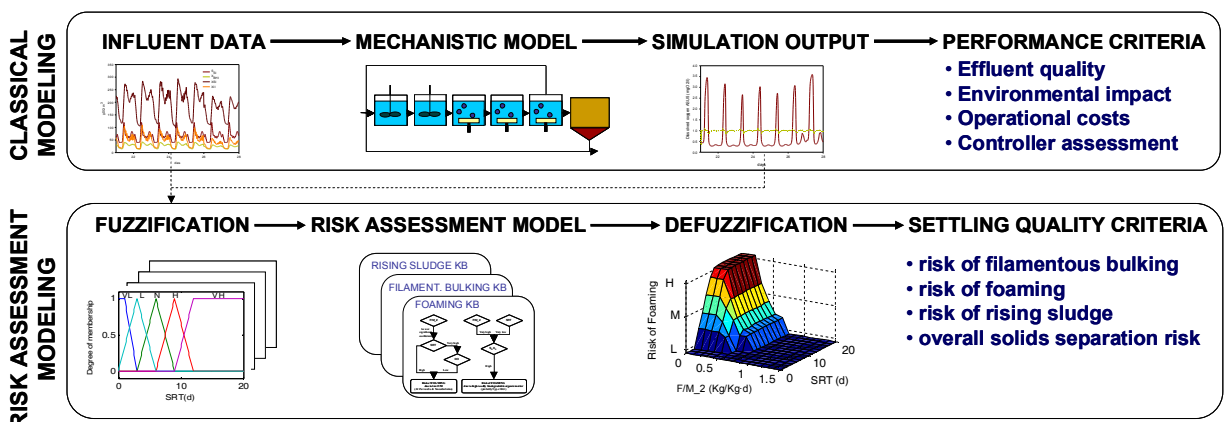


Figure 3.5] Relationship between the mechanistic model and the fuzzy knowledge base to estimate risk of microbiology-related solids separation problems.

The risk estimation involves three main steps:

- fuzzification;
- fuzzy inference of the risk through a Mamdani approach;
- defuzzification of the output variable.

Fuzzification is the process of converting values of numerical data into linguistic/qualitative descriptors or input fuzzy sets (i.e. low, high, etc.) by means of corresponding membership

functions. Membership functions are defined for each variable used as risk assessment indicators or symptoms in the decision trees (i.e. F/M_removed, F/M_fed, DO, SRT, BOD₅/N ratio, and S_s in this example). Triangular or pseudo-trapezoidal functions are used to define the membership functions. The limits of these membership functions as well as their degree of overlapping can be customized by the user according to the configuration and characteristics of the simulated activated sludge plant.

RESULTS I:

DEVELOPMENT OF A DECISION TREE
FOR THE INTEGRATED OPERATION
OF NUTRIENT REMOVAL MBRs
BASED ON SIMULATION STUDIES
AND EXPERT KNOWLEDGE

Redrafted from :

*Dalmau, M., Rodriguez-Roda, I., Ayesa, E., Odriozola, J., Sancho, L., Comas, J. (2013)
Development of a decision tree for the integrated operation of nutrient removal MBRs based on
simulation studies and expert knowledge. Chemical Engineering Journal 217, 174-18.*

4.1 OVERVIEW

The mathematical modelling and simulations of WWTPs have become very useful since their introduction in the mid-1990s as a support tool to select the appropriate design and operational parameters (Rivas et al. 2008). This is due, on one hand, to the publication of the well-known mathematical models for the different unit-processes, the Activated Sludge Model (ASM) family (Henze et al. 2000). On the other hand, the development of new computational platforms, with efficient methods for the numerical analysis of models (Copp 2002, Nopens et al. 2010) and the progressive elaboration of systematic procedures for the experimental calibration of the most common plant models and good modelling practices (Gillot et al. 2009) have also supported the rising use and implementation of models.

Although activated sludge models were initially developed to describe conventional activated sludge (CAS) processes, they have also been used in MBRs in the last decade. However, MBRs have different biological and filtration process specifications than CAS: higher control between sludge and hydraulic residence times, higher mixed liquor suspended solids concentrations and viscosity, accumulations of soluble microbial products (SMP) on the membrane (Tian et al. 2011b) and different aeration demands and performances, entailing the modification of standard ASM models (Naessens et al. 2012a). According to (Fenu et al. 2010a): modelling of biological processes in membrane bioreactor studies can be divided into two principal groups: (i) unmodified ASM and (ii) modified ASM to MBR processes. The unmodified models aim for good process descriptions, effluent characterizations, oxygen demand and sludge productions with standard ASM models and the adaptation of a few stoichiometric and kinetic parameters, mainly related to nitrification and denitrification, with respect to the default values, based on the experience (Fenu et al. 2010a, Monclús et al. 2010b). The modified models consider the MBR specificities in order to better describe the biokinetic models through the incorporation of additional compounds (SMP or exocellular polymeric substances, EPS) and/or processes (distinction between aerobic and membrane aeration). The use of these extended SMP-models increase the complexity of the model, while they do not improve the predictions for effluent characterization, sludge production or energy consumption. Besides, relations between SMP and fouling rates are still contradictories, e.g.: no correlation appears between SMP and the observed membrane fouling rate despite the efforts for modelling it (Fenu et al. 2011).

Apart from the biological processes, a filtration model is needed to describe the membrane operation. A filtration model aims to describe the permeate flux and pressure performance (transmembrane pressure (TMP) evolution, which is an indicator of fouling) over time. Most common ones are based on multi-series resistance models. For example, the resistance in series model in (Jiang 2007, Jiang et al. 2008) describes the fouling process as a progressive increase of the TMP, provoked by the material deposited on and inside the membrane pores. The accumulation of solid particles onto the filtering surface causes a rising resistance across the membrane. The total membrane resistance ($R_{tot}(t)$) is modelled by a sum of three different terms (Equation 4.1), two of them describing fouling mechanisms varying over the time ($R_c(t)$, $R_{irr}(t)$):

$$R_{tot}(t) = R_m + R_c(t) + R_{irr}(t) \quad (\text{Eq. 4.1})$$

where R_m denotes the constant intrinsic resistance of the membrane (m^{-1}), $R_c(t)$ is the cake resistance caused by the reversible accumulation of solids on the filtering surface during the filtration period (m^{-1}), and $R_{irr}(t)$ denotes the irreversible accumulation of solids (m^{-1}). Considering an incompressible filter cake, the cake resistance ($R_c(t)$) is modelled according to equation (Equation 4.2),

$$R_c(t) = \alpha \cdot (w(t)) / A_0 \quad (\text{Eq. 4.2})$$

where α represents the specific cake resistance according to cake thickness (m/g), $w(t)$ is the cake mass (g) related to the sludge solid concentration and to the flow rate of permeate, and A_0 is the surface area of the membrane (m^2). The irreversible fouling ($R_{irr}(t)$) is calculated as in the following:

$$R_{irr}(t) = R_m (A_0 / (A(t)) - 1) \quad (\text{Eq. 4.3})$$

where A indicates the irreversibly blocked membrane (m^2) depending on a pore blocking parameter, on a constant SMP concentration and on the flow rate of permeate over the time. Other similar approaches can be found in (Mannina et al. 2011).

Notwithstanding, several studies use model simplification by modelling an ideal membrane and ideal filtration and, thereby, disregarding the appearance and evolution of fouling (Maere et al. 2011, Verrecht et al. 2010a).

Model predictions are used by plant designers and operators to select the most appropriate combination of operational biological variables (aerobic dissolved oxygen set-point, recirculation flow rates, waste flow rates, etc.) to meet efficient removal and minimal cost requirements (Fang et al. 2011, Guerrero et al. 2012). In some papers, the operational variables for the filtration processes (membrane aeration, filtration flux or relaxation time) are also considered to ensure a good filtration performance, even though they are considered separately, i.e. independently from the biological processes. The study of both biological and filtration processes are a rising trend in this field (Mannina et al. 2011, Naessens et al. 2012b, Wu et al. 2012). Nevertheless, the above cited tools only considered descriptive parameters and none of them presented a real combined method which should couple with expert knowledge. The aim of the paper is the development of an operational decision tree for the integrated operation of MBRs for nutrient removal. In order to obtain it, a simulation-based study, based on sensitivity and scenario analysis and supplemented with expert process knowledge, was carried out for the identification of the most sensitive operational and their best set-point ranges/values for a UCT-MBR pilot plant.

4.2 MATERIALS AND METHODS

4.2.1 EXPERIMENTAL SYSTEM

The experimental pilot plant studied is an MBR with a UCT configuration able to biologically remove organic matter, nitrogen and phosphorous. Specifically, the UCT-MBR pilot plant is equipped with a primary settler and a screening system to prevent the entrance of large particles. The bioreactor has a total volume of 2.26 m³. It consists of an anaerobic (14% of the total volume), an anoxic (14%) and an aerobic compartment (23%), that are ultimately followed by a compartment (49%) with submerged microfiltration flat sheet membranes (Marti et al. 2011). The membranes used have a total membrane area of 8 m² (HF, Kubota, Japan), with a nominal pore size of 0.4 µm. A schematic representation of the pilot plant MBR is shown in Figure 4.1. The wastewater is obtained from the sewer that enters the full-scale wastewater treatment plant at Castell d'Aro (Catalonia, NE of Spain), where the MBR pilot plant is located.

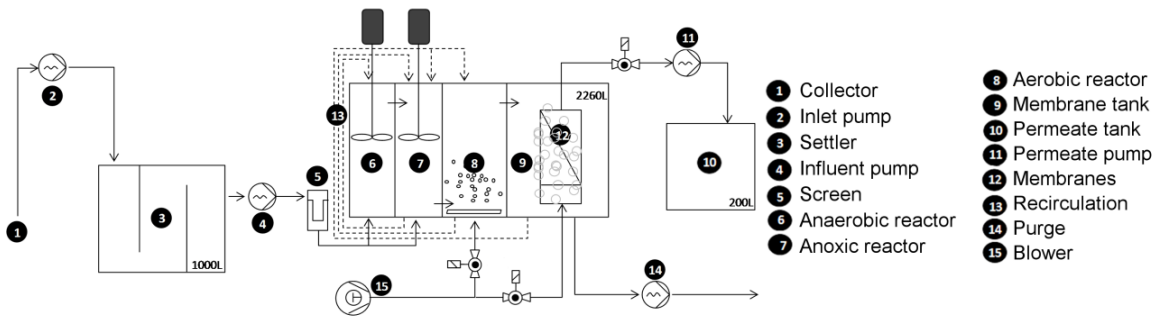


Figure 4.1| Schematic overview of the UCT-MBR pilot plant showing the different compartments, flow directions and main instruments and equipment.

4.2.2 MODEL-BASED METHODOLOGY FOR THE DEVELOPMENT OF OPERATIONAL DECISION TREES

A decision tree is explained as a representation of a causal chain of interactions from symptoms to problems, causes and solutions of a problem under evaluation (Comas et al. 2003). In this study, the evaluated problem is the proper operation of an UCT-MBR plant. Figure 4.2 illustrates the methodology followed for the development of a decision tree for the integrated operation.

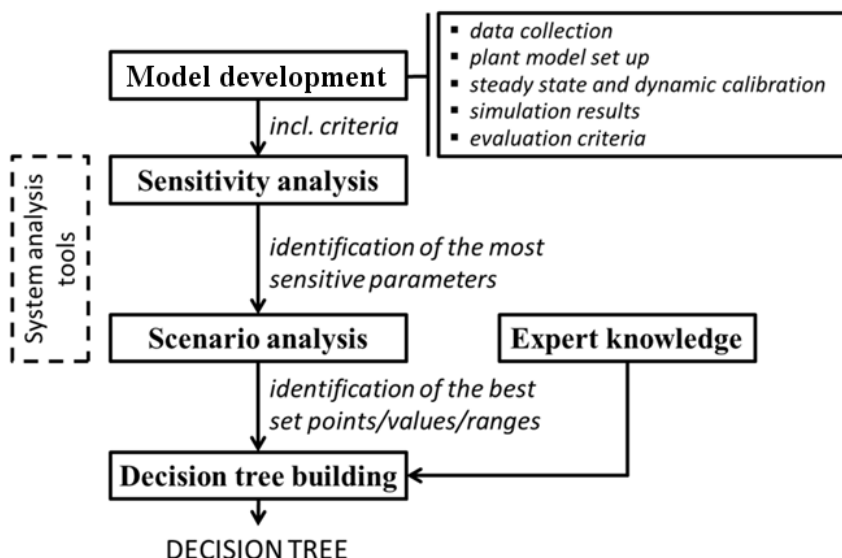


Figure 4.2| Methodology for the development of operational decision trees.

It is composed of 4 main steps (Figure 4.2): modeling, sensitivity and scenario analysis and building of the decision tree. The first step consists in setting up the plant model, as well as calibrating and validating it with experimental data. Once the plant is modeled, a local sensitive analysis (LSA) is performed in order to identify the most sensitive operational parameters (second step). Third, a scenario analysis (SCA) is carried out to find out the best set-point values/ranges for the most sensitive parameters (best operational parameter set). Finally, all the extracted information from the simulation results interpretation, supplemented with expert knowledge, allows developing the operational decision tree (fourth step).

4.2.3 MODEL DEVELOPMENT

The Unified Protocol developed by the IWA Good Modelling Practice task group (<http://www.iwahq.org/fc>) was adopted to develop the UCT-MBR pilot plant model and to carry out the corresponding simulations (Gillot et al. 2009). Focusing on the of UCT-MBR pilot plant (Figure 4.1), a simulation study of membrane bioreactors is carried out to identify the best control strategies for integrated MBR operation, updated with expert knowledge.

DATA COLLECTION AND RECONCILIATION

Data collection is divided in two main parts: the compilation of operational and design data and the characterization of influent wastewater. Table 4.1 summarizes the initial (or reference) operational conditions of the pilot plant.

To characterize influent wastewater for steady state and dynamic modelling, two experimental campaigns were held to measure influent chemical oxygen demand (COD), filtered COD, biochemical oxygen demand (BOD₅), ammonia (NH₄⁺-N), nitrates and nitrites (NO_x⁻-N), total Kjeldahl nitrogen (TKN-N), filtered TKN-N and phosphates (PO₄³⁻-P). From the SCADA data, membrane and anoxic mixed liquor suspended solids (MLSS), dissolved oxygen (DO) from the aerobic and the membrane tank, mixed liquor suspended solids (MLSS) concentrations from membrane tank, influent flow and transmembrane pressure (TMP) values were recorded every 10 seconds. During a seven-day experimental campaign (24-30 November 2010; first period), composite samples were taken every two hours. The steady state influent used for calibration

was based on average data of this period (Table 4.2). For the dynamic calibration, samples every two hours were used. During this period, the MBR pilot-plant was fed with municipal wastewater with a weekly average C:N:P ratio of 100: 16.76: 1.53. In order to validate the plant, the values of integrated samples from another 24-h campaign were used (15 January 2011; second period). In this case, the C:N:P ratio was 100: 10.91: 1.50. Effluent characterization was done following the same procedure.

Table 4.1 | Initial (reference) operational conditions of the pilot plant.

| Parameter | Units | Value |
|--|---|--|
| Influent flow | ($\text{m}^3 \cdot \text{d}^{-1}$) | 3800 (HRT \approx 0,6 d.) |
| Anoxic recirculation | (% of inflow) | 129 |
| Aerobic recirculation | (% of inflow) | 92 |
| External recirculation | (% of inflow) | 136 |
| Sludge retention time | (Days) | 22 days (waste flow rate: 1,8% inflow) |
| DO aerobic set-point | ($\text{mg O}_2 \cdot \text{L}^{-1}$) | 1.5 |
| $K_L a$ membranes | (d^{-1}) | 70 |
| Permeate; relaxation time | (minutes) | 9; 1 |
| Carbon dosage (pure commercial methanol) | ($\text{L} \cdot \text{d}^{-1}$) | 0 |

Analyses from influent and effluent were performed according to Standard Methods (APHA, 2005, APHA standard method 5220B for COD, APHA standard method 4500-Norg.B for TKN and APHA standard method B324 for NH_4^+ -N). The ammonia in the distillate was determined with a titrimetric method (Tritino 719S Metrohm, Herisau, Switzerland) using H_2SO_4 and a pH meter. Nitrites (NO_2^- -N), nitrates (NO_3^- -N) and phosphates (PO_4^{3-} -P) concentrations were analysed using ion chromatography (Metrohm 761-Compact; APHA standard method 4110B).

Table 4.2 | Average characteristics of the UCT-MBR pilot plant influent during the experimental campaign (after primary settler; daily samples during a week).

| Variable | Units | Average (SD) | | Variable | Units | Average (SD) | |
|-------------------------|---|--------------|--------|--|---------------------------------------|--------------|---------|
| BOD₅ | ($\text{mg BOD} \cdot \text{L}^{-1}$) | 115 | (36) | NH_4^+-N | ($\text{mg N} \cdot \text{L}^{-1}$) | 23.35 | (4.97) |
| BOD₃₀ | ($\text{mg} \cdot \text{L}^{-1}$) | 137 | (59) | NO_2^--N | ($\text{mg N} \cdot \text{L}^{-1}$) | 0.03 | (0.02) |
| COD | ($\text{mg COD} \cdot \text{L}^{-1}$) | 176 | (27) | NO_3^--N | ($\text{mg N} \cdot \text{L}^{-1}$) | 0.03 | (0.01) |
| COD_f | ($\text{mg COD} \cdot \text{L}^{-1}$) | 102 | (28) | PO_4^{3-}-P | ($\text{mg P} \cdot \text{L}^{-1}$) | 2.71 | (0.56) |
| TKN | ($\text{mg N} \cdot \text{L}^{-1}$) | 29.48 | (6.06) | TSS | ($\text{mg} \cdot \text{L}^{-1}$) | 42.26 | (12.00) |
| TKN_f | ($\text{mg N} \cdot \text{L}^{-1}$) | 25.81 | (6.62) | pH | - | 7.30 | (0.70) |

PLANT MODEL SET-UP

The conventional ASM2d (Henze et al. 1999) was chosen for this study as a biokinetic model for simultaneous C, N and P removal for both the steady state and dynamic simulation of the plant. Regarding the filtration processes, a filtration model based on a summation of in-series resistances was used (Jiang 2007). This model presents some limitations, such as the need to check the hydraulic balance across the membrane in every operational change (i.e. establishing filtration, backwashing and concentrate flux values, according to relaxation or backwashing times selected). In addition, cake resistance does not present any recuperation during the relaxation period. Finally, aeration in membranes is modelled in the same way as in conventional activated sludge units, considering fine bubbles instead of coarse bubbles. Hence, air scouring is not contemplated in the resistance model, and for this reason membrane aeration and fouling rates are not connected.

The plant was modelled and simulated using the modelling and simulation platform WEST® (mikebydhi.com) (Vanhooren et al. 2003).

STEADY STATE AND DYNAMIC CALIBRATION AND VALIDATION

The steady state calibration is run with an influent of constant flow and composition for 55 days, which corresponds to approximately three times the SRT (20 days), based on first period with a constant flow of 3800 m³·d⁻¹. The calibration was based on the dynamic influent profile of the seven-day experimental campaign (first period). The simulation was run with 40 days with steady state file, assuring constant nutrient removal profiles, followed by 15 days of dynamic influent, by repeating the seven characterized days twice. In addition, model validation was carried out on steady state data from the second period. The quantitative criteria to evaluate the simulation results are based on a mean square relative error (MSRE):

$$MSRE = 1/n \sum_{(i=1)}^n [[(y(t, \vartheta_{OBS})_i - (y(t, \vartheta_{SIM})_i)] / (y(t, \vartheta_{OBS})_i)]^2 \quad (\text{Eq. 4.4})$$

The MSRE is related to the corresponding observed or measured value at each time step. Minimum differences between the observed ($y(t, \vartheta_{OBS})$) and simulated ($y(t, \vartheta_{SIM})$) process variable values mean a good agreement between simulation and prediction (Hauduc et al. 2011). Taking

into account the purpose of the project, a MSRE below 15% is considered adequate. When necessary, modifications on default model parameters were done.

EVALUATION CRITERIA

Once the model is considered validated, several simulations were run following the same procedure: 40 days in steady state data followed by 15 days with dynamic influent. System analysis tools (section 2.4) are used to evaluate all the simulation runs, supporting the identification of best operational strategies. While BOD, COD, TSS, $\text{NH}_4^-\text{-N}$, $\text{NO}_x^-\text{-N}$ and $\text{PO}_4^{3-}\text{-P}$ are used as indicators for the efficiency of the nutrient removal processes, TMP is used as indicator of the fouling phenomena for the filtration processes. Besides, two additional global indicators, developed for the Benchmark Simulation Model (BSM, <http://www.BenchmarkWWTP.org>), are used to assess the impact of the operational strategies in MBRs: the effluent quality index (EQI) and the operational cost index (OCI)(Copp 2002, Nopens et al. 2010). In particular, the EQI combines the effluent loads of compounds that have a major influence on the quality of the receiving water. Specifically, the calculation of the EQI (in kg pollution units d^{-1}) is described in equation (4.5):

$$EQI = \frac{1}{1000(t_f - t_i)} \cdot \int_{t_f}^{t_i} [(PU_{TSS}(t) + PU_{COD}(t) + PU_{BOD}(t) + PU_{TKN}(t) + PU_{TKN}(t) + PU_{NO}(t) + PU_{Ptotal}(t)) \cdot Q_e(t) dt] \quad (\text{Eq. 4.5})$$

where t_i indicates the initial time and t_f the end day of the simulation period evaluated, $Q_e(t)$ is the effluent flow rate (L/d), and PU_k is the pollutant load of each component (mg/L) according to equation (4.6):

$$PU(t) = \beta_k \cdot C_k \quad (\text{Eq. 4.6})$$

where the weighting factors are $\beta_{TSS}=2$, $\beta_{BOD}=2$, $\beta_{TKN}=30$, $\beta_{NO}=10$ and $\beta_{PTOTAL}=50$, and C_k is the concentration of each composite variable (adapted from Nopens et al. 2010).

The operational cost index (OCI in kWh units d^{-1}) is estimated as follows (equation 4.7):

$$OCI = AE + PE + 3 \cdot SP + 3 \cdot EC + ME \quad (\text{Eq. 4.7})$$

This operational cost function is a weighted sum of aeration energy (AE), pumping energy (PE), sludge production (SP), external carbon addition (EC) and mixing energy (ME) (Copp 2002, Jeppsson 2005, Nopens et al. 2010). This equation estimates the energy costs of the system. Despite the effects of an elevated MLSS concentration on oxygen transfer and coarse bubble aeration are not taken into account in AE , for this study equation (4.7) is considered to adequately estimate the cost tendencies.

4.2.4 SYSTEM ANALYSIS TOOLS

SENSITIVITY ANALYSIS

Local sensitivity analysis (LSA) examines the impact of the modification of one operational parameter of the model on the resulting process variable, by applying a perturbation. The higher the difference between the perturbed and the default operational parameters (aerobic DO concentration, membrane K_La , anoxic recirculation, aerobic recirculation, filtration flux, relaxation time, carbon dosage and waste flow rate) related to each process variable (NH_4^+-N , $NO_3^- -N$, $PO_4^{3-}-P$, TMP), the higher the impact of the parameter on the model. All simulations were run using WEST® taking into account all adjusted parameters. Relative sensitivity function (RSF) evaluated the local sensitivity of the model. The RSF was calculated from the sensitivity function (SF) based on the finite forward difference method with a perturbation factor of $1 \cdot 10^{-7}$. The operational parameters were perturbed with an amount equal to $1 \cdot 10^{-7}$ for the SF calculation (equation 4.8):

$$SF = (y(t, \vartheta_j + \xi \vartheta_j) - y(t, \vartheta_j)) / (\xi \vartheta_j) \quad (\text{Eq. 4.8})$$

Where $y(t, \vartheta_j)$ represents the process variable, ϑ_j represents the operational parameter value and ξ the perturbation factor. The RSF calculation is based on equation 4.9:

$$RSF = (SF \cdot \vartheta) / (y(t, \vartheta)) \quad (\text{Eq. 4.9})$$

A value of $RSF < 0.25$ means a non-influential parameter. RSF values between 0.25 and 1 were moderately influential. Parameters extremely influential were considered when $RSF > 2$, according to Audenaert et al. (2011) and references therein.

SCENARIO ANALYSIS

To determine the best operational conditions a scenario analysis (SCA) has been carried out by experimentally varying values of the most sensitive parameters, i.e. those having the greatest impact on effluent quality and filtration process according to the previous LSA results. An SCA grid provides several operational conditions resulting from the different sensitive parameter combinations, leading to 768 different simulation runs. Each simulation of the SCA was run with an influent data file of 40 days in steady state followed by 15 days of dynamic influent. To find the best operational ranges for the most sensitive parameters, first a Pareto frontier considering the minimum TMP, EQI and OCI is applied. To reduce the extension of the front, a screening was performed by excluding all parameter sets which were worse than 50% of all sets for at least one criterion, thus focussing on the “compromise” area in the trade-off between performance criteria (Benedetti et al. 2009).

4.3 RESULTS AND DISCUSSION

4.3.1 MODEL CALIBRATION AND VALIDATION

An iterative evaluation of TMP and MLSS tendencies, as well as of COD, $\text{NH}_4^+\text{-N}$, $\text{NO}_3^-\text{-N}$ and $\text{PO}_4^{3-}\text{-P}$ profiles, was done based on a calibration method (Hulsbeek et al. 2002) and expert knowledge. Steady state calibration, using default parameters (Henze et al. 2000), resulted in low simulated nitrate and nitrite concentrations in the aerobic phases. For this reason, the nitrogen half saturation coefficient for autotrophs, K_{NH_4} , was increased from 1 up to $1.5 \text{ g N}\cdot\text{m}^{-3}$ due to the high ammonia concentration in the aerobic tanks. Moreover, as a second step, the reduction factor for denitrification ($\eta_{\text{NO}_3\text{-H}}$) was decreased from 0.8 to 0.4, diminishing the portion of the denitrifying biomass. With respect to the filtration model, all default parameters were used.

Table 4.3 illustrates that both simulated and experimental values denote an inefficient denitrification which is caused by an inadequate C:N:P ratio. Despite that, the estimated nutrient concentrations as well as the MLSS and TMP tendencies showed satisfactory values with respect to the experimental values. With the adjustment of K_{NH_4} and $\eta_{\text{NO}_3\text{-H}}$, dynamic calibration was also successful since experimental and simulated values presented a MSRE below 10% (Figure 4.3).

Table 4.3 | Steady state simulated values versus the experimental values.

| Parameter | Units | Experimental values | Simulated values | MSRE (%) |
|----------------------------------|-----------------------------|---------------------|------------------|----------|
| TMP | (mbar) | 170.66 | 188.01 | 1.03 |
| COD | (mg COD · L ⁻¹) | 31.50 | 31.02 | 0.02 |
| NH ₄ -N | (mg N · L ⁻¹) | 1.39 | 1.13 | 3.50 |
| NO _x ⁻ -N | (mg N · L ⁻¹) | 18.85 | 19.95 | 0.34 |
| PO ₄ ³⁻ -P | (mg P · L ⁻¹) | 3.31 | 3.01 | 0.82 |
| MLSS | (g · L ⁻¹) | 5.71 | 5.56 | 0.07 |

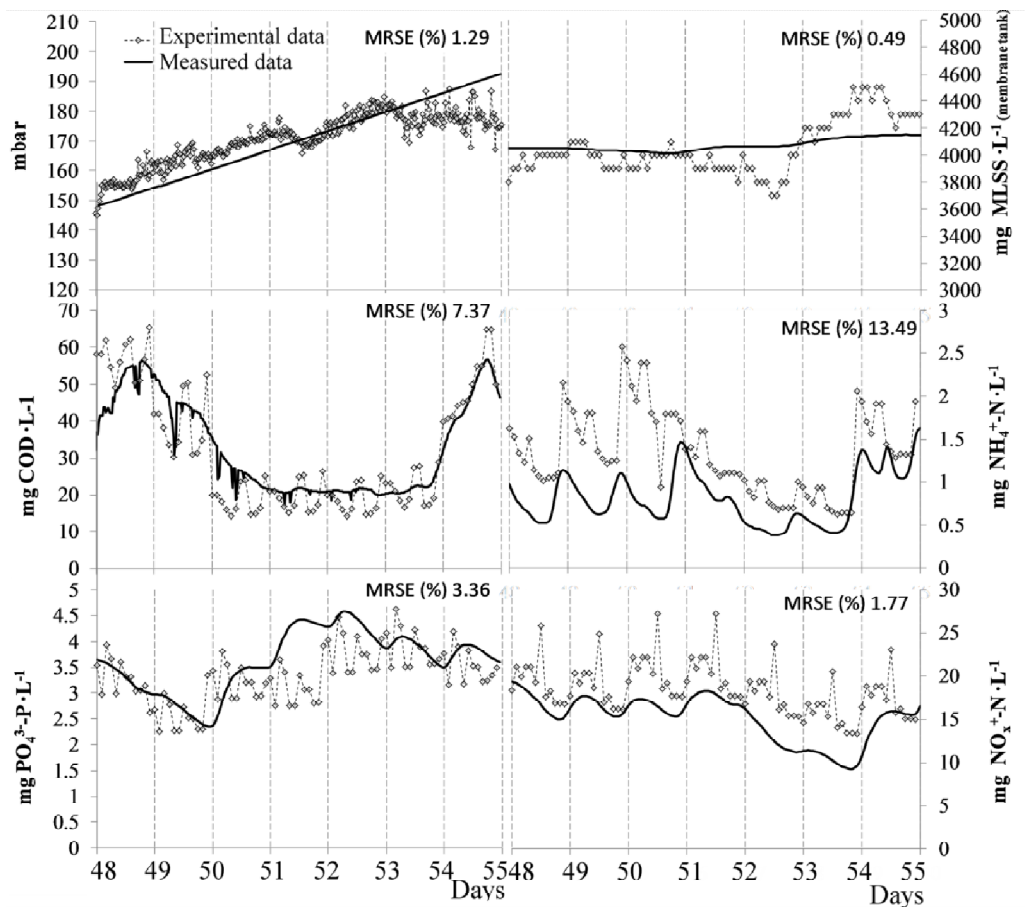


Figure 4.3| Relation between the dynamic simulation results (dark grey) and the experimental results (light grey), for TMP values at the end of each cycle (a), MLSS concentration into membrane compartment (b), and effluent concentrations for organic matter (c), ammonium (d), nitrates and nitrites (e) and phosphorous (f).

In order to validate the model, experimental data from the second period was used. Since the simulated values showed a mean percent error inferior to 10% with respect to the experimental values (i.e: 1.49% for TMP, 1.81% for membrane MLSS, 0.87 for COD, 2.10 for $\text{NH}_4^+\text{-N}$, 0.15 for $\text{NO}_3^-\text{-N}$ and 1.19 for $\text{PO}_4^{3-}\text{-P}$), the model was considered valid for reproducing process behaviour and for carrying out the local sensitivity analysis (LSA).

4.3.2 LOCAL SENSITIVITY ANALYSIS (LSA)

Taking into account all operational parameters that could alter not only the biological process but also the filtration processes (Table 4.1), a local sensitivity analysis was carried out (Figure 4.4). An external carbon addition was included to achieve good denitrification rates due to the low concentration of organic matter in the plant influent.

Regarding the filtration processes, only TMP was significantly sensitive to relaxation time, as well as filtration flux with the corresponding filtration time according to the mass balance (Figure 4.4a). From these observations it was concluded that an increase of relaxation time, implying and increase of filtration flux, leads to a TMP increase, in agreement with other studies (Wu et al. 2008).

In terms of EQI, specific sensitivity analyses over $\text{NH}_4^+\text{-N}$, $\text{NO}_3^-\text{-N}$ and $\text{PO}_4^{3-}\text{-P}$ effluent concentrations were run to determine the most sensitive operational parameters in the model ($\text{RSF} > 0.25$). DO set-point in the aerobic tank and aeration in the membrane tank were appreciated to be sensitive to $[\text{NH}_4^+\text{-N}]$ and $[\text{PO}_4^{3-}\text{-P}]$. These parameters were moderately influential to $[\text{NH}_4^+\text{-N}]$ in an indirect way ($\text{RSF} > 0.25$), meaning that higher aeration rates provoked better $[\text{NH}_4^+\text{-N}]$ removal. Contrary, these parameters presented a moderate direct influence on $[\text{PO}_4^{3-}\text{-P}]$. These relations could be explained by the fact that the quantity of returning nitrates to the anaerobic zone was increased due to high aeration. Nitrates give a competitive advantage to the heterotrophic bacteria in front of PAOs, which had slower growth using the same substrate. It is remarkable that aerobic recirculation presented an indirect proportional relation to $[\text{NO}_3^-\text{-N}]$.

Decreasing this value exerted a higher effluent $[\text{NO}_3^-\text{-N}]$ concentration. Carbon dosage was found to be important, as seen in $[\text{PO}_4^{3-}\text{-P}]$ and $[\text{NO}_3^-\text{-N}]$ RSF values. Due to the low C: N: P ratio in the influent, an external carbon dosage increases the denitrification yield. In addition, carbon dosage

enhanced phosphorus release phase, extending the phosphorus removal efficiency in both anoxic and aerobic zones (Figure 4.4b - d).

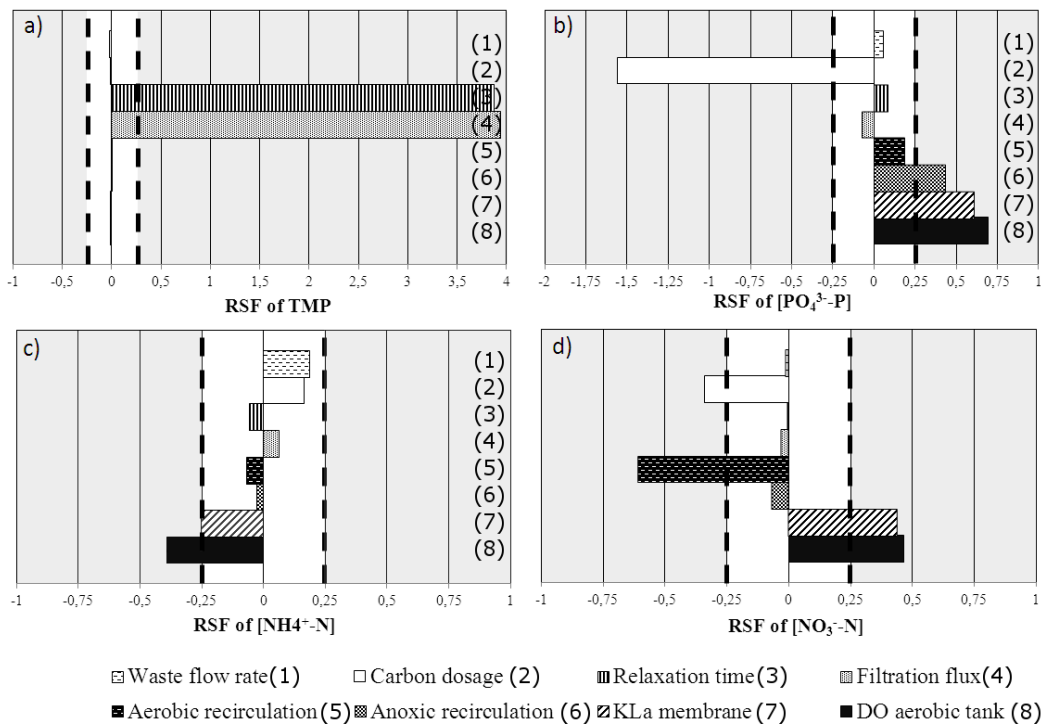


Figure 4.4 | Results obtained from the LSA, showing the most sensitive parameters related to the filtration process based on TMP (a) and effluent quality (b).

As a summary, the LSA results showed that aerobic recirculation, membrane aeration, relaxation time, DO aerobic set-point and carbon dosage are the most sensitive parameters, i.e. they have the greatest impact on effluent quality, OCI and TMP. Similar results were obtained by (Mannina et al. 2011), who distinguished two groups of sensitive operational parameters: one related to the biological processes and the other related to the physical filtration process. In agreement with our results, they also pointed out that the most sensitive operational parameters for biological processes did not significantly affect the TMP. This is clearly a strong drawback of the model since in practice operational parameters for biological processes can have substantial impact on TMP, e.g.: low levels of DO lower the cell hydrophobicity and thus causes floc deterioration and stronger interactions with the typically hydrophilic membrane, causing higher fouling (Drews 2010).

4.3.3 SCENARIO ANALYSIS

The scenario analysis was carried out with an adequate C:N:P relation in the influent. Thus an external dose of methanol was needed to increase the readily biodegradable organic substrate concentration (S_F , mg COD·L⁻¹) of the influent. The sludge retention time (SRT) was set in all the simulations as the reference one (20 days), in order to ensure nitrification and denitrification processes. An SCA grid providing several operational conditions was defined as a result of the combination of different set-point /values/ranges for the five more sensitive parameters (Table 4.4). These operational conditions are given by varying (i) aerobic recirculation, from 65 to 197% of influent; (ii) membrane aeration, with K_{La} between 50 and 90d⁻¹; (iii) relaxation time, tested on 0, 1 and 2 minutes; (iv) aerobic set-point of dissolved oxygen, between 0.5, 1, 1.5 and 2 mg O₂·L⁻¹, and finally, (v) carbon dosage, with an addition of 0.15, 0.17, 0.2 and 0.25 L CH₃COOH·d⁻¹. The combination of all these set-point values results in 768 different scenarios or simulation runs (Figure 4.5a).

Table 4.4 | Scenario analysis grid, showing the studied set-points for each sensitive parameter.

| Parameter | Studied values | | | | Units |
|-------------------------------------|----------------|------|-----|------|---------------------------------------|
| Aerobic recirculation | 65 | 92 | 130 | 197 | (% of the inflow) |
| Membrane k_{La} | 50 | 65 | 75 | 90 | (d ⁻¹) |
| Relaxation time | 0 | 1 | | 2 | (minutes) |
| DO aerobic set-point | 0.5 | 1 | 1.5 | 2 | (mg O ₂ ·L ⁻¹) |
| Carbon dosage | 0.15 | 0.17 | 0.2 | 0.25 | (L MeOH·d ⁻¹) |

To select the best values of the sensitive operational parameter among the 768 simulations run, the Pareto function was applied based on low OCI, EQI and TMP. The screening condensed the Pareto-optimal parameter sets from 48 to 10 (Figure 4.5b-c).

The study of the 10 optimal operational parameter set (Table 4.5) led to identifying that the best operational conditions involve working with a relaxation time of 0 minutes, a minimum aeration in the aerobic reactor (0.5 mg·L⁻¹) and in the membrane tank (50-75 d⁻¹ of K_{La} values), with the reference SRT (20 days). It must be emphasized that a minimum relaxation time (0 min.) is selected as the best option to maximize permeate production, and thus permeability, because the filtration model does not consider a significant recovery of TMP during relaxation. Since this is not a realistic situation, some of the 48 good operational conditions involving a relaxation time

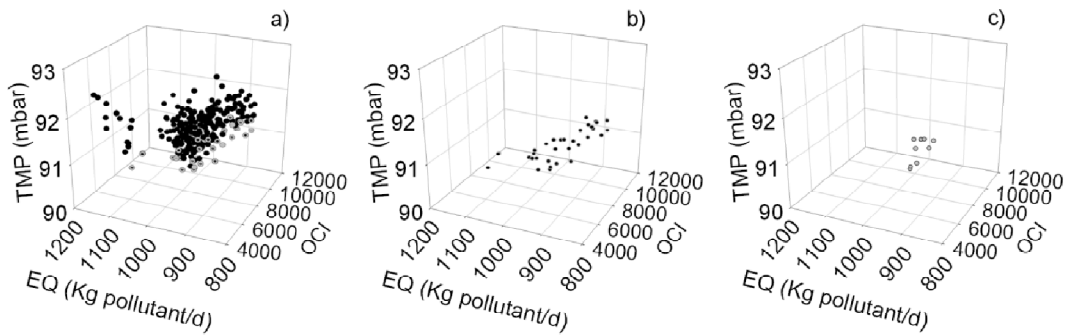


Figure 4.5 | Outputs of the scenario analysis in terms of operational costs (OCI), effluent quality and TMP: (a) represents all the set-point combinations (only strategies using relaxation time equal to 0), highlighting Pareto results; (b) only the 48 solutions corresponding to the Pareto front; and (c) the 10 best configurations after the screening method.

of 1 minute, for example, should be considered for practical implementation. Other modelling studies did not consider either the relaxation time or the filtration time as operational set-points (Maere et al. 2011, Verrecht et al. 2010b).

Table 4.5 |The best 10 operational parameters set obtained with the Pareto front and the screening over the SCA, allowing minor TMP, EQ and OCI, all of them fulfilling the EU Directive (91/271/CEE).

| | | | | | | | | | | | | |
|------------------------|--------------------------------------|-----------------------|---------|---------|---------|---------|---------|---------|---------|---------|---------|---------|
| Operational parameters | Relaxation time | (min) | 0.00 | 0.00 | 0.00 | 0.00 | 0.00 | 0.00 | 0.00 | 0.00 | 0.00 | 0.00 |
| | Filtration time | (min) | 10.00 | 10.00 | 10.00 | 10.00 | 10.00 | 10.00 | 10.00 | 10.00 | 10.00 | 10.00 |
| | Filtration flux | ($Lm^{-2}h^{-1}$) | 19.42 | 19.42 | 19.42 | 19.42 | 19.42 | 19.42 | 19.42 | 19.42 | 19.42 | 19.42 |
| | DO aerobic | ($mg \cdot L^{-1}$) | 0.50 | 0.50 | 0.50 | 0.50 | 0.50 | 0.50 | 1.00 | 0.50 | 0.50 | 0.50 |
| | K_{La} membranes | (d^{-1}) | 75.00 | 75.00 | 65.00 | 65.00 | 65.00 | 75.00 | 50.00 | 65.00 | 65.00 | 75.00 |
| | Aerobic recirculation | % of the inflow | 65.00 | 65.00 | 92.00 | 92.00 | 92.00 | 92.00 | 130.00 | 13.00 | 197.00 | 197.00 |
| | Methanol flow | ($L \cdot d^{-1}$) | 0.15 | 0.17 | 0.15 | 0.17 | 0.20 | 0.17 | 0.17 | 0.15 | 0.17 | 0.17 |
| Process variables | NH₄-N | ($mg \cdot L^{-1}$) | 2.85 | 2.84 | 3.31 | 3.35 | 3.54 | 2.89 | 3.62 | 3.22 | 3.20 | 2.89 |
| | NO_x⁻-N | ($mg \cdot L^{-1}$) | 6.58 | 6.42 | 5.70 | 5.25 | 4.98 | 6.50 | 4.39 | 5.69 | 5.28 | 6.14 |
| | PO₄³⁻-P | ($mg \cdot L^{-1}$) | 0.65 | 0.55 | 0.62 | 0.49 | 0.40 | 0.58 | 0.59 | 0.73 | 0.57 | 0.65 |
| | TMP | (mbar) | 91.07 | 91.15 | 91.49 | 91.16 | 91.73 | 91.44 | 91.35 | 91.31 | 91.11 | 91.19 |
| | EQI | ($kg \cdot d^{-1}$) | 932.22 | 907.79 | 948.69 | 912.56 | 908.31 | 922.29 | 926.84 | 962.32 | 913.21 | 924.65 |
| | OCI | -- | 5922.48 | 5984.52 | 5348.52 | 5493.95 | 5648.18 | 5941.02 | 6030.43 | 5320.11 | 5467.52 | 6050.57 |

Regarding aeration, the best operational condition involve a low DO set-point in the aerobic compartment and minimal values for K_{La} in the membrane compartment, enabling sufficient nitrification rates between aerobic and membrane compartments and ensuring membrane air-

scouring while reducing aeration costs and a recycling stream with high dissolved oxygen concentrations. A direct correlation between aeration in aerobic and membrane compartments and operational costs has also been found in full-scale MBRs elsewhere (Fenu et al. 2010b, Ferrero et al. 2011b). Since nitrification is partly carried out in the membrane compartment, the dissolved oxygen set-point in the aerobic compartment can be lowered. These conditions will also favour good denitrification rates and, consequently, phosphorous accumulating organisms as well. Finally, the SRT value selected is certainly enough for the development of nitrifying biomass.

In order to study the overall impact of all operational parameters on TMP, nutrient removal and costs, a global sensitivity analysis was carried out using standard regression coefficients (SRC) to identify their influences (Saltelli et al. 2004). A summary of the results is shown in Table 4.6.

Table 4.6 | Global sensitivity analysis results. If the coefficients of determination are $R^2 > 0.7$, SRC results are reliable sensitive measures (marked in bold). The higher the absolute values of the SRC, the stronger the influence of the corresponding parameter (θ_j) on the variable ($y(t, \theta_j)$).

| | Ammonium | Nitrates/ Nitrites | Phosphorous | TMP | EQ | OCI |
|-------------------|-----------------|---------------------------|--------------------|-------------|-----------|-------------|
| | R^2 | R^2 | R^2 | R^2 | R^2 | R^2 |
| | 0.29 | 0.86 | 0.84 | 0.96 | 0.42 | 0.93 |
| Relaxation time | -0.15 | -0.04 | -0.16 | 0.63 | 0.15 | 0.01 |
| Aerobic recycle | -0.02 | 0.20 | -0.06 | 0.00 | 0.13 | 0.02 |
| DO aerobic | 0.14 | 0.40 | 0.39 | 0.00 | 0.12 | 0.71 |
| $K_L a$ membranes | -0.26 | 0.61 | 0.25 | 0.00 | 0.12 | 0.57 |
| Methanol flow | -0.01 | -0.33 | -0.57 | 0.01 | -0.59 | 0.71 |

To sum up the main global sensitivity analysis results, the most significant parameters were related to costs, and they were ranked as aerobic DO set-point, methanol flow and membrane aeration. The significance of aeration in cost is well known (Ferrero et al. 2011b, Maere et al. 2011, Verrecht et al. 2010b), as well as an external contribution of external carbon dosage (appreciated in the OCI calculation). Increasing aeration or carbon dosage will cause higher operational cost, in agreement with the expectations arising from expert process knowledge.

Secondly, the most influential parameter affecting TMP was relaxation time.

4.3.4 OPERATIONAL DECISION TREE FOR THE INTEGRATED OPERATION OF MBRs

Based on the interpretation of the simulation results and complemented with expert and empirical knowledge, a decision tree for the integrated operation of both filtration and biological processes in any UCT MBRs has been developed (Figure 4.6). Even though many efforts have been made to match models with reality, they still present several limitations. Thus coupling of expert knowledge with simulation results is necessary to reach consistent rules for the integrated operation of MBRs. Expert knowledge involves human expertise acquired with MBR operation, as well as upgraded with empirical knowledge based on scientific research.

The developed decision tree consecutively evaluates five process variables: TMP, related to the filtration process, and $\text{NH}_4^+\text{-N}$, $\text{NO}_3^-\text{-N}$, $\text{PO}_4^{3-}\text{-P}$ concentrations related to the biological process. In addition, operational costs are included in the study as process variable. Sensitivity and scenario analysis results have been used for the tree development, supplemented by expert knowledge when necessary. For this reason, some restrictions were presented during the decision tree development and expert knowledge prevailed over simulating results when a conflict was detected. Biological and filtration processes are considered of paramount importance for experts since complying with them is essential before looking for potential cost savings. In addition, in order to guarantee an efficient nutrient removal, it was necessary to assess $\text{NH}_4^+\text{-N}$, $\text{NO}_3^-\text{-N}$, $\text{PO}_4^{3-}\text{-P}$ concentrations in this order, and consider carbon dosage as the last option for reaching biological nutrient removal. Analysing simulation results (point 4.3.3), several parameters are cost sensitive, and therefore they were considered in the last branch.

Taking into account these boundaries and according to the sensitivity analysis, the filtration process was presented as the first step of the tree, with relaxation time as the most sensitive parameter for TMP. Thus, the first step is focused on the control of the filtration process. In order to consider possible permeate flux fluctuations, permeability (K) has been selected instead of TMP in the decision tree. For these reason, the first action is checking for the permeability trend. In case of bad permeability, lowering the filtration flux is the subsequent action. Taking into account that filtration flux is related to relaxation time (it could be considered that the operation with higher fluxes implies higher relaxation times), lowering filtration flux resulted on an improvement of permeability trends, with the corresponding relaxation times. Consequently, other studies revealed that fouling dependence is higher on the applied instantaneous flux than

on filtration modes itself (Metzger et al. 2007). Taking into account expert process knowledge, membrane aeration is considered as an important factor to reduce TMP (LSA did not show any correlation because the filtration model does not consider air scouring). Consequently, checking permeability trends to reduce air-scouring costs while maintaining the correct filtration performance (Maere et al. 2011, Verrecht et al. 2010b) was presented as the following step in the decision tree.

If the control of filtration performance and the minimization of fouling affect biological processes, the following three steps are explored to ensure adequate nitrification, denitrification and phosphorous removal. According to expert knowledge and LSA results, the first action is to verify DO set-points of aerobic reactor needed for the conversion of ammonia into nitrates or nitrites. If the concentration of ammonia is higher than desired, it is important to check if the SRT is higher than the minimum required for nitrification.

The third level consists of achieving adequate nitrate and nitrite levels. Regarding to LSA results, the first control actions is focused on aerobic recirculation, according to whether DO is transported or not by recirculation from aerobic to anoxic tanks. If denitrification is not achieved, attention should be paid to aerobic aeration, and membrane aeration in second term, decreasing both when nitrate and nitrite concentration are too high. Eventually, if there are no other possible actions, this branch ends with the addition of organic matter.

The last branch is focused on phosphorous removal efficiency. To ensure a minimum level of phosphorous concentration, the most sensitive parameters (aerobic and membrane aeration) are taken into account. From a process engineering point of view, recirculation from anoxic played an important role on phosphorous removal. Thus, according to LSA, it can be considered a parameter to take it into consideration. Once again, the last action must be the external carbon dosage.

Once the filtration and nutrient removal processes are successfully achieved, then the costs can be reduced. For this reason, the closing branch of the tree is based on costs. As illustrated by the simulation results, aeration is the most important factor accordingly with expert knowledge and literature (Fenu et al. 2010b, Ferrero et al. 2011b, Verrecht et al. 2010b). In this case, aerobic aeration has a major effect on costs. Hence, cost reduction is focused on aerobic aeration.

4.4 CONCLUSIONS

- The combination of ASM2d as biokinetic model and an in-series resistance model as filtration model has provided a correct description of transmembrane pressure, nutrient removal and mixed liquor suspended solids in an UCT-MBR pilot plant.
- A local sensitivity analysis enabled to find the most sensitive parameters for the integrated operation of nutrient removal and filtration process of the MBRs, to be further examined via scenario analysis: aerobic recirculation, aeration in the membrane and aerobic tank and waste flow rate, all of them affecting the nutrient and organic matter removal, while the relaxation time and the filtration flux were the most sensitive parameters affecting the filtration performance.
- A Pareto front containing the best 48 operational conditions was found when examining the scenario analysis results. Then, in order to find the 10 best combinations of set-points among them, a screening method was applied.
- Simulation studies not only provided more information about the most sensitive parameters but also about the best set-point values/ranges, achieving a good relation with costs, effluent quality and lower TMP.
- Even though many efforts have been made to couple models to reality, they present several limitations. So the use of expert knowledge for simulation results interpretation is still essential.
- Based on the simulation results and expert knowledge, a decision tree for the integrated operation of both biological and filtration processes has been developed. The sensitivity analysis demonstrated the stronger relationship between relaxation time and filtration flux with TMP, gathered in the decision tree. However, due to model limitations, operational parameters (e.g. aerobic aeration) for biological processes may strongly affect TMP and it was not captured in the model results. Nutrient removal process variables presented higher dependence on biological and membrane aeration. Consequently, the first branches of the operational tree presented that relevant operational parameter whereas aerobic recirculation seemed to be important in denitrification. In addition, carbon dosage was very influential for denitrification and phosphorous removal. Both actions were used for decision tree development.

Operational costs were mainly influenced by aeration and carbon dosage, in agreement with engineering knowledge. The last branch of the tree was based on operational cost due to the relevancy of the biological nutrient removal process and filtration performance.

Further studies will concentrate on experimental verification of some relationships of the decision tree, e.g. between air scouring and fouling reduction in order to improve the filtration model.

RESULTS II:

**MODEL-BASED OPTIMISATION
OF A FULL-SCALE HYBRID MBR**

Redrafted from:

Dalmau M., Maere, T., Nopens, I., Rodriguez-Roda; I., Comas, J.

Model-based optimisation of a full-scale hybrid MBR

Submitted

5.1 OVERVIEW

MBRs becomes a rising choice in WWTPs, not only standalone, but also as an option to upgrade existing WWTP (Kraume and Drews 2010). That is why in the last decades a combination of conventional activated sludge (CAS) wastewater treatment technology with membrane filtration, known as hybrid MBR, have been taken into consideration (Bixio et al. 2008, Brepols et al. 2008). They mainly result from retrofitting conventional plants with strict effluent limits and little or no place for expansion or when a high quality effluent is needed for water reuse purposes. Flow treated by CAS generates lower effluent quality in terms of suspended solids, bacteria and viruses regarding standalone MBRs (Marti et al. 2011). However, several advantages of hybrid MBRs over standalone MBRs have been reported; effluent can either be produced through the secondary settlers or by filtration, which allows a reduction in the required membrane area (and thus costs) since peak flows can be treated by the settlers (Krzeminski et al. 2012b). Krzeminski et al. (2012b) identified a decrease of 17% in operational cost in hybrid concepts compared to standalone. However, to achieve the same effluent quality standalone MBRs are more efficient. Generally very little is known about the design and operation of hybrid MBRs.

Evaluation of different energy-saving strategies has already pointed out in several MBRs with different configurations. In all cases hydraulic load was found to be the main determinant factor for the energy consumption, which was highly dependent on membrane capacity usage. Specifically in hybrid MBRs, buffering the influent flow and optimization of both biological aeration and membrane air-scouring, reduced the specific energy demand by 14% (Gabarrón et al. 2014). The energy efficiency of an MBR is driven by the hydraulic utilization of the membranes and can be improved mainly by implementation of flow equalization, new aeration strategies and adjusting operational settings to incoming flow (Krzeminski et al. 2012b). Despite that fact, none of the improvements reported took into account the operational flexibility in hybrid MBRs, since in most of the full-scale facilities the operation is restricted to the manufacturers guarantee. Thus, there is a wide range of improvement in that field.

Mathematical modeling could be useful tool to identify the best operational strategies (Rivas et al. 2008), regarding effluent quality and costs in MBRs (Maere et al. 2011). There exist some examples focused on energy-saving strategies in MBRs at pilot-scale (Mannina and Cosenza 2013) or in full-scale standalone MBRs (Verrecht et al. 2010a). Regarding hybrid-MBRs, despite the

Embargoed until publication

Dalmau M., Maere, T., Nopens, I., Rodriguez-Roda, I., Comas, J. "Model-based optimisation of a full-scale hybrid MBR". *Submitted*

RESULTS III:

MODELLING MBR FOULING WITH DETERMINISTIC AND DATA-DRIVEN MODELS

Redrafted from:

Dalmau M., Atanasova N., Gabarrón S., Rodríguez-Roda I., Comas J.

Modelling MBR fouling with deterministic and data-driven models.

Chemical Engineering Journal, accepted for publication.

6.1 OVERVIEW

MBRs may have high operating energy requirements (Verrecht et al. 2010b), specifically to prevent fouling. The main MBR foulants are colloidal, dissolved and particulate substances excreted by microorganisms present in the biomass, including bound extracellular polymeric substances (EPS) and soluble microbial products (SMP) (Meng et al. 2009). Due to the complexity of the biological processes and membrane filtration phenomena taking place in MBRs, it is difficult to determine the optimal way to operate an MBR. For this reason, full scale MBRs are commonly run conservatively to avoid operational problems. Mathematical models can help to identify the best operating strategies through model-based optimisation (Verrecht et al. 2010a). However, a widely accepted general mathematical model able to cover all system variables does not yet exist (Naessens et al. 2012a). Although the biological processes have been described, fouling development within the filtration component is still under discussion. There are some successful efforts to model the biological processes occurring in MBRs that rely on activated sludge models (ASM) (Maere et al. 2011). In some cases, ASM-like models have been extended to include additional state variables to incorporate fouling descriptors (e.g., SMP), with limited success (Fenu et al. 2010a). Other models have focused more on the understanding of the physical processes to properly describe membrane aeration (Maere et al. 2011) and to determine operating costs for ideal membranes (Verrecht et al. 2010a) or optimal energy-saving strategies regarding fouling (Mannina and Cosenza 2013). However, the complexity of fouling, which is influenced by several factors and the lack of consensus on a specific fouling indicator (Drews 2010) increase the difficulty of modelling the filtration process. Overall, none of the *deterministic* approaches for modelling fouling have led to a widely accepted general model that has been validated at different scales and under operating conditions. Rather, deterministic models are only applicable in very specific cases. Empirical data and expert knowledge have also been applied to control fouling strategies (Ferrero et al. 2012), but the complexity of the process makes those systems vulnerable.

When there is a lack of fundamental knowledge about a specific process (e.g., fouling development) but a significant amount of experimental and historical data is present, data-driven models can be a good option. Currently, successful data-driven MBR models include chemometric approaches that have been used to predict transmembrane pressure (TMP) (Kaneko and Funatsu 2013) and chemical cleaning intervals (Kim et al. 2011) as linear regressions.

TMP has also been used to describe fouling behaviour by means of principal component analysis and fuzzy clustering (Maere et al. 2012). Furthermore, artificial neural networks have been adopted to predict TMP in ultrafiltration membranes for water treatment (Delgrange et al. 1998) or to predict the fouling behaviour of microfiltration membranes under constant flux conditions (Liu et al. 2009). A statistical approach linking long-term and short-term permeability evolution with operating variables in full-scale MBRs, with flux as the main factor affecting long-term fouling followed by temperature, food to microorganisms and sludge retention time, was also studied (Philippe et al. 2013). Other recent studies used 2-D fluorescence monitoring data to describe TMP, the effluent quality descriptors and biomass concentrations (Galinha et al. 2011, Galinha et al. 2012). However, the comparison of a deterministic model and a data-driven model to describe filtration can help to overcome the limitations of using a single model. Such a study would determine which approach better describes filtration processes and in which operating conditions.

The objective of this chapter is to illustrate the comparison of deterministic and data-driven models for the TMP description in MBRs and the utility of both approaches for a more reliable description of fouling. To that aim, two different models were developed and evaluated. The accuracy of both models was assessed and compared using experimental data from an industrial scale MBR pilot plant over 1.5 years of operation under different conditions.

6.2 MATERIALS AND METHODS

6.2.1 EXPERIMENTAL SYSTEM

The experimental pilot plant was an MBR with a University of Cape Town (UCT) configuration able to biologically remove organic matter, nitrogen and phosphorous. The influent wastewater ($4.25 \text{ m}^3 \cdot \text{d}^{-1}$) was obtained directly from the full-scale wastewater treatment plant sewer at Castell d'Aro (Catalonia, Spain), where the MBR pilot plant is located. Specifically, the UCT-MBR pilot plant was equipped with a primary settler and a screening system to prevent the entrance of large particles. The bioreactor had a total volume of 2.26 m^3 divided into anaerobic (14% of the total volume), anoxic (14%) and aerobic (23%) compartments and a compartment with

submerged microfiltration flat sheet membranes (49%). The membranes had a total membrane area of 8 m^2 (HF, Kubota, Japan), with a nominal pore size of $0.4 \mu\text{m}$, working at 9 minutes of filtration and 1 minute of relaxation. The permeate production for the whole period ranged from $120 \text{ L}\cdot\text{h}^{-1}$ to $200 \text{ L}\cdot\text{h}^{-1}$ ($15\text{-}25 \text{ L}\cdot\text{m}^{-2}\cdot\text{h}^{-1}$, LMH), and membrane aeration for the whole period fluctuated between 6 and $12 \text{ m}^3\cdot\text{h}^{-1}$. The UCT configuration pilot plant was operated at an average sludge retention time of $25\pm 6 \text{ d}$ and a hydraulic retention time of $0.50\pm 0.05 \text{ d}$. The suspended solids concentration in the membrane tank ranged from 3.55 to $11.85 \text{ g}\cdot\text{L}^{-1}$ and $1.27\text{-}4.08 \text{ g}\cdot\text{L}^{-1}$ in the anaerobic reactor. The plant was equipped with pH, OD, temperature and oxidation reduction potential (ORP) probes located in the aerobic reactor and flow sensors and solids concentration probes in the anaerobic and membrane compartments. A schematic representation of the pilot plant MBR is shown in Figure 6.1. More detailed information about the MBR influent and its configuration can be found in (Dalmau et al. 2013, Monclús et al. 2012).

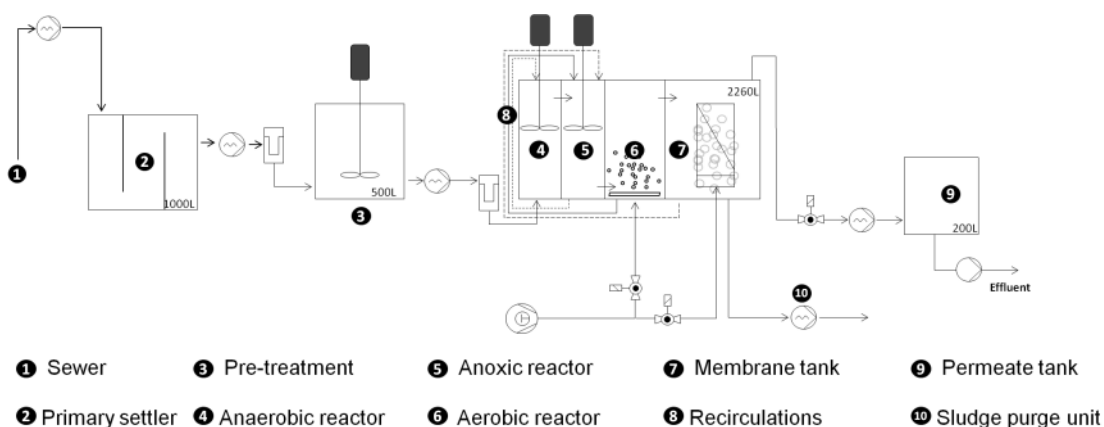


Figure 6.1| Schematic of the configuration of the MBR pilot-scale plant.

6.2.2 MODEL DEVELOPMENT AND EVALUATION

In the deterministic model, the TMP is described by differential equations to explain the physical, chemical and biological processes taking place in the system. In the data-driven modelling approach TMP is described by learning the model structure from compiled measured data only,

without previous introduction of any knowledge about the system in the modelling procedure. Although deterministic and data-driven models are conceptually different, the same data collection and processing were used to establish both models. The deterministic model was calibrated by adjusting the biological and physical parameters using a specified data set and was subsequently validated using a different data set, according to Rieger et al. (2012). Regarding the data-driven model, its structure was 'discovered' automatically from the measured data, thus there was no calibration. Validation was performed using a cross-validation method. The deterministic model was evaluated using local sensitivity analysis and by comparing the accuracy of the simulated and experimental TMP values.

6.2.3 DATA COLLECTION AND PROCESSING

On-line data from operating variables and parameters related to the filtration and biological processes as well as the biomass characteristics were gathered every ten seconds for 1.5 years (462 days). Data include the TMP, temperature, ORP, mixed liquor suspended solids concentration of the membrane compartment (MLSS_m) and mixed liquor suspended solids concentration of the anaerobic tank (MLSS_{ana}), dissolved oxygen (DO) in the aerobic reactor, waste flow rate, membrane air-scouring flow rate and permeate flow rate.

In addition, integrated grab samples were taken twice per week from the influent, permeate and each sludge compartment (anaerobic, anoxic, aerobic and membranes). From the influent and permeate, chemical oxygen demand (COD); total Kjeldahl nitrogen (TKN); and $\text{NH}_4^+\text{-N}$, $\text{NO}_3^-\text{-N}$, $\text{NO}_2^-\text{-N}$, $\text{PO}_4^{3-}\text{-P}$ concentrations were measured (APHA 2005) (Table 6.2). The total suspended solids (MLSS) from the influent and from the sludge of each compartment as well as the SMP concentrations from the membrane tank were also analysed. The SMP characterisation was based on the analysis of soluble microbial products (SMP), the protein analysis and the polysaccharide fractions (Dubois et al. 1956, Frølund et al. 1996). Finally, the operating parameters and chemical cleanings performed during the study were taken into account. Chemical cleanings were identified to explain the increase in TMP and the consequent decrease in pressure after cleaning.

Once all the data were collected, they were processed to filter outliers and remove periods with atypical behaviour, i.e., operational failures, according to Comas et al. (2010). Daily averages of the 10 second on-line measurements were used to describe the TMP performance, providing adequate information and avoiding noise. An extrapolation of the grab sample results was performed for days when information was not available, by considering the same value until the next analysis was performed.

The time between each chemical cleaning was considered a different experimental period, yielding 9 different periods with different operating conditions (Table 6.2). During periods 4 (P4) and 5 (P5), an intensive experimental campaign was performed to characterise the influent of the plant (full details in (Dalmau et al. 2013)).

6.2.4 MODEL SET UP

DETERMINISTIC MODEL

ASM2d (Henze et al. 1999) was selected as the biochemical model for simultaneous C, N and P removal for both the steady state and dynamic simulations of the plant. For the filtration component, the deterministic TMP model was based on a resistance-in-series model based on Jiang (Jiang 2008), which describes the fouling process as a progressive increase in TMP (mbar) caused by material deposited on and inside the membrane pores (equation 6.1).

$$TMP = \frac{\eta(T,t)}{3.6 \cdot 10^5} \cdot \frac{J(t)}{3.6 \cdot 10^5} \cdot R_{tot}(t) \quad (\text{Eq. 6.1})$$

In equation 6.1, $\eta(T,t)$ is the viscosity ($\text{g} \cdot \text{h}^{-1} \cdot \text{m}^{-1}$), $J(t)$ is the permeate flux ($\text{L} \cdot \text{m}^{-2} \cdot \text{h}^{-1}$) and R_{tot} is the total resistance of the membrane (m^{-1}), expressed as a resistance increment across the membrane due to the accumulation of particles in the filtering area.

Table 6.1 | Operating conditions of the different periods used for simulation.

| Period | Days | Membrane air-flow (m ³ ·h ⁻¹) | Permeate flow (l·h ⁻¹) | Permeate flux (LMH) | MLSSm (kg·m ⁻³) | MLSSana (kg·m ⁻³) | SMP concentration (mg·L ⁻¹) | Temperature (°C) | Aerobic DO set-point (mg·L ⁻¹) | pH | ORP (mV) |
|---------------|------|--|---------------------------------------|------------------------|--------------------------------|----------------------------------|---|---------------------|--|-------------|-----------------|
| Period 1 (P1) | 27 | 12.00 - 12.01 | 156.78 - 196.01 | 19.60 - 24.50 | 6.29 - 80.10 | 1.75 - 2.65 | 8.00 ± 1.50 | 17.83 - 21.48 | 1.09 - 2.52 | 6.61 - 7.04 | 450.11 - 493.06 |
| Period 2 (P2) | 24 | 10.00 - 12.00 | 176.98 - 203.99 | 22.12 - 25.50 | 6.92 - 7.46 | 2.26 - 2.46 | 10.00 ± 0.50 | 20.64 - 22.88 | 1.63 - 1.77 | 7.09 - 6.96 | 494.70 - 483.23 |
| Period 3 (P3) | 96 | 6.71 - 8.86 | 175.98 - 176.53 | 22.00 - 22.07 | 9.41 - 11.84 | 3.37 - 4.08 | 9.50 ± 12.50 | 24.07 - 28.50 | 1.53 - 1.70 | 6.80 - 6.95 | 314.09 - 381.11 |
| Period 4 (P4) | 41 | 7.40 - 8.20 | 175.55 - 176.95 | 21.94 - 22.12 | 3.55 - 4.52 | 1.47 - 3.35 | 12.00 ± 3.25 | 18.74 - 22.41 | 1.70 - 1.96 | 6.86 - 7.17 | 413.73 - 446.75 |
| Period 5 (P5) | 18 | 10.00 - 10.01 | 140.00 - 156.25 | 17.50 - 19.53 | 4.79 - 5.78 | 1.23 - 2.42 | 8.50 ± 2.00 | 14.89 - 16.54 | 1.53 - 1.62 | 5.95 - 6.07 | 229.76 - 245.10 |
| Period 6 (P6) | 63 | 10.99 - 11.20 | 125.77 - 126.98 | 15.72 - 15.87 | 5.30 - 6.96 | 1.49 - 2.60 | 3.00 ± 0.50 | 15.74 - 19.46 | 1.53 - 1.81 | 4.70 - 5.48 | 238.39 - 255.72 |
| Period 7 (P7) | 128 | 7.28 - 10.44 | 146.57 - 149.50 | 18.32 - 18.69 | 5.34 - 8.96 | 1.37 - 2.45 | 2.35 ± 0.50 | 21.83 - 27.38 | 1.52 - 1.79 | 5.18 - 5.63 | 242.06 - 341.22 |
| Period 8 (P8) | 32 | 10.00 - 10.23 | 169.06 - 183.55 | 21.13 - 22.94 | 8.38 - 9.33 | 2.24 - 2.87 | 7.75 ± 0.15 | 24.51 - 26.77 | 1.48 - 1.59 | 6.39 - 6.64 | 346.42 - 352.15 |
| Period 9 (P9) | 33 | 10.00 - 10.29 | 174.71 - 177.56 | 21.84 - 22.20 | 7.02 - 10.71 | 1.97 - 3.98 | 5.35 ± 1.25 | 22.93 - 25.98 | 1.50 - 1.53 | 6.14 - 6.51 | 457.49 - 533.49 |

Table 6.2 | Influent and effluent characteristics along the different periods (units: mg·L⁻¹)

| Period | COD _T (in) | COD _S (in) | COD _T (out) | TKN _T (in) | TKN _S (in) | TKN (out) | NH ₄ ⁺ (in) | NH ₄ ⁺ (out) | NO ₂ ⁻ (in) | NO ₂ ⁻ (out) | NO ₃ ⁻ (in) | NO ₃ ⁻ (out) | PO ₄ ³⁻ (in) | PO ₄ ³⁻ (out) |
|--------|-----------------------|-----------------------|------------------------|-----------------------|-----------------------|-----------|-----------------------------------|------------------------------------|-----------------------------------|------------------------------------|-----------------------------------|------------------------------------|------------------------------------|-------------------------------------|
| P1 | 122.03 ± | 112 ± 62 | 71 ± 30 | 14.95 | 10.70 ± | 0.71 ± | 16.68 ± | 2.71 ± | 0.01 ± | 0.06 ± | 0.40 ± | 16.53 ± | 1.77 ± | 2.66 ± |
| | 61.10 | | | ±7.82 | 9.14 | 0.53 | 3.58 | 1.01 | 0.00 | 0.04 | 0.10 | 1.70 | 0.62 | 0.80 |
| P2 | 226.75 ± | 79.82 ± | 69.64 ± | 30.13 ± | 22.13 ± | 2.13 | 17.37 ± | 2.16 ± | 0.03 ± | 0.08 ± | 0.31 ± | 13.45 ± | 2.46 ±1.17 | 1.98 |
| | 145.43 | 49.94 | 40.65 | 17.87 | 12.31 | ±1.91 | 6.63 | 1.25 | 0.01 | 0.01 | 0.14 | 5.11 | | ±1.10 |
| P3 | 717.56 ± | 138.33 ± | 48.76 ± | 85.82 ± | 67.31 ± | 6.93 ± | 37.59 ± | 2.35 ± | 0.09 ± | 0.04 ± | 1.74 | 11.63 ± | 15.00 ± | 7.17 ± |
| | 278.12 | 48.67 | 29.91 | 51.42 | 10.95 | 3.05 | 10.12 | 1.71 | 0.11 | 0.02 | ±0.64 | 7.34 | 14.04 | 4.14 |
| P4 | 458.67 ± | 96.67 ± | 35.36 ± | 25.11 ± | 21.96 ± | 1.87 ± | 18.83 ± | 1.27 ± | 0.04± | 0.10 ± | 0.41 ± | 13.45 ± | 2.49 ± | 1.98 ± |
| | 49.03 | 31.46 | 22.22 | 10.28 | 9.61 | 1.12 | 9.40 | 0.79 | 0.03 | 0.08 | 0.31 | 5.11 | 1.17 | 1.10 |
| P5 | 232.29 ± | 82.00 ± | 35.25 ± | 24.93 ± | 19.39 ± | 1.76 ± | 20.08 ± | 17.09 ± | 0.31 ± | 0.10 ± | 0.79 ± | 14.45 ± | 2.14 ± | 1.99 ± |
| | 180.92 | 60.01 | 21.68 | 12.46 | 8.89 | 0.60 | 6.11 | 5.88 | 0.24 | 0.04 | 0.55 | 2.67 | 0.96 | 0.76 |
| P6 | 207.41 ± | 115.82 ± | 29.29 ± | 42.40 ± | 26.79 ± | 1.77 ± | 28.48 ± | 28.48 ± | 2.17 ± | 0.05 ± | 0.05 ± | 0.06 ± | 11.06 ± | 1.47 ± |
| | 127.41 | 60.75 | 14.30 | 31.66 | 12.40 | 1.05 | 17.08 | 17.08 | 1.73 | 0.04 | 0.01 | 0.05 | 2.91 | 0.77 |
| P7 | 466.37 ± | 179.33 ± | 20.26 ± | 54.99 ± | 33.99 ± | 4.43 ± | 47.41 ± | 3.51 ± | 2.28 ± | 1.63 ± | 0.76 ± | 4.86 ± | 11.93 ± | 1.70 |
| | 210.26 | 97.27 | 14.95 | 18.06 | 30.26 | 6.44 | 28.46 | 2.40 | 0.53 | 0.47 | 0.27 | 3.89 | 6.70 | ±1.35 |
| P8 | 433.77 ± | 137.96 ± | 23.45 ± | 42.68 ± | 35.01 ± | 4.47 ± | 33.71 ± | 5.51 ± | 0.10 ± | 0.26 ± | 0.11 ± | 7.22 ± | 3.25 ± | 3.24 ± |
| | 137.48 | 95.13 | 9.35 | 16.32 | 12.47 | 3.21 | 13.74 | 2.67 | 0.05 | 0.12 | 0.03 | 5.84 | 1.25 | 1.22 |
| P9 | 274.70 ± | 97.78 ± | 26.17 ± | 44.20 ± | 29.18 ± | 2.70 ± | 29.59 ± | 7.07 ± | 0.17 ± | 0.11 ± | 0.45 ± | 5.78 ± | 2.51 ± | 1.62 ± |
| | 107.54 | 73.75 | 17.26 | 41.55 | 15.67 | 2.09 | 19.36 | 2.72 | 0.11 | 0.04 | 0.28 | 4.17 | 1.73 | 0.30 |

The total membrane resistance ($R_{tot}(t)$) is modelled by the sum of three different terms (equation 2):

$$R_{tot}(t) = R_m + R_c(t) + R_{irr}(t) \quad (\text{Eq. 6.2})$$

where R_m denotes the constant intrinsic resistance of the membrane (m-1), $R_c(t)$ is the cake resistance caused by the reversible accumulation of solids on the filtering surface during the filtration period (m-1), and $R_{irr}(t)$ denotes the irreversible accumulation of solids (m-1). The reversible accumulation cake resistance ($R_c(t)$) is modelled according to equation 6.3,

$$R_c(t) = \alpha \cdot w(t) / A_0 \quad (\text{Eq. 6.3})$$

where α represents the specific cake resistance according to cake thickness ($\text{m} \cdot \text{g}^{-1}$), $w(t)$ is the cake mass (g) related to the sludge solids concentration and to the flow rate of permeate, and A_0 is the surface area of the membrane (m^2). The irreversible fouling ($R_{irr}(t)$) is calculated as follows:

$$R_{irr}(t) = R_m \cdot \left(\frac{A_0}{A(t)} - 1 \right) \quad (\text{Eq. 6.4})$$

Where $A(t)$ indicates the irreversibly blocked membrane (m^2) determined from a pore-blocking parameter, the SMP concentration ($\text{g} \cdot \text{L}^{-1}$) and the flow rate of permeate over the time. The deterministic model was developed using West^(R) (www.mikebydhi.com) as the modelling and simulation tool.

DATA DRIVEN

In contrast to the deterministic model, where the relationship between the dependent and independent variables is presented with known functions, data-driven approaches identify the functional dependencies between variables from measured data. In the case of a model tree, these functional dependencies are a set of regression equations following specific conditions for their use. Thus, unlike a simple linear regression, which calculates a single regression function for a given domain, a model tree identifies a set of sub-domains that can be characterised with regression functions of the dependent variable. The division into sub-

domains is based on tests of the values of the independent variables, which are entered as nodes in the model tree (Witten et al. 2011). Thus, model trees are hierarchical structures composed of nodes and branches where the internal nodes contain tests on the input variables. Each branch of an internal test corresponds to an outcome of the test, and the predictions for the values of the dependant variable are stored in the leaves, which are the terminal nodes in the tree, containing a regression equation. The data-driven model, i.e., a model tree, was induced with the M5' algorithm embedded in the WEKA® software package. The algorithm M5' embedded in the WEKA® is a variation of the M5 algorithm (Quinlan 1992).

MODEL CALIBRATION AND VALIDATION

The deterministic model was calibrated for steady and dynamic states over a period equal to three times the sludge retention time, using the experimental campaign data from period 4 (P4). Biological parameters were adjusted when required by comparing the simulated and measured values. Once calibrated, the model was then validated using the experimental campaign values from period 5 (P5), working under different conditions. The other periods were also calibrated with the available experimental data.

The validation of the model tree was performed by cross-validation, wherein the dataset is partitioned into a chosen number of folds (n). Each fold is used for testing in turn, while the remainders ($n-1$ folds) are used for training. The final error is the averaged error of all the models throughout the procedure. In our case, we used 10-fold cross-validation and the root mean square error were used.

MODEL EVALUATION

Local sensitivity analysis was conducted to determine which filtration parameters in the deterministic model had the strongest effect on the TMP. Following the same procedure as Dalmau et al. (2013), a relative sensitivity function (RSF) was used to evaluate the local sensitivity of the model by perturbing the operating parameters by $1 \cdot 10^{-7}$. Greater differences between the perturbed and the default operating parameters imply greater impact of the parameter on the TMP. A value of $RSF < 0.25$ means the parameter is non-

influential. RSF values between 0.25 and 1 are moderately influential. Parameters are considered extremely influential when the $RSF > 2$, according to Audenaert et al. (2011) and references therein.

The root mean square error (RMSE) (equation 6.5) was used to compare the accuracy of the simulated TMP values for each model compared to the experimental values. The RMSE is commonly used to predict the divergence between simulated results and observed values. This criterion avoids error compensation and indicates the average magnitude of the errors, which should be as low as possible. Therefore, the model with the lowest RMSE, deterministic or data-driven, is better at describing the TMP.

$$RMSE = \sqrt{\left[\frac{1}{n} \cdot \sum (y_{i,\text{measured}} - y_{i,\text{simulated}})^2 \right]} \quad (\text{Eq. 6.5})$$

where $y_{i,\text{measured}}$ is the observed, experimental or measured TMP value in the MBR process, while $y_{i,\text{simulated}}$ is the value given by the simulation results and n the total number of values.

6.3 RESULTS AND DISCUSSION

6.3.1 MODEL SET-UP, CALIBRATION AND VALIDATION

DETERMINISTIC MODEL

A deterministic model was developed following the layout shown in Fig. 6.1. It consisted of three activated sludge units: anaerobic, anoxic and aerobic tanks, each of which were described with an ASM2d biological process model. The oxygen transfer rate was adapted in the aerobic tank to attain the experimental DO set-point. The fourth tank represented the membrane compartment, where the filtration processes were described with a resistance-in-series model. Influent fractions for COD, N and P in the deterministic model were determined from influent and effluent grab samples taken during the experimental campaign. Total suspended solids from the influent and tanks as well as SMP measurements were also taken into account in the deterministic model. In addition, daily averages of the on-line measurements of temperature, aerobic reactor DO, waste flow rate and permeate flow were used in the model.

The biological model was calibrated using default parameters for ASM2d, except for the nitrogen half-saturation coefficient for autotrophs, K_{NH_4} , which was increased from 1 to $1.5 \text{ g N}\cdot\text{m}^{-3}$, and the anoxic reduction factor for the growth of heterotrophic organisms ($\eta_{\text{NO}_3\text{-H}}$), which was decreased from 0.8 to 0.4, diminishing the proportion of the denitrifying biomass. The RMSE values for TMP in the calibration and validation periods were 14.83 and 13.65, respectively (detailed results in Dalmau et al. (2013)).

DATA-DRIVEN MODEL

The model tree (MT) generated from measured data was primarily used for finding functional dependencies between the operating parameters and the TMP and thus modelling the TMP values under different conditions. Additionally the MT, unlike many commonly used data-driven methods, can partly explain the system and reveal hidden patterns from the data. All on-line daily data, that is, temperature, ORP, MLSS_m, MLSS_{sana}, aerobic reactor DO, membrane air-scouring and permeate flow, were used to induce the data-driven model. Offline measurements were too scarce (two to three times per week) for reliable induction of data-driven model. Thus, they were not taken into account. The model tree (Figure 6.2) was composed of 35 multivariable linear equations (or linear models, LM), each of which is valid under specific operating conditions in the system given by specific values of the operation conditions (on-line daily data). The 10-fold cross-validations of the developed model tree led to a RMSE of 20.08.

Starting from the top of the tree, it is necessary to discern along the tree branches (between the different operating conditions) until reaching each LM in the leaves. The operating parameters at the top of the tree were the most discriminating. Each LM enables the estimation of the TMP as a linear regression of multiple operating parameters. LM1, for example, is valid when the temperature is below 22.44°C , the membrane airflow is under $10.631 \text{ m}^3\cdot\text{h}^{-1}$, the ORP is under 426.78 mV , the pH is 6.89 and, finally, the temperature is below 19.46°C . All of the LMs are listed at the end of the chapter (6.5 Annex). From the LM equations, it is possible to know which parameters are the most influential because each parameter is multiplied by a weighting factor. The higher the weighting factor, the greater the influence on the predicted TMP value. Finally, positive weighting factors indicate a direct relation to the TMP, while a negative value denotes an inverse relation to TMP.

The RMSE of the simulated results with respect to real values for the whole evaluation period is slightly higher for the data-driven model compared to the deterministic model (19.34 and 20.08, respectively). The accuracy of both models for different periods was also calculated (Table 6.3).

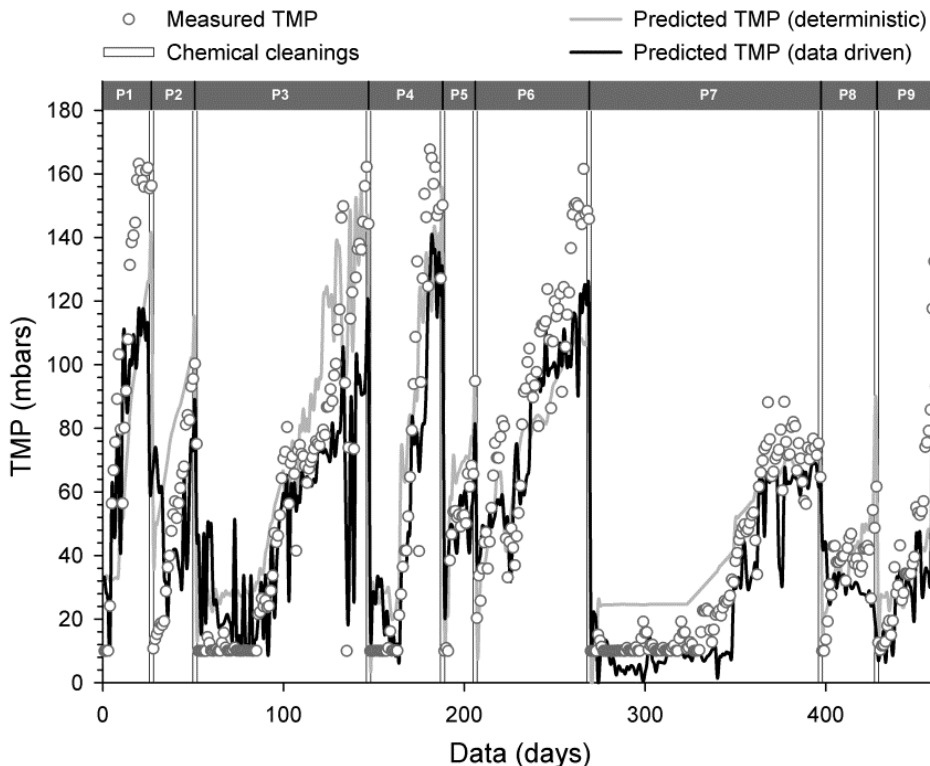


Figure 6.3 | Measured TMP and simulated TMP values using both data-driven and deterministic models versus time.

Table 6.3 | RMSE for each period for both models. The lowest value for each period is in bold.

| Periods | Deterministic | Data Driven |
|-----------------------|---------------|--------------|
| Overall period | 19.34 | 20.08 |
| P1 | 36.93 | 29.62 |
| P2 | 15.56 | 31.81 |
| P3 | 20.73 | 23.61 |
| P4 | 14.83 | 14.46 |
| P5 | 13.65 | 10.03 |
| P6 | 23.38 | 20.46 |
| P7 | 10.61 | 9.96 |
| P8 | 10.60 | 17.68 |
| P9 | 18.81 | 19.36 |

The sensitivity analysis performed on the deterministic model demonstrated that permeate flux (with an RSF > 2) is the most influential parameter affecting the TMP in the deterministic model, implying a direct relationship between the TMP and the permeate flux, i.e., an increase in the permeate flux leads to an increase in TMP (Figure 6.4). This relationship was also confirmed by the experimental results (Figure 6.5a). Additionally, permeate fluxes close to the critical flux defined by the manufacturer yield a steeper slope for the TMP (i.e., higher fouling rates, also in Figure 6.5a), in agreement with other results reported (Ng and Ng 2010).

In addition, the SMP concentration and temperature had a moderate influence on the TMP, according to RSF values (Figure 6.4). The direct impact on TMP after an increase of SMP concentrations was also observed in the experimental results; higher SMP concentrations led to slightly higher TMP values (Figure 6.5b). On the other hand, a decrease in temperature resulted in a slight increase in TMP (Figure 6.5b). Membrane filtration resistance was highly affected by temperature in the deterministic model, as it has an impact on sludge morphology and, specifically, the sludge viscosity. Indeed several studies reported seasonal variations in the TMP due to temperature (Al-Amri et al. 2010, van den Brink et al. 2011).

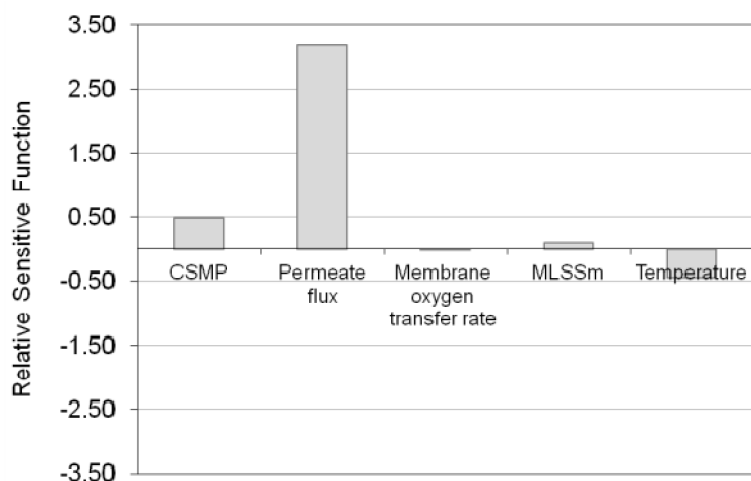


Figure 6.4 | Sensitivity of different parameters in the deterministic TMP model.

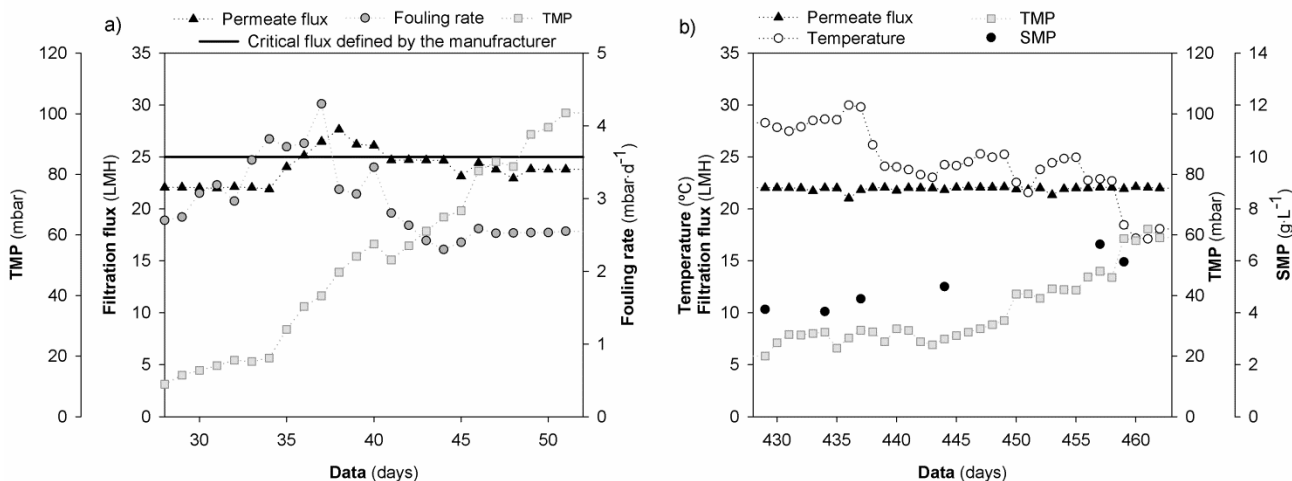


Figure 6.5 | Experimental influence of TMP vs. the permeate flux increase (a) and SMP increase and temperature decrease (b).

In general, TMP values fell into five different subdomains, as revealed in the model tree. These subdomains are defined by different operating conditions (Figure 6.2). Taking into account all the operating conditions, the most discriminating variable was temperature. As an overall trend, the TMP values predicted by the model tree at temperatures over 22.44 °C (left-hand side of the tree) were lower than those estimated at temperatures below 22.44 °C (right-hand side of the tree). In addition, there was a negative relationship between temperature and TMP in all linear models for temperatures >22.44 °C (i.e., negative coefficients in LM20-35). In general, high TMP values are expected at lower temperatures because there is an increase in the mixed liquor viscosity, a reduction of biomass floc size and higher release of SMP into the mixed liquor (van den Brink et al. 2011).

The second most discriminating variable was the membrane air scouring flow rate. Higher membrane airflows (>10 m³·h⁻¹) had a positive influence on the TMP trend in several linear models (Figure 6.2 LM14-19, 27-33). An increase in aeration rates is expected to reduce membrane fouling (Ji and Zhou 2006), as is observed in subdomain 5b of Figure 6.2. However, the highest estimated TMP values were found in subdomain 3, with air flow rates greater than 10.63 m³·h⁻¹. These high TMP values can be explained due to excessive aeration intensity, which can cause sludge floc breakage, i.e., deflocculation, leading to higher SMP release and thus an

increase in TMP, thereby increasing fouling (Gil et al. 2012). This situation is more favoured at lower temperatures (Bewtra et al. 1970).

Robles et al. (2012) reported that pH values under 7 could reduce fouling problems related to chemical precipitation, thus leading to low TMP. This observation is also in agreement with the model tree, where several conditions (represented in subdomains 1, 4 and 5 in Figure 6.2) yielded slightly better TMP predictions at pH values less than 7, independent of the other parameters.

ORP, which is related to the concentration of nitrates and nitrites in the tank, had a positive effect on TMP, as shown in subdomain 1 of Figure 6.2 and is reflected in the LM (LM1-12). De la Torre et al. (2010) reported a direct statistical relationship between nitrite concentration and sludge filterability. Accordingly, membrane fouling could increase by biofilm denitrification (Kim and Nakhla 2009), and Drews et al. (2007) reported that SMP increased with decreasing nitrate concentrations in post-denitrification biological nutrient removal systems.

Permeate flow has a strong influence on TMP (Judd and Judd 2011, Ng and Ng 2010), especially when working above the critical flux (Monclús et al. 2010b, Ng and Ng 2010), (> 25 LMH, e.g., LM7). However, critical flux conditions were not reached in the majority of experimental studies. However, our model suggests that when working under critical conditions, permeate flux is not the most discriminatory parameter for TMP, thus it is not at the top of the tree.

DIFFERENCES ON MODEL PERFORMANCE DURING THE DIFFERENT PERIODS

To establish which conditions enabled the best representation of the TMP in each model, all of the periods were studied separately. However, after an adjustment of each model based on the RMSE values (Table 6.3), neither model was capable of describing the TMP in all of the periods. Depending on the conditions, one model predicted the TMP better than the other. P2, P3, P8, and P9, the hottest periods with less temperature variation, were better explained by the deterministic model. In contrast, P1, P4, P5, P6, and P7, which had lower temperatures overall and more variation in temperature, were better explained by the data-driven model.

The data-driven model fitted better in period 1 ($RMSE_{det}$ 39.93, $RMSE_{data-driven}$ 29.62), likely because of the high variation in the dissolved oxygen in the aerobic compartment and pH, which are considered in the data-driven model (e.g., LM1-LM4), but not in the deterministic model equations.

Regarding the second period (P2), when the flux changed noticeably (22.12 – 25.50 LMH), even though the flux conditions were mostly subcritical and critical flux (J_c , 25 LMH, [21]) was reached in very few cases, the deterministic model fitted better ($RMSE_{det}$ 15.56, $RMSE_{data-driven}$ 31.81).

P3, P8 and P9 were periods without large changes in operation. Specifically, the conditions were a MLSSm greater than $6 \text{ g}\cdot\text{L}^{-1}$, relatively high temperature (above $22 \text{ }^\circ\text{C}$), pH of approximately 7 and, the use of subcritical flux conditions ($<25 \text{ LMH}$), all of which led to better performance by the deterministic model. In period 8, higher accuracy was achieved with the deterministic model ($RMSE_{det}$ 10.60), as opposed to the data-driven model ($RMSE_{data-driven}$ 17.68), which could be due to permeate flux variation (21.13 - 22.94 LMH), in alignment with P2 results.

Monclús et al. (2011) reported that critical flux is 21 LMH when the MLSSm concentration is under $6 \text{ g}\cdot\text{L}^{-1}$. Using these criteria, operation in P4 was over the critical flux (21.94-22.12 LMH), with the highest SMP values (12 ± 3.25) and a wide range of temperatures ($18.74\text{-}22.41 \text{ }^\circ\text{C}$). According to Ng and Ng (2010), fouling mechanisms change when working at critical conditions. In these conditions, the data-driven model yielded more accurate results ($RMSE_{det}$ 15.56, $RMSE_{data-driven}$ 31.81). The data-driven model also performed better in P5 ($RMSE_{det}$ 13.63, $RMSE_{data-driven}$ 10.03), where low MLSSm concentrations ($4.79\text{-}5.78 \text{ g}\cdot\text{L}^{-1}$) and temperatures ($14.89\text{-}16.54 \text{ }^\circ\text{C}$) were predominant, although the operating flux was not over the critical flux (17.50-19.53 LMH). Finally, the data-driven model gave a more accurate description in periods with low pH values: P6 (4.70-5.48) and P7 (5.18-5.63). Although fouling problems related to chemical precipitation can be avoided at pHs of less than 7 (Robles et al. 2012), pH is not normally considered in deterministic models, thus neither is its effect on fouling phenomena, which could explain the lower accuracy obtained from the deterministic model.

To summarize, the deterministic model describes better the TMP under subcritical and stable operating conditions, while the data-driven model outperforms the deterministic model in periods with higher perturbations, explicitly under critical conditions (e.g. low temperature

and/or MLSS) and sudden variations of operational conditions (e.g. DO changes). Since the data-driven model is learning from relationships between data values of real cases, it is able to capture those cases better, i.e. when there are significant changes in the filtration process, reflected on the TMP evolution. On the other hand, the deterministic model describes relatively well the filtration processes when MBR system is working as expected but it is not able to capture the effect of the perturbations, except from permeate changes. Permeate flux is the most influential variable introduced in the deterministic model affecting the TMP, followed by TMP is also sensitive to other variables, such temperature or SMP concentration, considered in the deterministic model. However, pH variations or ORP oscillations are not considered in the mechanistic model equations. In that sense, the data-driven model can go one step further in the prediction of TMP whereas deterministic models are not detailed enough, especially if these variables are modified due to perturbations. In any case, filtration models need to be integrated with the deterministic ASM models to describe the biological processes in order to have a complete description of the MBR systems. The combined use of both models enabled a better understanding of this phenomenon as a function of the different operating conditions. Next studies will involve the validation of combined use in other pilot and full-scale plants and implementation of variables such pH or ORP in deterministic models.

6.4 CONCLUSIONS

Two different models (deterministic and data-driven) were used to describe fouling phenomena as measured by TMP over 462 days at an MBR pilot plant operated under different conditions. Neither model best described fouling under all of the simulated operating conditions. The combined use of both models led to a better understanding of this phenomenon as a function of the different operating conditions. In general, the deterministic model performed better at high temperatures (20 °C); at constant MLSS_m, DO and pH; subcritical filtration conditions; and with permeate fluctuations. In contrast, the data-driven model worked better at low temperatures (under 20 °C), low pH, under critical filtration conditions and in periods with relevant variations in other operating parameters, such as pH or DO in the aerobic reactor. The combination of both models led a better understanding of fouling under different operating conditions.

6.5 ANNEX

Table 6.4 | . List of all linear models developed by the data driven model.

| Linear Model | Equation |
|--------------|--|
| LM1 | $TMP = 0.01 \cdot (\text{Permeate flow}) - 10.35 \cdot (\text{Aerobic DO}) - 8.17 \cdot (\text{Membrane air-flow}) - 0.79 \cdot (\text{MLSSm}) + 8.22 \cdot (\text{MLSSana}) + 5.23 \cdot (\text{Temperature}) - 0.21 \cdot (\text{pH}) - 0.01 \cdot (\text{ORP}) + 54.30$ |
| LM2 | $TMP = 0.06 \cdot (\text{Permeate flow}) - 13.09 \cdot (\text{Aerobic DO}) - 0.09 \cdot (\text{Membrane air-flow}) - 0.61 \cdot (\text{MLSSm}) + 0.97 \cdot (\text{MLSSana}) + 0.94 \cdot (\text{Temperature}) - 1.25 \cdot (\text{pH}) - 0.01 \cdot (\text{ORP}) + 65.08$ |
| LM3 | $TMP = 0.18 \cdot (\text{Permeate flow}) - 18.96 \cdot (\text{Aerobic DO}) - 0.12 \cdot (\text{Membrane air-flow}) - 0.47 \cdot (\text{MLSSm}) + 0.97 \cdot (\text{MLSSana}) + 0.94 \cdot (\text{Temperature}) - 2.15 \cdot (\text{pH}) - 0.00 \cdot (\text{ORP}) + 62.20$ |
| LM4 | $TMP = 0.18 \cdot (\text{Permeate flow}) - 18.46 \cdot (\text{Aerobic DO}) - 0.12 \cdot (\text{Membrane air-flow}) - 0.47 \cdot (\text{MLSSm}) + 0.97 \cdot (\text{MLSSana}) + 0.94 \cdot (\text{Temperature}) - 2.15 \cdot (\text{pH}) - 0.01 \cdot (\text{ORP}) + 58.97$ |
| LM5 | $TMP = -0.33 \cdot (\text{Permeate flow}) - 4.36 \cdot (\text{Aerobic DO}) - 0.05 \cdot (\text{Membrane air-flow}) - 1.00 \cdot (\text{MLSSm}) + 1.04 \cdot (\text{MLSSana}) + 1.25 \cdot (\text{Temperature}) + 1.93 \cdot (\text{pH}) - 0.01 \cdot (\text{ORP}) + 110.26$ |
| LM6 | $TMP = -0.41 \cdot (\text{Permeate flow}) - 4.36 \cdot (\text{Aerobic DO}) + 0.19 \cdot (\text{Membrane air-flow}) - 1.00 \cdot (\text{MLSSm}) + 1.04 \cdot (\text{MLSSana}) + 1.25 \cdot (\text{Temperature}) + 1.93 \cdot (\text{pH}) - 0.01 \cdot (\text{ORP}) + 123.45$ |
| LM7 | $TMP = 15.88 \cdot (\text{Permeate flow}) - 9.79 \cdot (\text{Aerobic DO}) - 1.40 \cdot (\text{Membrane air-flow}) - 1.00 \cdot (\text{MLSSm}) + 1.04 \cdot (\text{MLSSana}) + 1.25 \cdot (\text{Temperature}) + 1.93 \cdot (\text{pH}) - 0.01 \cdot (\text{ORP}) - 273.20$ |
| LM8 | $TMP = -0.10 \cdot (\text{Permeate flow}) - 12.10 \cdot (\text{Aerobic DO}) - 0.61 \cdot (\text{Membrane air-flow}) - 3.96 \cdot (\text{MLSSm}) - 2.77 \cdot (\text{MLSSana}) - 0.03 \cdot (\text{Temperature}) + 16.08 \cdot (\text{pH}) + 0.10 \cdot (\text{ORP}) - 44.40$ |
| LM9 | $TMP = -0.10 \cdot (\text{Permeate flow}) - 12.10 \cdot (\text{Aerobic DO}) - 0.61 \cdot (\text{Membrane air-flow}) - 3.12 \cdot (\text{MLSSm}) - 3.26 \cdot (\text{MLSSana}) - 0.03 \cdot (\text{Temperature}) + 16.64 \cdot (\text{pH}) + 0.10 \cdot (\text{ORP}) - 48.80$ |
| LM10 | $TMP = -0.10 \cdot (\text{Permeate flow}) - 12.10 \cdot (\text{Aerobic DO}) - 0.61 \cdot (\text{Membrane air-flow}) - 2.59 \cdot (\text{MLSSm}) - 2.09 \cdot (\text{MLSSana}) - 0.03 \cdot (\text{Temperature}) + 14.07 \cdot (\text{pH}) + 0.10 \cdot (\text{ORP}) - 41.80$ |
| LM11 | $TMP = 0.06 \cdot (\text{Permeate flow}) - 13.90 \cdot (\text{Aerobic DO}) - 0.61 \cdot (\text{Membrane air-flow}) - 3.49 \cdot (\text{MLSSm}) - 0.45 \cdot (\text{MLSSana}) - 0.03 \cdot (\text{Temperature}) + 8.57 \cdot (\text{pH}) + 0.14 \cdot (\text{ORP}) - 24.02$ |
| LM12 | $TMP = 0.09 \cdot (\text{Permeate flow}) - 13.90 \cdot (\text{Aerobic DO}) - 0.61 \cdot (\text{Membrane air-flow}) - 4.64 \cdot (\text{MLSSm}) - 0.45 \cdot (\text{MLSSana}) - 0.03 \cdot (\text{Temperature}) + 8.57 \cdot (\text{pH}) + 0.14 \cdot (\text{ORP}) - 18.77$ |
| LM13 | $TMP = 0.62 \cdot (\text{Permeate flow}) - 5.69 \cdot (\text{Aerobic DO}) + 7.25 \cdot (\text{Membrane air-flow}) + 2.27 \cdot (\text{MLSSm}) + 3.61 \cdot (\text{MLSSana}) + 0.37 \cdot (\text{Temperature}) - 1.68 \cdot (\text{pH}) + 0.07 \cdot (\text{ORP}) - 67.25$ |
| LM14 | $TMP = -0.34 \cdot (\text{Permeate flow}) - 6.58 \cdot (\text{Aerobic DO}) - 18.56 \cdot (\text{Membrane air-flow}) + 2.27 \cdot (\text{MLSSm}) - 15.53 \cdot (\text{MLSSana}) + 1.89 \cdot (\text{Temperature}) - 2.45 \cdot (\text{pH}) + 0.08 \cdot (\text{ORP}) + 319.43$ |
| LM15 | $TMP = -0.79 \cdot (\text{Permeate flow}) - 1.45 \cdot (\text{Aerobic DO}) + 27.55 \cdot (\text{Membrane air-flow}) + 6.55 \cdot (\text{MLSSm}) - 10.41 \cdot (\text{MLSSana}) - 3.44 \cdot (\text{Temperature}) + 2.52 \cdot (\text{pH}) + 0.03 \cdot (\text{ORP}) - 214.83$ |
| LM16 | $TMP = -1.40 \cdot (\text{Permeate flow}) - 16.67 \cdot (\text{Aerobic DO}) - 5.56 \cdot (\text{Membrane air-flow}) + 17.58 \cdot (\text{MLSSm}) - 3.49 \cdot (\text{MLSSana}) + 0.37 \cdot (\text{Temperature}) + 19.44 \cdot (\text{pH}) - 0.43 \cdot (\text{ORP}) + 383.98$ |
| LM17 | $TMP = -1.31 \cdot (\text{Permeate flow}) - 1.45 \cdot (\text{Aerobic DO}) - 3.10 \cdot (\text{Membrane air-flow}) + 27.04 \cdot (\text{MLSSm}) - 43.63 \cdot (\text{MLSSana}) + 0.37 \cdot (\text{Temperature}) + 16.96 \cdot (\text{pH}) - 0.32 \cdot (\text{ORP}) + 275.05$ |
| LM18 | $TMP = -1.37 \cdot (\text{Permeate flow}) - 1.45 \cdot (\text{Aerobic DO}) - 3.10 \cdot (\text{Membrane air-flow}) + 27.04 \cdot (\text{MLSSm}) - 34.26 \cdot (\text{MLSSana}) + 0.37 \cdot (\text{Temperature}) + 16.30 \cdot (\text{pH}) - 0.32 \cdot (\text{ORP}) + 263.07$ |

| | |
|------|---|
| LM19 | $\text{TMP} = -1.90 \cdot (\text{Permeate flow}) - 1.45 \cdot (\text{Aerobic DO}) - 3.10 \cdot (\text{Membrane air-flow}) + 31.93 \cdot (\text{MLSSm}) - 29.82 \cdot (\text{MLSSana}) - 0.37 \cdot (\text{Temperature}) + 16.96 \cdot (\text{pH}) - 0.32 \cdot (\text{ORP}) + 323.41$ |
| LM20 | $\text{TMP} = 0.06 \cdot (\text{Permeate flow}) - 2.43 \cdot (\text{Membrane air-flow}) + 1.71 \cdot (\text{MLSSm}) - 6.55 \cdot (\text{Temperature}) + 3.07 \cdot (\text{pH}) - 0.01 \cdot (\text{ORP}) + 178.41$ |
| LM21 | $\text{TMP} = 0.06 \cdot (\text{Permeate flow}) + 1.35 \cdot (\text{Aerobic DO}) - 2.43 \cdot (\text{Membrane air-flow}) + 2.58 \cdot (\text{MLSSm}) - 5.87 \cdot (\text{Temperature}) + 3.07 \cdot (\text{pH}) - 0.01 \cdot (\text{ORP}) + 149.08$ |
| LM22 | $\text{TMP} = 0.06 \cdot (\text{Permeate flow}) - 3.07 \cdot (\text{Membrane air-flow}) + 2.06 \cdot (\text{MLSSm}) - 5.48 \cdot (\text{Temperature}) + 3.07 \cdot (\text{pH}) - 0.01 \cdot (\text{ORP}) + 143.67$ |
| LM23 | $\text{TMP} = 0.33 \cdot (\text{Permeate flow}) - 1.29 \cdot (\text{Membrane air-flow}) + 0.61 \cdot (\text{MLSSm}) - 1.71 \cdot (\text{Temperature}) + 3.07 \cdot (\text{pH}) - 0.01 \cdot (\text{ORP}) - 2.17$ |
| LM24 | $\text{TMP} = -0.03 \cdot (\text{Permeate flow}) + 3.54 \cdot (\text{Aerobic DO}) + 0.33 \cdot (\text{Membrane air-flow}) + 1.07 \cdot (\text{MLSSm}) - 2.26 \cdot (\text{MLSSana}) - 1.34 \cdot (\text{Temperature}) - 1.06 \cdot (\text{pH}) - 0.02 \cdot (\text{ORP}) + 59.28$ |
| LM25 | $\text{TMP} = -0.03 \cdot (\text{Permeate flow}) + 3.54 \cdot (\text{Aerobic DO}) + 0.36 \cdot (\text{Membrane air-flow}) + 1.07 \cdot (\text{MLSSm}) - 2.26 \cdot (\text{MLSSana}) - 1.34 \cdot (\text{Temperature}) - 1.06 \cdot (\text{pH}) - 0.02 \cdot (\text{ORP}) + 58.70$ |
| LM26 | $\text{TMP} = -0.03 \cdot (\text{Permeate flow}) + 3.54 \cdot (\text{Aerobic DO}) + 0.71 \cdot (\text{Membrane air-flow}) + 1.07 \cdot (\text{MLSSm}) - 2.26 \cdot (\text{MLSSana}) - 1.34 \cdot (\text{Temperature}) - 1.06 \cdot (\text{pH}) - 0.02 \cdot (\text{ORP}) + 55.27$ |
| LM27 | $\text{TMP} = 0.02 \cdot (\text{Permeate flow}) - 16.25 \cdot (\text{Aerobic DO}) + 4.04 \cdot (\text{Membrane air-flow}) + 0.88 \cdot (\text{MLSSm}) + 0.57 \cdot (\text{MLSSana}) - 1.89 \cdot (\text{Temperature}) - 1.06 \cdot (\text{pH}) - 0.00 \cdot (\text{ORP}) + 53.20$ |
| LM28 | $\text{TMP} = 0.02 \cdot (\text{Permeate flow}) - 21.63 \cdot (\text{Aerobic DO}) - 2.70 \cdot (\text{Membrane air-flow}) + 0.88 \cdot (\text{MLSSm}) + 0.27 \cdot (\text{MLSSana}) - 1.89 \cdot (\text{Temperature}) - 1.06 \cdot (\text{pH}) - 0.00 \cdot (\text{ORP}) + 128.90$ |
| LM29 | $\text{TMP} = 0.02 \cdot (\text{Permeate flow}) - 21.38 \cdot (\text{Aerobic DO}) - 2.70 \cdot (\text{Membrane air-flow}) + 0.88 \cdot (\text{MLSSm}) + 0.27 \cdot (\text{MLSSana}) - 1.89 \cdot (\text{Temperature}) - 1.06 \cdot (\text{pH}) - 0.00 \cdot (\text{ORP}) + 128.38$ |
| LM30 | $\text{TMP} = 0.02 \cdot (\text{Permeate flow}) - 15.86 \cdot (\text{Aerobic DO}) - 1.64 \cdot (\text{Membrane air-flow}) + 0.88 \cdot (\text{MLSSm}) - 1.22 \cdot (\text{MLSSana}) - 1.89 \cdot (\text{Temperature}) - 1.06 \cdot (\text{pH}) - 0.00 \cdot (\text{ORP}) + 111.93$ |
| LM31 | $\text{TMP} = 0.02 \cdot (\text{Permeate flow}) - 14.88 \cdot (\text{Aerobic DO}) - 1.64 \cdot (\text{Membrane air-flow}) + 0.88 \cdot (\text{MLSSm}) - 1.22 \cdot (\text{MLSSana}) - 1.89 \cdot (\text{Temperature}) - 1.06 \cdot (\text{pH}) - 0.02 \cdot (\text{ORP}) + 108.38$ |
| LM32 | $\text{TMP} = 0.02 \cdot (\text{Permeate flow}) - 14.88 \cdot (\text{Aerobic DO}) - 1.64 \cdot (\text{Membrane air-flow}) + 0.88 \cdot (\text{MLSSm}) - 1.22 \cdot (\text{MLSSana}) - 1.89 \cdot (\text{Temperature}) - 1.06 \cdot (\text{pH}) - 0.02 \cdot (\text{ORP}) + 108.99$ |
| LM33 | $\text{TMP} = 0.02 \cdot (\text{Permeate flow}) + 3.54 \cdot (\text{Aerobic DO}) - 1.90 \cdot (\text{Membrane air-flow}) + 0.88 \cdot (\text{MLSSm}) - 1.22 \cdot (\text{MLSSana}) - 1.94 \cdot (\text{Temperature}) - 1.06 \cdot (\text{pH}) - 0.02 \cdot (\text{ORP}) + 101.13$ |
| LM34 | $\text{TMP} = 0.41 \cdot (\text{Permeate flow}) - 29.24 \cdot (\text{Aerobic DO}) + 8.59 \cdot (\text{Membrane air-flow}) - 2.05 \cdot (\text{MLSSm}) + 3.54 \cdot (\text{Temperature}) - 11.70 \cdot (\text{pH}) - 0.84 \cdot (\text{ORP}) + 474.80$ |
| LM35 | $\text{TMP} = 0.11 \cdot (\text{Permeate flow}) - 4.09 \cdot (\text{Aerobic DO}) + 8.71 \cdot (\text{Membrane air-flow}) + 3.96 \cdot (\text{MLSSm}) - 2.69 \cdot (\text{Temperature}) - 7.05 \cdot (\text{pH}) - 0.15 \cdot (\text{ORP}) + 96.24$ |

RESULTS IV:**TOWARDS INTEGRATED OPERATION
OF MBRS: EFFECTS OF AERATION
ON BIOLOGICAL AND
FILTRATION PERFORMANCE**

Redrafted from:

*Dalmau, M., Monclús, H., Gabarrón, S., Rodriguez-Roda, I., Comas, J.
Towards integrated operation of MBRS: effects on aeration on biological
and filtration performance.*

Bioresource Technology, accepted for publication

7.1 OVERVIEW

MBR aeration control is still rare in practice (Ferrero et al. 2012), although more than 50% of total operation costs are due to aeration (Krzeminski et al. 2012c). Thus, aeration control presents a wide range of opportunities for optimisation.

The effects of aeration on biological nutrient removal have been widely studied in recent decades, frequently with reliable activated sludge models (ASM, Henze et al., (2000)). Model-based studies using ASMs have enabled successful optimisations of wastewater treatment plants with different configurations with respect to nutrient removal efficiencies and operating costs (Rivas et al. 2008).

Focusing on MBR studies, a model-based optimisation of a modified benchmark-MBR plant was carried out to investigate carbon (C) and nitrogen (N) removal via the appropriate manipulation of dissolved oxygen (DO) and recirculation flow at different temperatures (Odriozola et al. 2013). Additionally, optimisation studies carried out in a small-centralised MBR with specific aeration efficiencies for fine and coarse bubbles at the bioreactor and membrane compartment were used to determine the optimal strategy for biological removal processes and energy demand (Verrecht et al. 2010a). Sarioglu et al. (2008) also carried out a model-based optimisation of nitrogen removal in an MBR plant, taking advantage of the high sludge age, the high mixed liquor suspended solids (MLSS) concentration and the lower DO diffusion rate, enabling simultaneous nitrification/denitrification. However, none of the previous studies have dealt with the description of fouling phenomena, but rather considered the filtration processes as ideal. A standard model to describe fouling is not yet available because there are complex relationships between operational parameters, biological and physical processes and activated sludge characteristics. A few authors have presented a mathematical model considering both membrane fouling filtration and biological nutrient removal processes (Mannina et al. 2011, Zarragoitia-González et al. 2008). However, as reported by Zuthi et al. (2012), those modelling studies were focused on steady-state processes; other studies presented some drawbacks, and still others had too many parameters for calibration or were only validated in a specific pilot plant.

Experimental studies are necessary to quantify the relationships among biomass characteristics, filtration performance and biological nutrient removal, especially for the aeration process. A few experimental aeration studies have reported the effects of membrane aeration. These studies

have been focused on the influence of shear stress provoked by membrane aeration on the physicochemical and biological properties of the biomass, whether focusing on the break-up of the flocculation and the formation of smaller particles (Germain and Stephenson 2005) or on the production of extracellular polymeric substance (EPS) (Menniti and Morgenroth 2010a) and the membrane fouling rate. Gao et al. (2011) studied how DO concentration influenced the generation of EPS and soluble microbial products (SMP) in mixed liquor and biocake to control fouling. However, the study of how both biological and membrane aeration affect the filtration performance, the properties (physical and biological) of the biomass and the biological nutrient removal (BNR) performance has not been reported. The aim of this chapter is to study the effect of changes in biological and membrane aeration on the filtration processes (i.e., fouling behaviour), the biological nutrient removal processes and the biomass characteristics.

7.2 MATERIALS AND METHODS

7.2.1 UCT-MBR PILOT PLANT

The pilot plant for this study is an MBR with a University Cape Town (UCT) configuration that is able to biologically remove organic matter, nitrogen and phosphorous (Monclús et al. 2010a). The pilot plant was fed with real municipal wastewater, without industrial contributions, directly collected from the sewer system. It was sent to the UCT-MBR pilot plant is equipped with a primary settler and a screening system (0.01 m) to prevent the entrance of large particles. The bioreactor has a total volume of 2.26 m³. It consists of anaerobic (14% of the total volume), anoxic (14%) and aerobic (23%) compartments that are ultimately followed by a fourth compartment (49%) with submerged microfiltration (MF) flat sheet (FS) membranes. The membranes have a total membrane area of 8 m² (LF-10, Kubota, Japan), with a nominal pore size of 0.4 µm. In the aerobic reactor, a PID (proportional-integral-derivative) controller maintains the DO at the desired concentration using a blower and membrane diffusers. A scheme of the pilot plant is shown in Figure 7.1. Details for the operating conditions in the pilot plant are provided in Table 7.1.

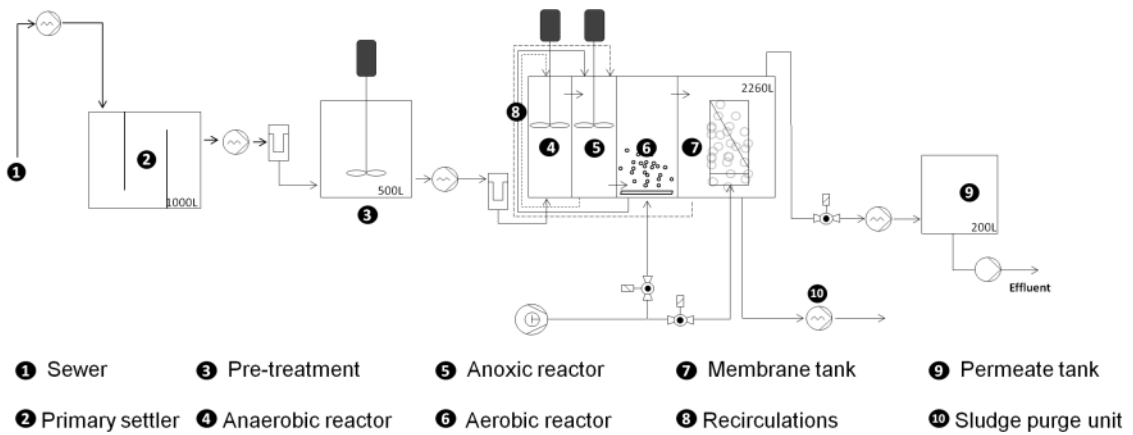


Figure 7.1 | Pilot plant diagram.

Table 7.1 | Design and operating parameters.

| Parameter | | Units | Value | Standard deviation |
|--|-------------------|-------------------------------------|-------|--------------------|
| Design influent flow | | $\text{m}^3 \cdot \text{d}^{-1}$ | 4.5 | |
| Instantaneous flux | | LMH | 25 | 0.2 |
| Membrane surface | | m^2 | 8 | - |
| Filtration/relaxation periods | | min | 9/1 | - |
| Default specific energy demand (SADm) | | $\text{m} \cdot \text{h}^{-1}$ | 1.25 | - |
| Default Aerobic DO set-point | | $\text{mg O}_2 \cdot \text{L}^{-1}$ | 1.5 | |
| Temperature | | $^{\circ}\text{C}$ | 16 | 1.83 |
| TSS | anaerobic reactor | $\text{mg} \cdot \text{L}^{-1}$ | 2.17 | 0.75 |
| | anoxic reactor | $\text{mg} \cdot \text{L}^{-1}$ | 4.48 | 1.20 |
| | aerobic reactor | $\text{mg} \cdot \text{L}^{-1}$ | 4.95 | 1.58 |
| | membrane tank | $\text{mg} \cdot \text{L}^{-1}$ | 9.28 | 2.41 |
| Recirculation to anoxic to anaerobic | | % influent flow | 129 | |
| Recirculation to aerobic to anoxic | | % influent flow | 92 | |
| External recycle (to membrane to anoxic) | | % influent flow | 136 | |
| Wastage pump | | % influent flow | 1.8 | |

7.2.2 EXPERIMENTAL PROCEDURE

Two different studies were carried out to determine the effects of aeration in an MBR: Experiment A uses a modification of the DO set-point in the aerobic compartment and Experiment B involves a modification of the air-scouring flow rate in the membrane tank.

The aeration of the aerobic compartment in Experiment A was modified by gradually reducing the DO set-point of the aerobic compartment from 1.5 to 0 mg O₂·L⁻¹ over the course of 35 days. Experimentally, 0.1 mg O₂·L⁻¹ was reduced each day by adjusting the aerobic DO set-point, from 1.5 mg O₂·L⁻¹ to 0.5 mg O₂·L⁻¹. After one week at 0.5 mg O₂·L⁻¹, the decrease continued with a gradual decrease of 0.1 mg O₂·L⁻¹ per day to 0 mg O₂·L⁻¹. In this experiment, the air-scouring flow was fixed at 1.25 m·h⁻¹. The same procedure was applied for Experiment B, in which the aerobic DO set-point was maintained at 0.5 mg O₂·L⁻¹ and the membrane air-scouring flow rate was reduced from 10 m³·h⁻¹ to 6 m³·h⁻¹ (SADm, of 1.25 to 0.75 m·h⁻¹). The manufacturer recommends applying an average air-scouring flow of 10 m³·h⁻¹ at this pilot-scale size. Daily air-scouring flow rate changes of 1 m³·h⁻¹ were applied until 6 m³·h⁻¹ (SADm of 0.75 m·h⁻¹) was reached; the plant was operated using this rate for 3 days. A subsequent daily increase of the air-flow was applied up to 1.25 m·h⁻¹. The second part of the experiment lasted for 15 days.

Before starting each experiment, there was a stabilisation period in which nutrient removal remained constant and the TMP was maintained at an approximate value of 50 mbar. A chemical cleaning was applied before starting Experiment B.

7.2.3 EXPERIMENTAL MONITORING

BIOLOGICAL NUTRIENT REMOVAL MONITORING

Three times per week, grab samples were gathered from the influent, the effluent, and each of the pilot plant compartments. The chemical oxygen demand (COD), the total suspended solids (TSS), and the volatile suspended solids (VSS) were measured in the samples from the influent and each compartment according to Standard Methods for the Examination of Water and Wastewater (APHA 2005). Influent and effluent nitrogen species and phosphates were analysed in accordance with Standard Methods (APHA 2005). All the soluble fractions were filtered using

0.45 mm cellulose acetate filters, and all samples were analysed on the day of collection. An average of the influent measurements during the entire experiment is provided in Table 7.2. In addition, on-line measurements of ammonia (Amtax®, Hach Lange), nitrates and nitrites (Nitratax®, Hach Lange) and phosphates (Phosphax®, Hach Lange) from the effluent were recorded every 10 seconds during the whole experiment. The plant was operated at a constant sludge retention time of 25 ± 2 days, with a constant concentration of solids throughout the experiment (Table 7.1).

Table 7.2 | Influent characteristics.

| Measurement | Units | Value | Standard deviation |
|----------------------------------|------------------------------------|--------|--------------------|
| COD total | mg O ₂ ·L ⁻¹ | 211.50 | 73.35 |
| soluble | mg O ₂ ·L ⁻¹ | 77.59 | 74.74 |
| TKN total | mg N ·L ⁻¹ | 26.80 | 14.23 |
| soluble | mg N ·L ⁻¹ | 20.86 | 14.65 |
| NH ₄ ⁺ -N | mg N ·L ⁻¹ | 20.51 | 11.15 |
| NO _x ⁻ -N | mg N ·L ⁻¹ | 0.42 | 0.18 |
| PO ₄ ³⁻ -P | mg P ·L ⁻¹ | 1.58 | 1.07 |
| Influent TSS | mg ·L ⁻¹ | 150 | 111 |

BATCH TESTS FOR BIOLOGICAL NUTRIENT REMOVAL RATES

Batch tests were carried out for Experiment A at 1.5, 1, 0.5 and 0 mg O₂ ·L⁻¹ and for Experiment B at the beginning and the end of the experiment; these batch tests were used to determine the biological activity of the polyphosphate-accumulating organisms (PAO) and denitrifying PAO (DPAO) responsible for aerobic and anoxic phosphorus removal based on Monclús et al. (2010a).

The oxidation of ammonium to nitrite by ammonium oxidising bacteria (AOB) and nitrite-oxidising bacteria (NOB) were also tested using batch experiments at 1.5, 0.5 and 0 mg O₂ ·L⁻¹ in Experiment A and at the beginning and the end of Experiment B. The flasks were inoculated with 2 L of sludge from the MBR after washing them three times with tap water. Predetermined amounts of NaHCO₃ and NH₄Cl were added as a feed to enable nitrification under oxygen saturation. Samples were taken every 15 minutes, and NO₃⁻-N, NO₂⁻-N and TSS concentrations were measured and recorded.

SLUDGE CHARACTERISATION

The sludge characterisation was performed by analysing sludge samples from the membrane tank 3 times per week in Experiment A and 5 times per week in Experiment B. The characterisation was based on the analysis of soluble microbial products (SMP), the protein analysis (Frolund et al. 1995) and the polysaccharide (Dubois et al. 1956) fractions. Due to high concentrations of activated sludge, the diluted sludge volumetric index (DSVI) was considered using the methodology described by Lee et al. (1983). Particle size distribution (PSD) analyses were carried out using an LS 13320 Multi-Wavelength Particle Size Analyser. In addition, relative hydrophobicity, expressed as percentage of hydrophobic sludge, was performed using the protocol described by Rosenberg (1980). Microscopic examinations were performed using a Nikon model Eclipse E200 microscope, and the microscope pictures were recorded using the Zeiss KS100.3 software. Microscopic analysis was used to determine the filamentous index (FI) based on the method for filamentous bacteria abundance scoring suggested by Eikelboom (2000). The capillarity suction time (CST) (Triton electronics Ltd., type 304 B, (Scholz 2005)) was used daily to determine the dewaterability of the sludge, and a sludge filterability test was also performed daily (Monclús et al. 2011). Differences among samples were determined by 1-way ANOVA, where a p-value <0.05 was considered significant. All statistical calculations were generated using Microsoft Excel 2007 (Microsoft).

FOULING AND FILTRATION PERFORMANCE

The transmembrane pressure (TMP) and the fouling rate (FR) calculations were recorded every 10 seconds. The FR per cycle was obtained as the slope of all TMP values for each cycle according to the equation 7.1, following the procedure described by Monclús et al. (2011):

$$FR = \left(\frac{dTMP}{dt} \right)_{\text{cycle}} \quad (\text{mbar} \cdot \text{s}^{-1}) \quad (\text{eq. 7.1})$$

Moreover, the irreversible fouling that was not recovered by physical cleaning was calculated by comparing the initial values of two consecutive cycles using equation 2:

$$F_{irr} = \frac{TMP_2 - TMP_1}{t_2 - t_1} \quad (\text{mbar} \cdot \text{d}^{-1}), \quad (\text{eq. 7.2})$$

where TMP_1 and TMP_2 are the TMP (in mbar) at the beginning of the two consecutive cycles and t_1 and t_2 their corresponding times (days).

Additionally, at the beginning and end of the experiments, a flux step test was used to determine the critical flux based on the protocol of Tiranuntakul et al. (2011).

7.3 RESULTS

7.3.1 EXPERIMENT A: MODIFICATION OF THE DO SET-POINT IN THE AEROBIC COMPARTMENT

EFFECTS ON BIOLOGICAL NUTRIENT REMOVAL

Decreasing the aerobic DO set-point led to significant changes in the nutrient removal performance (Figure 7.2). Regarding the ammonium concentration, complete nitrification efficiencies were achieved above the $0 \text{ mg O}_2 \cdot \text{L}^{-1}$ DO set-point, with effluent concentrations below $0.1 \text{ mg NH}_4^+ \cdot \text{N} \cdot \text{L}^{-1}$. Then, with an aerobic DO at $0 \text{ mg O}_2 \cdot \text{L}^{-1}$, $\text{NH}_4^+ \cdot \text{N}$ increased up to $12 \text{ mg NH}_4^+ \cdot \text{N} \cdot \text{L}^{-1}$. Nitrification tests showed a 30% decrease in the nitrification rate from the start of the experiment until the end (Table 7.3). With respect to denitrification, peaks of NO_x^- that exceeded the standard limits were reached when operating at $1.5 \text{ mg O}_2 \cdot \text{L}^{-1}$ of DO; however, at $0.5 \text{ mg O}_2 \cdot \text{L}^{-1}$, an improvement in the denitrification rate was achieved without increasing the ammonium concentration. Thus, as observed by Sarioglu et al. (2008), simultaneous nitrification and denitrification were most likely occurring at $0.5 \text{ mg O}_2 \cdot \text{L}^{-1}$. The overall total nitrogen concentration decreased as much as 30%, from $13.36 \pm 3.70 \text{ mg N} \cdot \text{L}^{-1}$ (the DO set-point at $1.5 \text{ mg O}_2 \cdot \text{L}^{-1}$) to $9.39 \pm 3.70 \text{ mg N} \cdot \text{L}^{-1}$ (when operating at $0.5 \text{ mg O}_2 \cdot \text{L}^{-1}$).

In the case of phosphorous removal, anaerobic plus anoxic conditions stimulated the development of denitrifying phosphate-accumulating organisms (DPAOs). Table 7.3 summarises the evolution of the phosphate accumulating organisms (PAO) and the DPAO activity. The P_{release} activities were mostly constant throughout the experiment, with a slight decrease from 6.41 to $5.16 \text{ mg P} \cdot \text{gVSS}^{-1} \cdot \text{h}^{-1}$ in PAOs and 4.97 to $3.94 \text{ mg P} \cdot \text{gVSS}^{-1} \cdot \text{h}^{-1}$ in DPAOs. Regarding P_{uptake} , PAO P_{uptake} activity was higher than that of DPAOs, as has been observed elsewhere (Oehmen et al. 2007), with a decrease in both communities of 47% in PAOs and 44% in DPAOs activities

throughout the experiment. Specifically, the P_{uptake} rate decreased twice as much as the P_{release} rates, which is evident in the phosphate concentration increase with the aerobic DO set-point of $0.5 \text{ mg O}_2 \cdot \text{L}^{-1}$ (Figure 7.2). Therefore, under these conditions, there was an accumulation of phosphorous in the system up to values of $8 \text{ mg PO}_4^{3-} \cdot \text{P} \cdot \text{L}^{-1}$.

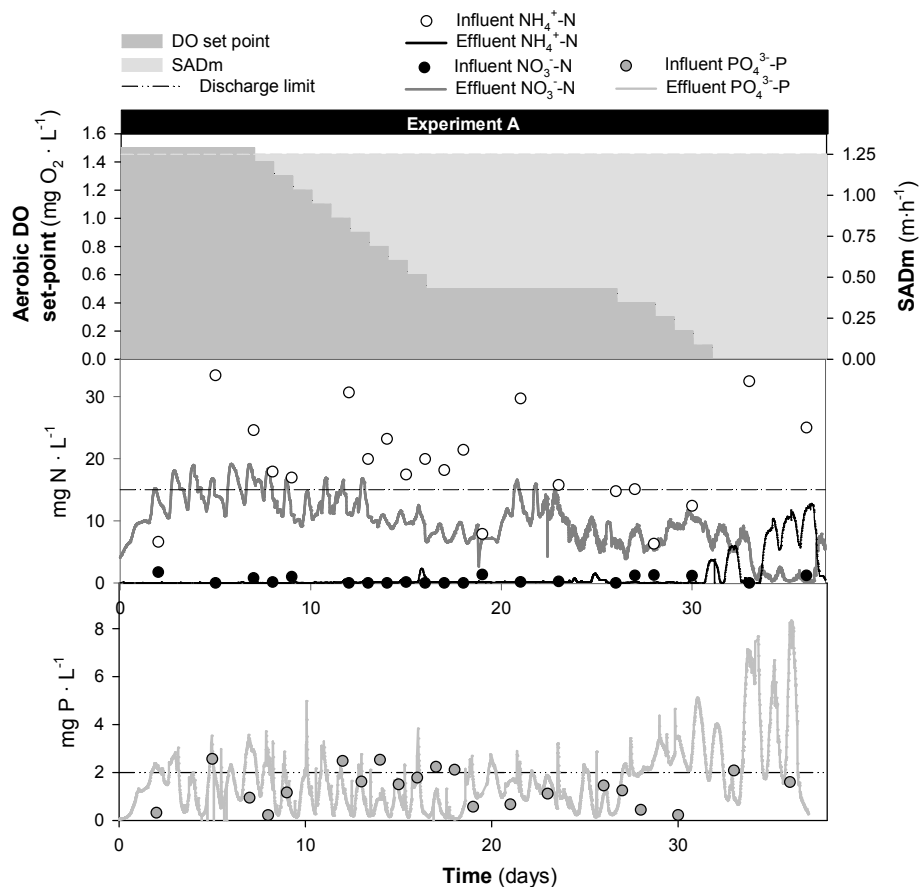


Figure 7.2 | Evolution of nutrient concentrations in the effluent and influent grab samples along the aerobic DO set-point modification.

Table 7.3 | AOB, NOB, PAOS and DPAOS in Experiment A.

| | | Parameter | Units | Aerobic DO set-point ($\text{mg O}_2 \cdot \text{L}^{-1}$) | | | |
|------------------------|--|----------------------|--|--|--|------|------|
| | | | | 1.5 | 1.0 | 0.5 | 0 |
| Nitrogen | Nitrification test | NO_x^- rate | $\text{mg N} \cdot \text{gVSS}^{-1} \cdot \text{h}^{-1}$ | 3.38 | -- | 2.60 | 2.34 |
| | | Phosphorous removal | PAO test | $P_{\text{rel.}}$ rate | $\text{mg P} \cdot \text{gVSS}^{-1} \cdot \text{h}^{-1}$ | 6.41 | 6.48 |
| $P_{\text{upt.}}$ rate | $\text{mg P} \cdot \text{gVSS}^{-1} \cdot \text{h}^{-1}$ | | | 10.20 | 8.56 | 8.88 | 5.37 |
| DPAO test | $P_{\text{rel.}}$ rate | | $\text{mg P} \cdot \text{gVSS}^{-1} \cdot \text{h}^{-1}$ | 4.97 | 4.82 | 4.85 | 3.94 |
| | $P_{\text{upt.}}$ rate | | $\text{mg P} \cdot \text{gVSS}^{-1} \cdot \text{h}^{-1}$ | 4.02 | 3.81 | 3.02 | 2.24 |
| % DPAO | PUR ratio | | | 0.39 | 0.35 | 0.33 | 0.37 |

EFFECTS ON SLUDGE CHARACTERISTICS

The PSD decreased throughout the entire experimental period. Although the median of the particle sizes was maintained ($139.44 \pm 9.31 \mu\text{m}$), smaller particles were observed at the end of the experiment. This reduction was noticed in the 90th percentile, which decreased 20% from $194.10 \pm 20.01 \mu\text{m}$ to $153.23 \pm 14.20 \mu\text{m}$ (significant differences ($p=0.003$) were found between means).

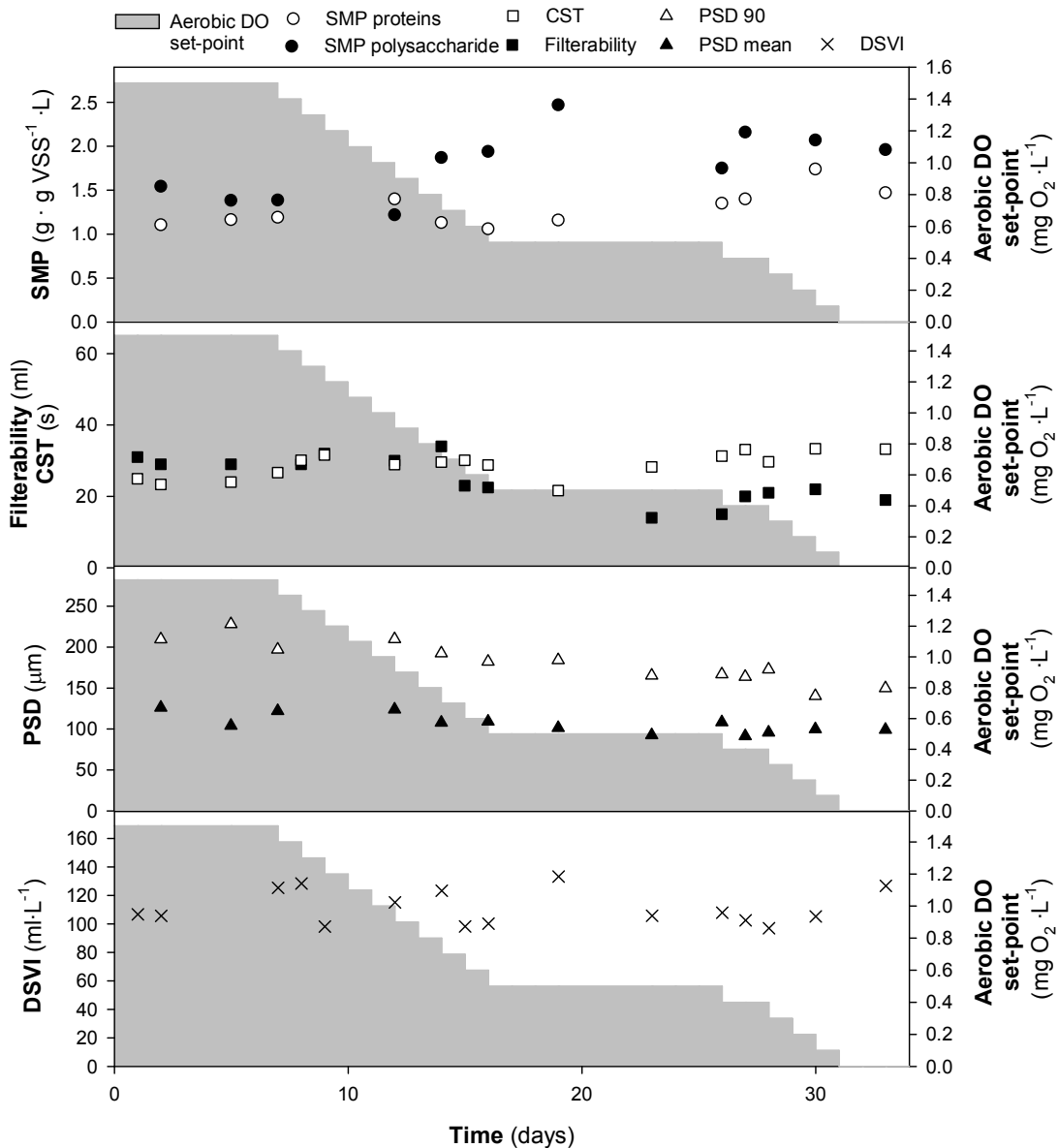


Figure 7.3 | Sludge characteristics evolution in Experiment A.

SMP analysis revealed an increase in protein ranging from 1.06 ± 0.32 to 1.74 ± 0.28 mg SMP · L · g SSV⁻¹ and an increase in the polysaccharide fraction from 1.14 ± 0.46 to 2.06 ± 0.23 mg SMP · L · g SSV⁻¹.

In addition, significant differences were found in the protein fraction ($p=0.034$). Relative hydrophobicity values remained constant, with values of $80.7 \pm 7.1\%$, reinforced by the statistical analysis ($p=0.084$). The number of filaments obtained by microscopic analysis did not show any increase in the filamentous index (always between 2 and 3) at the lowest DO concentrations, and the DSVI values were 138 ± 19 mL · mg⁻¹ ($p=0.722$). However, proliferation of *Spirillum spp.* in the system was observed. A decrease in the filterability (3.55 ± 0.21 to 2.85 ± 0.18 mL · g SSV⁻¹ · L) and an increase in CST (3.86 ± 0.51 to 4.50 ± 0.26 s · g SSV⁻¹ · L) were also observed when comparing values above and below 0.5 mg O₂ · L⁻¹. Filterability values were consistently different, while CST values were significantly different ($p=0.001$).

EFFECTS ON FILTRATION PERFORMANCE

There was an increase in the TMP and the FR during the experimental period. Specifically, the TMP values increased from 70 to 175 mbars, while FR rose 75% from the beginning to the end of the experiment (Figure 7.4). However, both changes were greater when the aerobic DO set-point values were lower than 0.5 mg O₂ · L⁻¹, which can be identified as the lower limit for the DO set-point. When DO values were below 0.5 mg O₂ · L⁻¹, the TMP ranged from 100 mbars to 175 mbars and the FR values doubled. When operating at 0 mg O₂ · L⁻¹, the FR values exceeded the FR critical condition values of 0.008 mbar · s⁻¹ (Monclús et al. 2010b) (see A1, A2 and A3 in Figure 7.4). Irreversible fouling was also observed; when working above 0.5 mg O₂ · L⁻¹, F_{irr} showed an average TMP increase of 1.05 mbar · day⁻¹, whereas below 0.5 mg O₂ · L⁻¹, F_{irr} values increased 6.94 mbar · day⁻¹.

The flux step tests indicated a reduction of the critical flux by 36%, from 27.5 LMH at the beginning to 17.5 LMH at the end of Experiment A; this indicates that the system was operated over the critical conditions, and it explains the high increase in fouling (Figure 7.4).

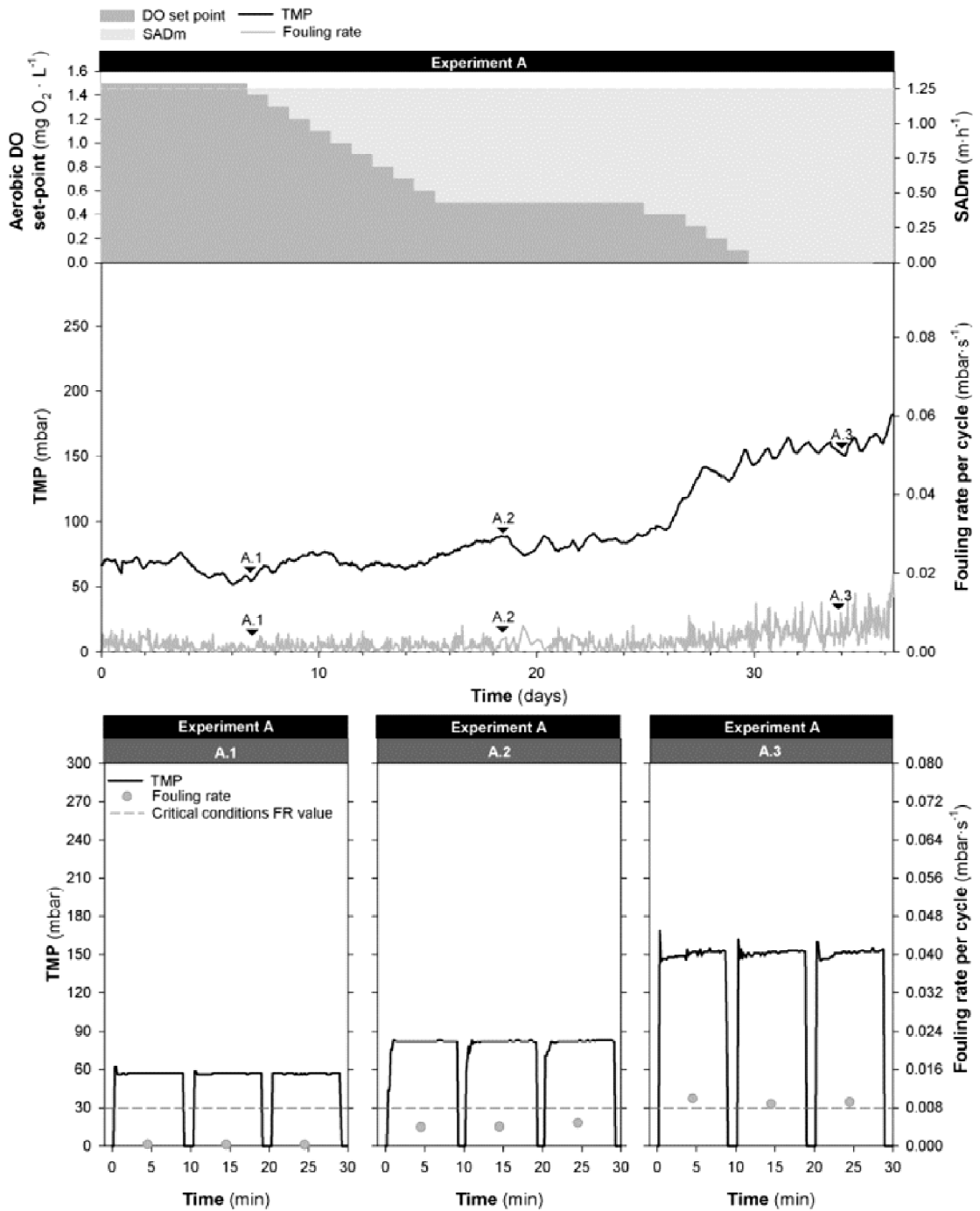


Figure 7.4 | Evolution of the TMP and the fouling rates during the aerobic DO set-point modification in Experiment A. A.1, A.2 and A.3 illustrate the evolution of the TMP and the fouling rates three experimental cycles operating at 1.5, 0.5 and 0 mg O₂ · L⁻¹, respectively.

7.3.2 EXPERIMENT B: MODIFICATION OF THE AIR-SCOURING FLOW IN THE MEMBRANE COMPARTMENT

EFFECTS ON BIOLOGICAL NUTRIENT REMOVAL

Although the experiment lasted for two weeks, the effects of the membrane air-scouring flow modification on nutrient removal were observed almost immediately (Figure 7.5). Membrane aeration reduction led to an increase in anoxic zones that were detrimental to the aerobic zones. Therefore, a decrease in nitrates and an increase in ammonium were observed. As a consequence, the effluent $\text{NH}_4^+\text{-N}$ concentrations exceeded the discharging limit ($5 \text{ mg N}\cdot\text{L}^{-1}$). However, when membrane aeration was increased again to an SAD_m value of $1.25 \text{ m}\cdot\text{h}^{-1}$, the total N removal efficiency recovered. In comparison with Experiment A, similar nitrification rates were identified (Table 7.4). However, the influent varied on the 8th day of the experiment with lower ammonium and phosphate concentrations, and the lower concentrations were reflected in the effluent discharge.

Table 7.4 | AOB, NOB, PAOS and DPAOS activities in Experiment B.

| Nutrient | Test | Parameter | Units | Air-scouring flow at $10 \text{ m}^3\cdot\text{h}^{-1}$ | |
|-------------|--------------------|------------------------|--|---|--------|
| | | | | Day 0 | Day 14 |
| Nitrogen | Nitrification test | NO_x^- rate | $\text{mg N}\cdot\text{gVSS}^{-1}\cdot\text{h}^{-1}$ | 3.04 | 3.02 |
| | | | | | |
| Phosphorous | Test PAO | $P_{\text{rel.}}$ rate | $\text{mg P}\cdot\text{gVSS}^{-1}\cdot\text{h}^{-1}$ | 5.83 | 5.67 |
| | | $P_{\text{upt.}}$ rate | $\text{mg P}\cdot\text{gVSS}^{-1}\cdot\text{h}^{-1}$ | 10.54 | 9.17 |
| | Test DPAO | $P_{\text{rel.}}$ rate | $\text{mg P}\cdot\text{gVSS}^{-1}\cdot\text{h}^{-1}$ | 4.41 | 4.93 |
| | | $P_{\text{upt.}}$ rate | $\text{mg P}\cdot\text{gVSS}^{-1}\cdot\text{h}^{-1}$ | 3.30 | 2.97 |
| | % DPAO | PUR ratio | | 0.32 | 0.32 |

Phosphorous removal was not affected by the membrane aeration decrease, as shown in Figure 7.4. The PAOs and the DPAOs tests demonstrated that both the PUR ratio and the aerobic and anoxic phosphorous release rates and the phosphorous uptake were essentially maintained (Table 7.4).

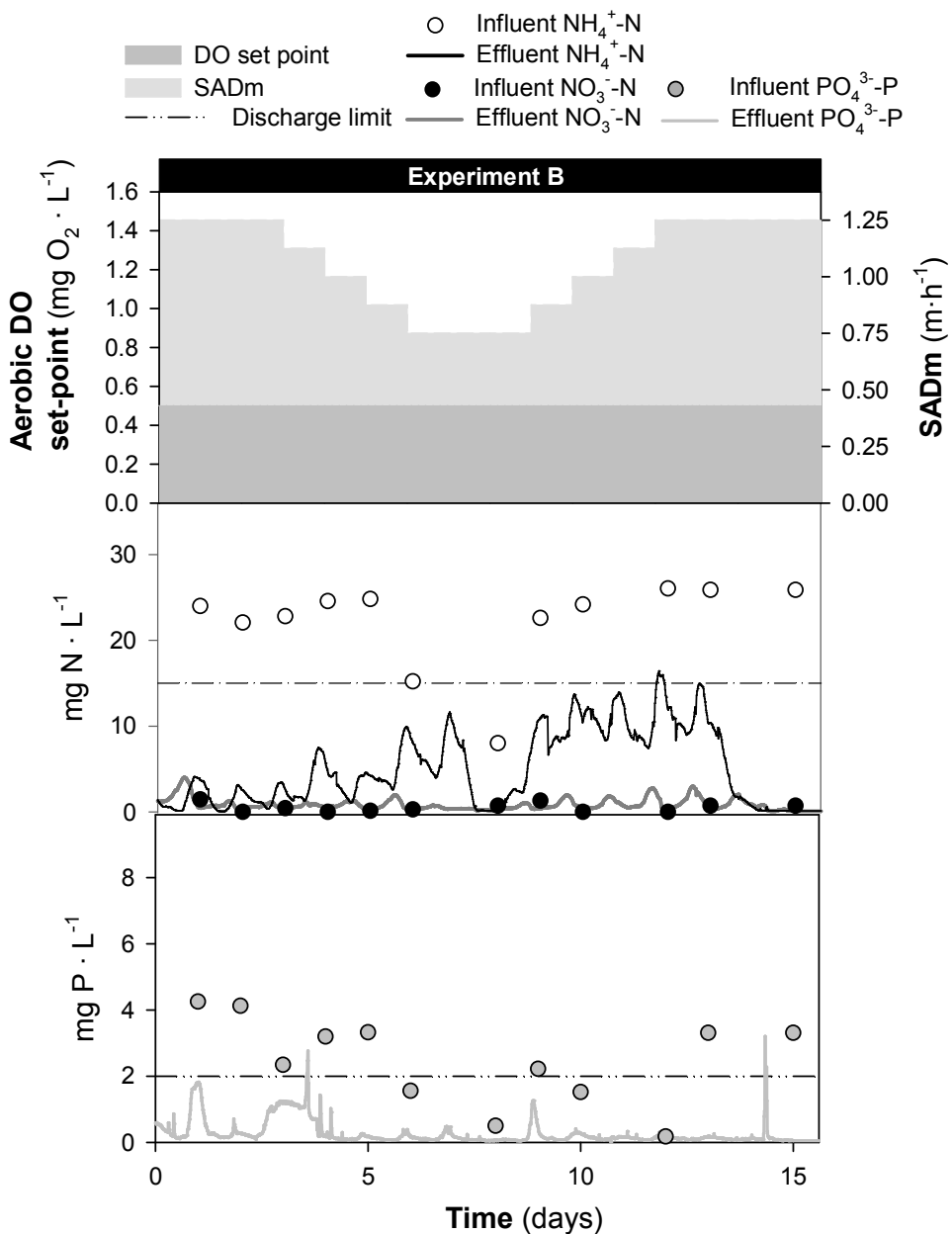


Figure 7.5 | Evolution of the nutrient concentrations in the effluent and influent grab samples during the membrane air-scouring flow rate modification of Experiment B.

EFFECTS ON SLUDGE CHARACTERISTICS

The PSD did not show any significant differences ($p > 0.050$) during the experiment; the average particle size was $125 \pm 10 \mu\text{m}$, and the 90th percentile of the particles was $243 \pm 23 \mu\text{m}$.

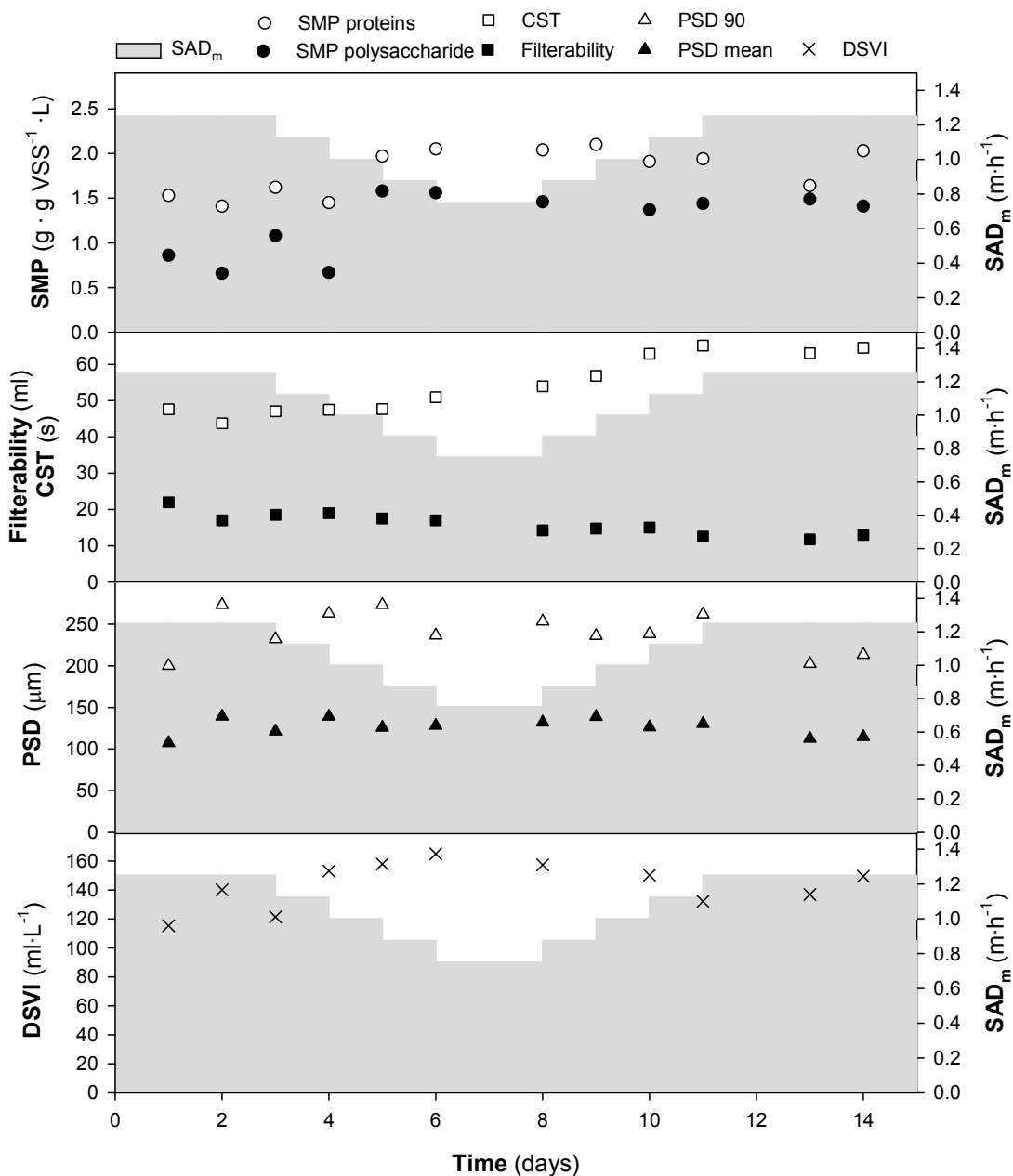


Figure 7.6 | Sludge characteristics evolution in Experiment B.

The polysaccharide SMP increased by 19.5% when SAD_m was less than 1 m · h⁻¹ (from 1.62 ± 0.15 to 1.94 ± 0.19 g · mg VSS⁻¹), and the protein fraction increased by 20% (from 1.08 ± 0.11 to 1.29 ±

0.13 g·mg VSS⁻¹). Despite of the increment, statistical analysis did not show significant differences. In contrast to the SMP results, the relative hydrophobicity of the sludge decreased from 80% to 30% with the air-scouring flow rate reduction. However, hydrophobicity increased to values similar to the initial values when aeration was restored. No changes in the filamentous bacteria index were noticed (the index remained between 2 and 3); there were no significant changes observed in the DSVI ($127 \pm 16.36 \text{ mL}\cdot\text{mg}^{-1}$), either. Filterability values decreased 15% when the air-scouring flow rate decreased to SAD_m values lower than 1 m·h⁻¹. A similar trend was observed for CST, with values rising from $4.99 \pm 0.22 \text{ s}\cdot\text{VSS}^{-1}$ to $5.90 \text{ s}\cdot\text{VSS}^{-1}$ for SAD_m values below 1 m·h⁻¹, and means were significantly different ($p=0.025$).

EFFECT ON FILTRATION PERFORMANCE

A reduction in the air-scouring flow rate, measured as SAD_m, from 1.25 to 0.75 m·h⁻¹ resulted in a rise in the TMP from 50 to 100 mbar (Figure 7.7). There was also an increase of approximately 99% in the FR, compared to the initial values. Moreover, the subsequent SAD_m increase (from 0.75 to 1.25 m·h⁻¹) did not result in a TMP recovery. At the beginning of Experiment B, the FRs were higher than in the beginning of Experiment A. However, the FR values (Figure 7.4-B.2) agree with the values observed in Experiment A under the same operating conditions (Figure 7.7-A.2). The irreversible fouling, F_{irr}, values were calculated to be 1.18 mbar·d⁻¹ when the air-scouring flow decreased from 1.25 to 1 m·h⁻¹ and were 17.68 mbar·d⁻¹ when the air-scouring flow was reduced from 1 to 0,75 m·h⁻¹. F_{irr} increased to 22.57 mbar·d⁻¹ after increasing the air-scouring from 0.75 to 1.25 m · h⁻¹; this shows that the TMP did not recover. The critical flux decreased from 27.5 LMH to 12.5 LMH from the beginning to the end of the experiment, i.e., a reduction of 56%, which corroborated the deterioration of the filtration performance. This confirms that the last part of the experiment was operated over a critical flux.

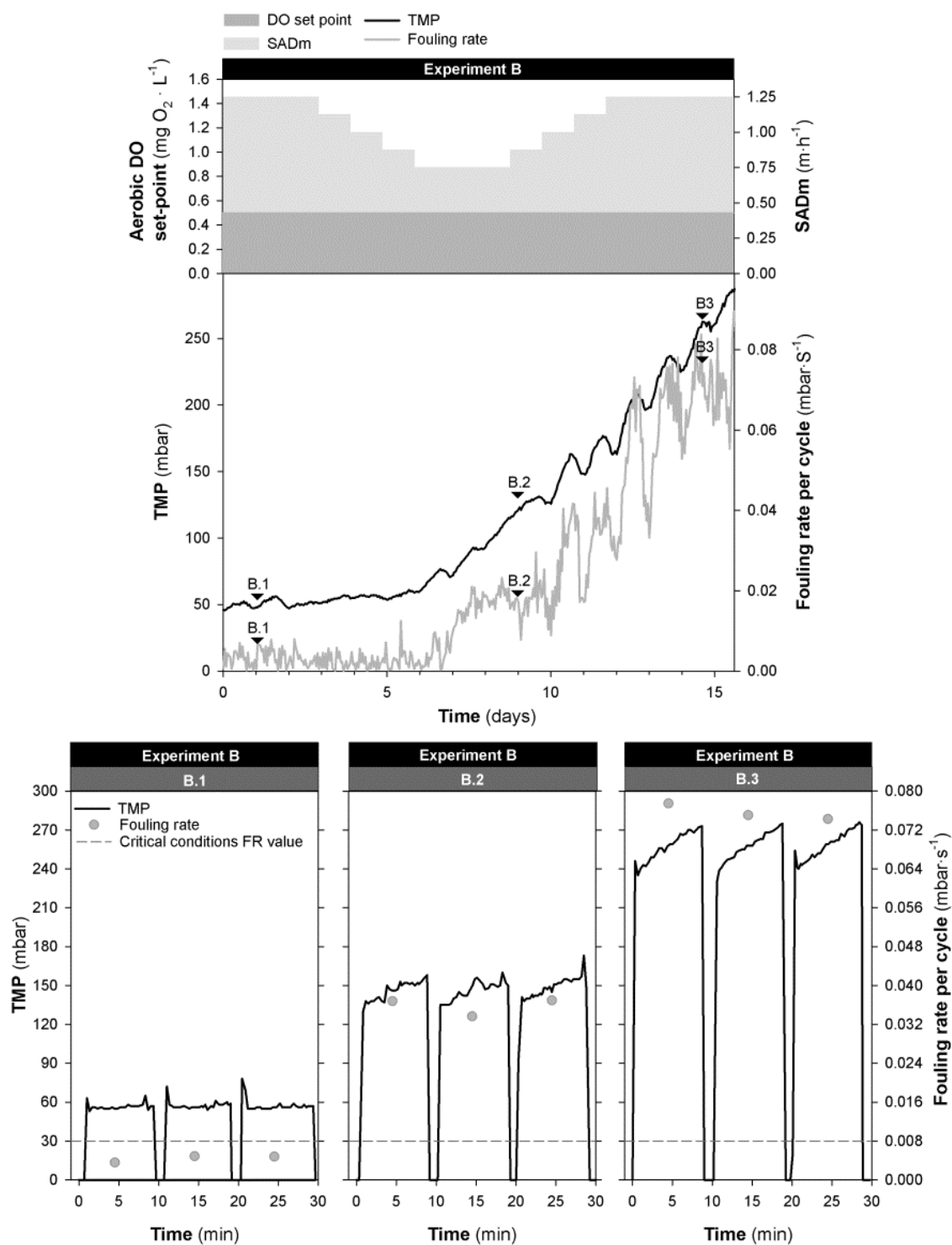


Figure 7.7 | The evolution of the TMP and the fouling rates during the membrane air-scouring flow modification in Experiment B. B.1, B.2 and B.3 illustrate the evolution of the TMP and the fouling rate of three specific filtration cycles working at different SAD_m values (1.25, 0.75 and 1.25 mbar·s⁻¹) on day 1, 8 and 14, respectively.

7.4 DISCUSSION

The results presented in this study reveal the importance of the interrelations between biological nutrient removal processes, filtration processes and sludge characteristics and establish the basis for the development of integrated control strategies for the two most important control parameters in MBR: biological and membrane aeration. The Discussion has thus been divided in four sections: a) biological nutrient removal, b) sludge characteristics, c) filtration performance and d) the evaluation of energy savings.

7.4.1 BIOLOGICAL NUTRIENT REMOVAL

Biological and membrane aeration reductions of 66% and 20%, respectively, were carried out. These reductions had positive effects on nutrient removal efficiencies because denitrification was improved and nitrification was complete in the membrane compartment. Even in a system in which the membrane tank is double the volume of the aerobic compartment, it is necessary to maintain a minimum of $0.5 \text{ mg O}_2 \cdot \text{L}^{-1}$ in the aerobic compartment. Lower DO set-point values in the aerobic compartment lead to a severe deterioration of sludge flocs and reduce biological nutrient removal processes due to lower transfer efficiency caused by coarse-bubble aeration in the membrane compartment compared to fine-bubble aeration in the aerobic tank (Rosso et al. 2008).

MBR operational conditions typically enhance nitrification, especially under stress conditions (Liebig et al. 2001); however, the activity of nitrifiers was significantly reduced (33%) when the DO set-point was decreased to values lower than $0.5 \text{ mg} \cdot \text{L}^{-1}$ or when the SAD_m decreased lower than $1 \text{ m} \cdot \text{h}^{-1}$. In addition, for both cases, it was revealed that the nitrogen removal efficiencies recovered after aeration was increased again.

Phosphorous evolution is directly related to NO_x^- concentrations in the biological nutrient removal system. This was observed in the results shown in Figure 7.2, where PO_3^{4-} is not stable due to the lack of oxygen under $0.5 \text{ mg O}_2 \cdot \text{L}^{-1}$, and the conditions are not suitable to uptake phosphorous completely. However, Experiment B (Figure 7.5) demonstrated that an aerobic DO set-point of $0.5 \text{ mg O}_2 \cdot \text{L}^{-1}$ was sufficient to ensure enhanced biological phosphorous removal despite the decrease in air-scouring flow. Both aeration experiments showed similar trends

regarding P removal efficiencies according to the PAOs and DPAOs tests, but with a greater decrease of the P_{uptake} in Experiment A under $0.5 \text{ mg O}_2 \cdot \text{L}^{-1}$ and minor changes in the P_{release} ratio. According to Kuba et al. (1996), the rate of P_{uptake} by PAOs under anoxic conditions is generally lower than that under aerobic conditions. Some authors have noted the existence of two different groups of PAOs (Oehmen et al. 2007) and have debated whether PAOs and DPAOs are the same organisms. The ratio of DPAO/PAO (P_{uptake} rate, PUR) was relatively constant in our experiments, which suggests that DPAOs are PAOs capable of utilising nitrate as an electron acceptor.

7.4.2 SLUDGE CHARACTERISTICS

The sludge characteristics deteriorated when the DO set-point was lowered to values below $0.5 \text{ mg O}_2 \cdot \text{L}^{-1}$. This decrease led to smaller sludge particles. A 25% decrease in the average PSD was observed due to the reduction of the bigger particles, which intensify the fouling propensity, even though the median size of the particles was maintained. In anaerobic MBRs similar results were found, where lower aggregate sizes were identified due to high dispersive growth associated to the anaerobic systems, leading to high fouling propensities (Martin-Garcia et al. 2011). Faster FR were observed when the DO set-point values were lower than $0.5 \text{ mg O}_2 \cdot \text{L}^{-1}$ because small particles in the solution were deposited on the membrane surface intensifying the fouling propensity. Air-scouring flow rate changes in the membrane tank did not significantly affect the PSD. Lower filterability values were observed at concentrations below $0.5 \text{ mg O}_2 \cdot \text{L}^{-1}$, which is in agreement with the results of Wilén and Bálmer (1999). Regarding the SMP in Experiments A and B, the polysaccharide fractions increased by 20% and 15%, respectively, and the protein fractions increased up to 20% and 19%, respectively, because the low DO set-points and the low air-scouring flow rates intensified the stress of the microorganisms and enabled greater release of EPS (Gao et al. 2011). The results achieved in this study are also in agreement with those of Arabi and Nakhla (2009), who observed higher carbohydrate SMP concentrations in a simultaneous nitrification and denitrification MBRs, determining that anoxic conditions impact membrane fouling more than the shear rate.

In addition, a rapid reduction of relative hydrophobicity was observed when the membrane air-scouring flow rate SAD_m values were below $1 \text{ m} \cdot \text{h}^{-1}$. Lower relative hydrophobicity values are

correlated with increased fouling because of the hydrophilic characteristics of the membranes and the higher flock deterioration (Van den Broeck et al. 2011). Other studies have shown similar behaviour of relative hydrophobicity and fouling propensity in MBR pilot plants (Arabi and Nakhla 2009) or full-scale municipal MBRs (Van den Broeck et al. 2011).

Biological aeration affects the properties of the sludge and has an effect on the deterioration of the filtration performance, which was observed for the PSD, the CST, the filterability and the SMP. However, sludge characteristics also deteriorated when the membrane air-scouring flow rate decreased; there was a noteworthy decrease in hydrophobicity and significant changes in the SMP, the filterability and the CST.

Filamentous bacteria did not show any specific changes in either of the experiments, with the DSVI confirming the filamentous index results. Although Ma et al. (2013) noted that some filamentous bacteria are related to membrane fouling, the presence of *Spirillum spp.* bacteria has not been reported to have an effect on the filtration efficiency.

7.4.3 FILTRATION PERFORMANCE

A DO set-point of $0.5 \text{ mg O}_2 \cdot \text{L}^{-1}$ in the aerobic tank and an SAD_m of $1 \text{ m} \cdot \text{h}^{-1}$ in the membrane tank are the optimal values for the filtration performance of this pilot plant based on the TMP, the FR and the F_{irr} values. For operational conditions with lower aeration, in both the aerobic and the membrane tanks, the TMP and the FR values doubled and irreversible fouling was observed (Figure 7.4 and Figure 7.7). However, higher irreversible fouling was observed in Experiment B with an F_{irr} value 2.5 times higher than in Experiment A (from 0.5 to $0 \text{ mg O}_2 \cdot \text{L}^{-1}$ and from 1 to $0.75 \text{ m}^3 \cdot \text{h}^{-1}$). Moreover, when decreasing the membrane aeration so that SAD_m values were below $1 \text{ m} \cdot \text{h}^{-1}$, Experiment B also experienced reversible fouling, with FR values 10 times higher than in Experiment A.

After operating with SAD_m values lower than $1 \text{ m} \cdot \text{h}^{-1}$ in Experiment B, the following aeration increase did not provide any recovery for the TMP; an F_{irr} of $25.83 \text{ mbar} \cdot \text{day}^{-1}$ was observed. In addition, despite achieving the same initial aeration conditions ($\text{SAD}_m = 1.25 \text{ m} \cdot \text{h}^{-1}$), the observed FRs at the end of the experiments were 99% higher. The optimal aeration conditions enabled the reactor to operate with FRs lower than $0.008 \text{ mbar} \cdot \text{s}^{-1}$; operating at higher FR values is a

determinant for critical conditions. These operational critical conditions were reinforced by the critical flux values, which decreased 1.6 and 2.3 times compared to the initial conditions in Experiments A and B, respectively. A non-returnable point was observed when working at an aerobic DO set-point below $0.5 \text{ mg O}_2\cdot\text{L}^{-1}$ and with SAD_m values lower than $1 \text{ m}\cdot\text{h}^{-1}$; operating under these conditions resulted in requiring chemical cleaning to recover stable conditions.

It could be concluded that the fouling propensity in Experiment A is due to the deterioration of the sludge, which is caused by an increase in SMP fractions and a reduction of the PSD, causing increased fouling. This was reflected by the filterability decrease and the CST increase. In Experiment B, despite similar changes in sludge characteristics, a reduction of the SAD_m directly deteriorated the sludge characteristics (SMP increased, filterability and relative hydrophobicity were reduced and CST increased) and increased the fouling phenomenon.

7.4.4 ENERGY EFFICIENCIES

Aerobic aeration can be reduced up to 81% (at $0.5 \text{ mg O}_2\cdot\text{L}^{-1}$, decreasing aeration flow from 5.74 to $1.08 \text{ m}^3\cdot\text{h}^{-1}$), and membrane aeration can be reduced up to a 20% (at $1 \text{ m}\cdot\text{h}^{-1}$ of SAD_m , which represents a decrease of air-scouring from 10 to $8 \text{ m}^3\cdot\text{h}^{-1}$). With these operational conditions, filtration performance and sludge characteristics were not negatively affected and nutrient removal efficiency was improved. Therefore, the optimised total air flow rate was $9.08 \text{ m}^3\cdot\text{h}^{-1}$, and the initial value was $15.79 \text{ m}^3\cdot\text{h}^{-1}$. The average airflow rate saved was 42%, which, when using a centrifugal blower, represents an energy savings of 75% compared to the initial operating conditions.

7.5 CONCLUSIONS

Interrelations between biological nutrient removal processes, filtration processes and sludge characteristics determine the strategies for the integrated control of the two most important operating parameters in MBRs: biological and membrane aeration. Optimal values include a DO set-point of $0.5 \text{ mg O}_2\cdot\text{L}^{-1}$ or an SAD_m of $1 \text{ m}\cdot\text{h}^{-1}$ (75% of energy reduction), during which the membrane compartment can be used to complete nitrification even though denitrification was favoured due to simultaneous nitrification/denitrification. Filtration performance and sludge

characteristics were not negatively affected. An irreversible point was noted when operating under the optimal conditions: the BNR and the sludge characteristics deteriorated, and chemical cleaning was required to recover the original conditions.

RESULTS V:

**FULL-SCALE VALIDATION OF A
CONTROL SYSTEM FOR ENERGY
SAVING IN MEMBRANE BIOREACTORS
FOR WASTEWATER TREATMENT**

Redrafted from:

Monclús, H., Dalmau, M., Ferrero, G., Gabarron, S., Comas, J, Rodriguez-Roda, I.

*Full-scale validation of a control system for energy saving in
membrane bioreactors for wastewater treatment.*

Submitted

8.1 OVERVIEW

Since the late 1990s, several improvements in the operational conditions of filtration and the decrease in the total capital expenditure required for the MBRs has led to its wider adoption in municipal wastewater treatment facilities (Ferrero et al. 2012). According to market expansion stabilisation at the turn of the 21st century, MBR technology is currently a consolidated technology (Judd 2011, Santos et al. 2011, Lesjean et al. 2009).

The energy requirements of MBR systems are greater than the requirements of conventional activated sludge systems coupled with tertiary treatment. One of the parameters that significantly contributes to the total operational cost is membrane aeration (Santos et al. 2011, Verrecht et al. 2010). Because membrane aeration represents between 25-50% of the operational costs (Judd, 2011), several new automatic control systems or module configurations have focused on aeration reduction (i.e., reusing the air-scouring between different modules or using intermittent aeration) (Judd 2011, Verrecht et al. 2008, Drews 2010). However, robust control systems that are capable of reducing aeration requirements while maintaining optimum filtration performance are lacking. Ferrero et al. (2012) compared different control systems that aimed to reduce operational costs by modifying operational conditions (flux, cycle length, etc.). These authors stressed that the number of patents and scientific publications regarding control systems for membrane bioreactors remains very limited. In addition, the patents are usually very general and based on large assumptions to cover a wide spectrum of intellectual property. However, these statements are not always scientifically proven or validated, at least for long term conditions (Ferrero et al. 2012). There are very few research publications on control systems that have been developed at the pilot scale, and none of these systems has been validated in closed-loop at full scale (Huyskens et al. 2011, Lorain et al. 2010).

The membrane air-scouring flow rates that are adopted in practice are generally very conservative according to the manufacturers' recommendations. The most recent developments on the module configuration and aeration strategies have resulted in considerable improvements (i.e., using cyclic aeration for hollow fiber membranes (Barillon et al. 2013). However, in most cases, the air-scouring flow rate remains fixed in most cases regardless of the sludge quality or membrane permeability. Thus, automatic control systems are needed to optimise aeration in termf of the membrane performance and sludge characteristics.

Ferrero et al. (2011a) developed a control algorithm for air-scouring reduction based on permeability evolution, which was successfully tested at the pilot scale (Ferrero et al. 2011b). This control system was patented and registered as Smart Air MBR®.

The aim of this chapter is to report a full-scale validation of this MBR air-scouring control system and to illustrate that energy savings can be achieved without affecting the filtration process performance, the nutrient removal efficiencies or the sludge characteristics.

8.2 MATERIALS AND METHODS

8.2.1 LA BISBAL D'EMPORDÀ WWTP

The membrane air-scouring control system was validated over two years at La Bisbal d'Empordà WWTP (LBE, North East of Spain). This full-scale MBR plant (Figure 8.1) was designed to treat a maximum daily flow rate of 3200 m³ of municipal wastewater.

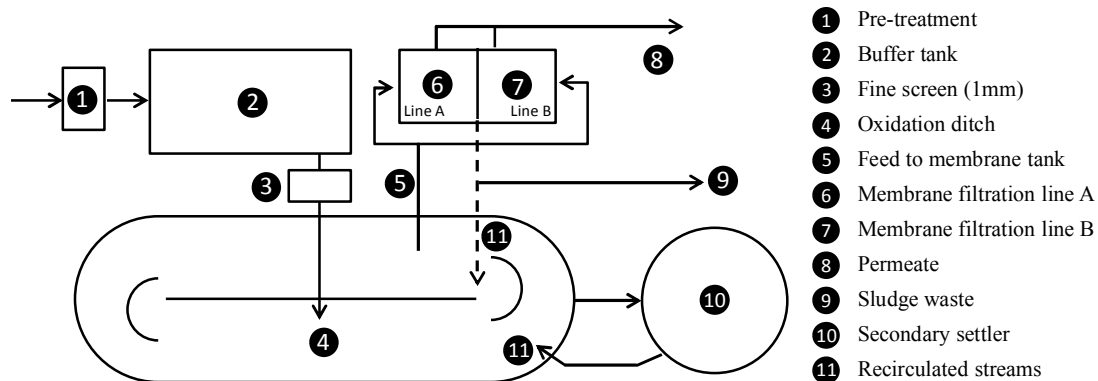


Figure 8.1 | Flow diagram of LBE water line.

The treatment steps consist a coarse screen (8 cm), a grit chamber, a buffer tank (1110 m³), a fine screen (1 mm), an oxidation ditch bioreactor (3636 m³), two parallel membrane lines (30 m³) with submerged ultrafiltration membranes (ZeeWeed 500C, Zenon, GE), and an additional secondary settler that is employed during wet weather and peak flows. Each filtration line is equipped with an independent positive displacement air blower (GM 25S, Aerzen, Germany) that provides a fixed aeration of 17.8 m³·min⁻¹ for each line. Each blower is operated at 3500 rpm (50 Hz),

corresponding to an energy consumption of 289.5 kWh per day. A detailed description of the MBR is presented in Table 8.1.

Table 8.1 | Membrane characteristics at *La Bisbal d'Empordà* WWTP.

| | | Filtration Line A | Filtration Line B |
|-------------------------------------|--|--|-------------------|
| MBR capacity | $\text{m}^3 \cdot \text{day}^{-1}$ | 1,600 | 1,600 |
| Membranes manufacturer | | Zenon, General Electric | |
| Membranes model | | <i>ZeeWeed 500c</i> | |
| Pore size | μm | 0.04 | |
| Total membrane area | m^2 | 2,904 | 2,904 |
| Air-scouring flow | $\text{m}^3 \cdot \text{min}^{-1}$ | 17.8 - 14.24 | 17.8 |
| SAD _m [*] | $\text{Nm}^3 \cdot \text{m}^{-2} \cdot \text{h}^{-1}$ | 0.37 - 0.29 | 0.37 |
| SAD _p ^{**} | $\text{Nm}^3 \cdot \text{h}^{-1} \cdot \text{m}^{-3} \cdot \text{h}^1$ | 16.02 - 12.82 | 16.02 |
| Filtration cycle | filtration/backpulse | 10 min / 40 sec | |
| Average permeate flux | $\text{L} \cdot \text{m}^{-2} \cdot \text{h}^{-1}$ (LMH) | 23 ± 2 | |
| Average permeate net flux | $\text{L} \cdot \text{m}^{-2} \cdot \text{h}^{-1}$ (LMH) | 21.6 ± 2 | |
| Standard maintenance cleaning: | | 140 $\text{mg} \cdot \text{L}^{-1}$ of NaClO + 200 $\text{mg} \cdot \text{L}^{-1}$ of EDTA | |
| Chemically-enhanced backflush (CEB) | 45 minutes of CEB | when the TMP < 0,45bars | |
| Recovery chemical cleaning | 6–12 hours of in-situ cleaning | Soaking the membranes in basic or acid solution (1,500ppm) | |

*SAD_m: Specific Aeration Demand with respect to membrane area, according to membrane manufacturer

**SAD_p: Specific Aeration Demand with respect to permeate flow, according to membrane manufacturer

Membranes were installed in 2003, and only 5.7% of the total area has been replaced over 10 years of operation. A visual inspection carried out in 2011 revealed that the membranes were in good condition (i.e., less than 1% of the membranes were damaged). The membranes were installed in 2003, and only 5.7% of the total area has been replaced over 10 years of operation. A visual inspection carried out in 2011 revealed that the membranes were in good condition (i.e., less than 1% of the membranes were damaged). Chemically-enhanced backflush (CEB) is performed as a maintenance routine procedure when the TMP exceeds a threshold of 0.4 bars (usually every week). First, a solution of 140 $\text{mg} \cdot \text{L}^{-1}$ sodium hypochlorite and 200 $\text{mg} \cdot \text{L}^{-1}$ EDTA is applied for 5 backflush pulses of 15 seconds, with a 5-minute relaxation between pulses, at a flux of approximately 23 $\text{L} \cdot \text{m}^{-2} \cdot \text{h}^{-1}$ (LMH). Every 6 months, recovery chemical cleanings are carried out

by soaking the membranes in an alkaline solution (a $1500 \text{ mg}\cdot\text{L}^{-1}$ sodium hypochlorite solution) or an acid solution (a $1500 \text{ mg}\cdot\text{L}^{-1}$ citric acid solution) for 6-12 h. Manual cleanings are performed every two years (Gabarrón et al. 2013).

8.2.2 AIR-SCOURING CONTROL SYSTEM: SMART AIR MBR®

SmartAir MBR® control system modifies the membrane air-scouring flow rate based on the permeability evolution, which is used as an indicator of the membrane performance and sludge characteristics (Comas et al. 2010). TMP and permeate flow are monitored in real time. Long-term (LT) and short-term (ST) permeability trends are evaluated and compared to identify savings opportunities and alarms. The controlled variable is the slope ratio (SR), which is calculated as the ratio between the ST and the LT permeabilities. The SR is proportional to the control action, which in this case is the daily regulation of the air scour flow rate by increasing or decreasing the blower frequency (the manipulated variable) (Ferrero et al. 2011a).

Normally, the permeability decreases in proportion to the cake layer resistance, which is roughly proportional to the volume of sludge filtered. However, corrective actions such as chemical cleaning or a decrease in the permeate flux, can cause the permeability to increase. Operational conditions (the temperature, the suspended solids concentration, the sludge age, etc.) can also affect the sludge permeability. Thus, four different scenarios (i.e., relationships between ST and LT) have been defined for the air scour control system (Figure 8.2).

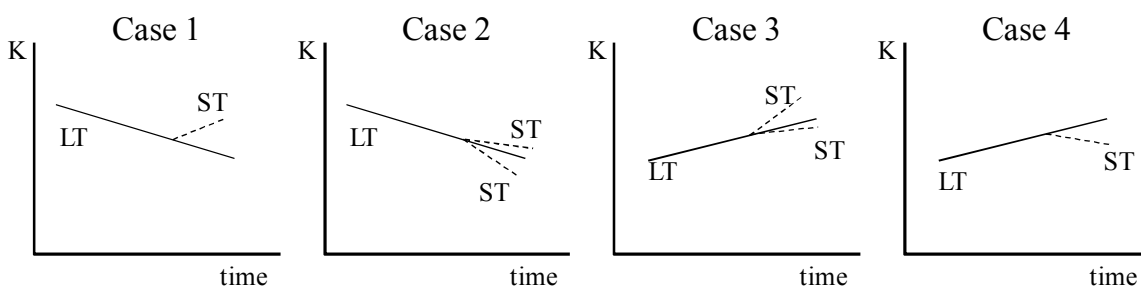


Figure 8.2 | Different relationships between LT and ST permeability.

- Case 1: The long term permeability slope is negative ($LT < 0$), and the short term permeability slope is positive or equal to zero ($ST \geq 0$), corresponding to a moderate energy saving opportunity.
- Case 2: The long term permeability slope is negative ($LT < 0$), and the short term permeability slope is negative ($ST < 0$, lower or higher than LT), corresponding to a low or a non-energy saving opportunity.
- Case 3: The long term permeability slope is positive or equal to zero ($LT \geq 0$), and the short term permeability is positive or equal to zero ($ST \geq 0$, lower or higher than LT) corresponding to a moderate or high energy saving opportunity.
- Case 4: The long term permeability slope is positive or equal to zero ($LT \geq 0$), and the short term permeability is negative ($ST < 0$), corresponding to a moderate or low energy saving opportunity.

EXPERIMENTAL PLANNING

The experimental work was divided in two main phases:

- PHASE 1: DATA GATHERING AND CALIBRATION OF THE CONTROL SYSTEM.

The air scour control system was operated in an open-loop regime under the conditions recommended by the membrane suppliers for 4 months (Table 8.1). Data on the TMP, the permeate flux and the working hours per day of both process lines were collected in real time, processed and compared. The information acquired over this period was used to calibrate the control system parameters. The ST was determined to be 4 days, and the LT was determined to be 14 days (Ferrero et al. 2011b).

- PHASE 2: VALIDATION.

The air scour control system was operated in a closed-loop regime for filtration line A, whereas line B was used as a reference with a constant air scour flow rate of $17.8 \text{ m}^3 \cdot \text{min}^{-1}$ (as recommended by the membrane manufacturers). Figure 8.3 is a schematic of the membrane tank that shows the two filtration lines and the equipment for the control system. In Phase 2, the maximum flow rate reduction allowed for the air scour control system in line A was increased progressively from 5% of the air scour flow rate to 10%, 15% and 20% of the air scour flow rate. The permeability decay was used as an indicator of the

general fouling evolution, and the fouling rate (which was measured as the slope of the permeability for each permeate cycle, as in Monclús et al. (2011)), was used to estimate the fouling that accumulated in each cycle. The filtration performance, energy consumption and economic savings were evaluated and compared for the two filtration lines. The biological nutrient removal efficiencies and sludge characteristics were also measured and compared for the last three years.

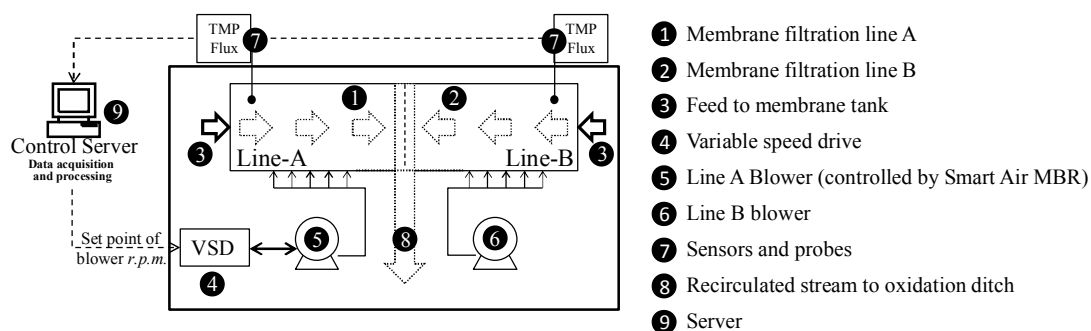


Figure 8.3| Schematic diagram of the control system of the LBE WWTP.

8.3 RESULTS AND DISCUSSION

8.3.1 PHASE 1: DATA GATHERING AND CALIBRATION OF THE CONTROL SYSTEM

The evolution of the daily averaged TMP and the permeability values for both lines exhibited very similar behavior for both lines during the entire phase: the average permeability was 66.9 ± 7.3 LMH·bar⁻¹ for line A and 62.1 ± 4.1 LMH·bar⁻¹ for line B (Figure 8.4). Line A exhibited a slightly higher permeability than line B until February 16th when both permeabilities began to fluctuate, such that the lines exhibited almost the same permeability at the end of Phase 2 (52.5 LMH·bar⁻¹ for line A and 51.7 LMH·bar⁻¹ for line B). Similar filtration times were observed for both lines (18.2 ± 0.1 working hours·day⁻¹ for line A and 18.1 ± 0.3 working hours·day⁻¹ for line B), and the number of maintenance CEB cleanings for both lines was also very similar (13 for line A and 14 for line B).

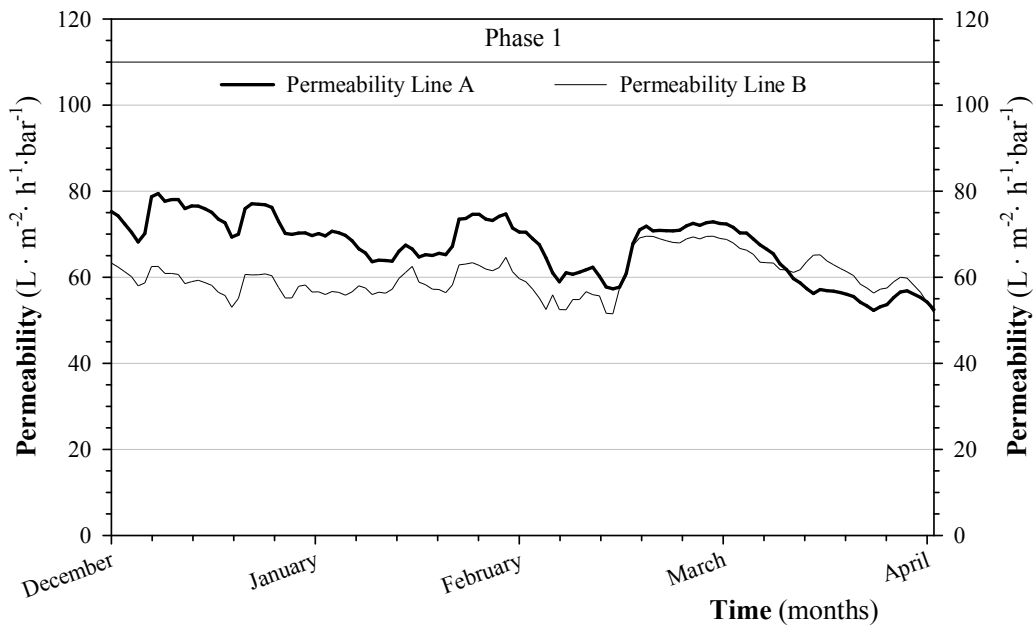


Figure 8.4 | Fouling evolution (permeability) during 4 months previous of the control system activation.

The daily TMP and the permeate flux for both lines were registered to calibrate the control system parameters based on the most common ranges for the ST, LT and SR. For filtration line A, for which the control system was implemented, the SR ranged from +2 to -2, showing the highest percentage of occurrence and represented 43% of the total cases (Figure 8.5A). In defining the entire SR range, 63% of the total cases were taken into account, where the lowest value was -2.5 and the highest value was +5.0 (Figure 8.5B). These historical SR values were used to set the variation in the air scour flow rate (in % or in $m^3 \cdot min^{-1}$). The control system regulated variations in the air scour flow rate using a positive displacement air blower through a frequency driver.

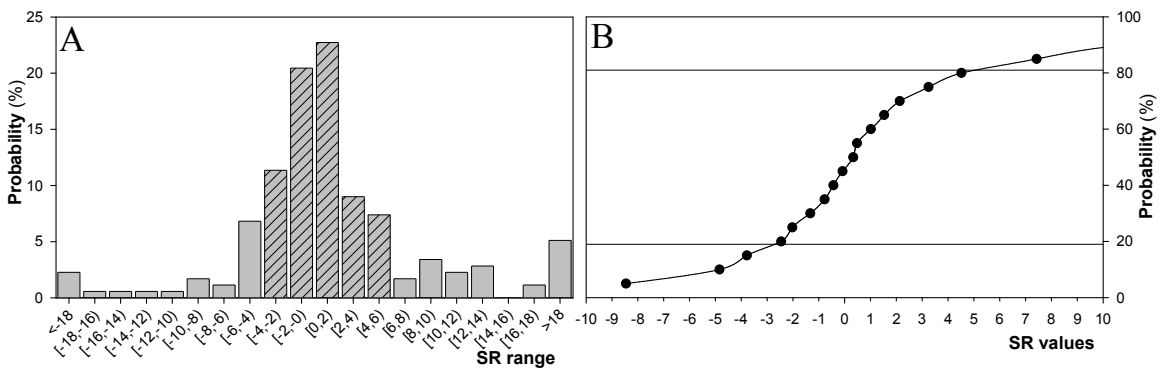


Figure 8.5 | SR percentage of occurrence. A) Probability B) Accumulated probability.

Table 8.2 shows the relationships between the SR and the variations in the air scour flow rate that were used in the second phase of the validation project.

Table 8.2 | Control system actions

| LT | ST | Slope Ratio $SR = ST/LT$ [...] | Airflow Variation (%) | Airflow variation ($m^3 \cdot min^{-1}$) | Saving | |
|------------------|------------------------------------|---------------------------------------|-----------------------------|--|-------------------|-------------------|
| LT < 0 | CASE 1 ST ≥ 0 | <-2.5 | -3% | -0,53 | Moderate | |
| | | [-2.5; -2) | -2.6% | -0,46 | | |
| | | [-2; -1.5) | -2.2% | -0,39 | | |
| | | [-1.5; -1) | -1.8% | -0,32 | | |
| | | [-1; -0.5) | -1.4% | -0,25 | | |
| | | [-0.5; 0) | -1% | -0,18 | | |
| | | [0; 0.2) | -1% | -0,18 | | |
| | | [0.2; 0.4) | -0.8% | -0,14 | <i>ST ≥ LT</i> | |
| | | [0.4; 0.6) | -0.6% | -0,11 | | |
| | | [0.6; 0.8) | -0.4% | -0,07 | Moderate | |
| | | [0.8; 1) | -0.2% | -0,04 | | |
| | | [1; 1.2) | +0.3 % | +0,05 | | |
| | | CASE 2 ST < 0 | [1.2; 1.4) | +0.6% | +0,11 | |
| | | | [1.4; 1.6) | +0.9% | +0,16 | |
| | | | [1.6; 1.8) | +1.2% | +0,21 | |
| | | | [1.8; 2) | +1.5% | +0,27 | <i>ST < LT</i> |
| | | | [2; 2.5) | +1.8% | +0,32 | |
| | | [2.5; 3) | +2.1% | +0,37 | No savings | |
| | | [3; 3.5) | +2.5% | +0,45 | | |
| | | [3.5; 4) | +3% | +0,53 | | |
| | [4; 5) | +4% | +0,71 | | | |
| | ≥5 | +5% | +0,89 | | | |
| LT > 0 | CASE 3 ST ≥ 0 | [0; 0.2) | -0.4% | -0,07 | <i>ST < LT</i> | |
| | | [0.2; 0.4) | -0.8% | -0,14 | | |
| | | [0.4; 0.6) | -1.2% | -0,21 | | |
| | | [0.6; 0.8) | -1.4% | -0,25 | Moderate | |
| | | [0.8; 1) | -1.8% | -0,32 | | |
| | | [1; 1.2) | -2.5% | -0,45 | | |
| | | [1.2; 1.4) | -3% | -0,53 | <i>ST ≥ LT</i> | |
| | | [1.4; 1.6) | -3.5% | -0,62 | | |
| | | [1.6; 1.8) | -4% | -0,71 | High | |
| | | ≥1.8 | -5% | -0,89 | | |
| | | CASE 4 ST < 0 | <-2 | 0% | 0,00 | Low |
| | | | [-2; 0) | -0.5% | -0,09 | |

8.3.2 PHASE 2: VALIDATION

FOULING EVOLUTION

The fouling behavior was monitored based on the evolution of the permeability and the fouling rate (FR) to ensure that there were no differences between the filtration line that was regulated by the air scour control system (line A) and the reference line B.

Figure 8.6 shows the permeability (K) evolution of both filtration lines. At the end of Phase 1 (before the closed-loop implementation, from day -50 to day 0), the difference between the permeabilities of the lines was less than 0.6% (i.e., the permeability was $57.1 \pm 10 \text{ LMH}\cdot\text{bar}^{-1}$ for line A and $57.4 \pm 9.7 \text{ LMH}\cdot\text{bar}^{-1}$ for line B). The air scour control system was then operated in a closed-loop regime (day 0) with a maximum air flow reduction of 5% (i.e., an air-scouring flow rate of $16.9 \text{ m}^3\cdot\text{min}^{-1}$): the evolution of the permeability was very similar for both lines. After two weeks, the maximum allowable reduction in the flow rate was increased to 10% over 47 days (from day 14 to day 61). The maximum reduction in the air scour flow rate was then increased up to 15%. Over this period, the permeabilities of both lines were almost identical, except for days 115-130 when a recovery cleaning was performed on both lines (the permeability reached the minimum value set by the operators), and the permeability rose to $80 \text{ LMH}\cdot\text{bar}^{-1}$ and $95 \text{ LMH}\cdot\text{bar}^{-1}$ for lines A and B, respectively. The high fluctuations in both permeabilities, which were generally parallel, were caused by the CEB. This behavior reflected that following a CEB, the permeability decreased until a subsequent CEB was performed.

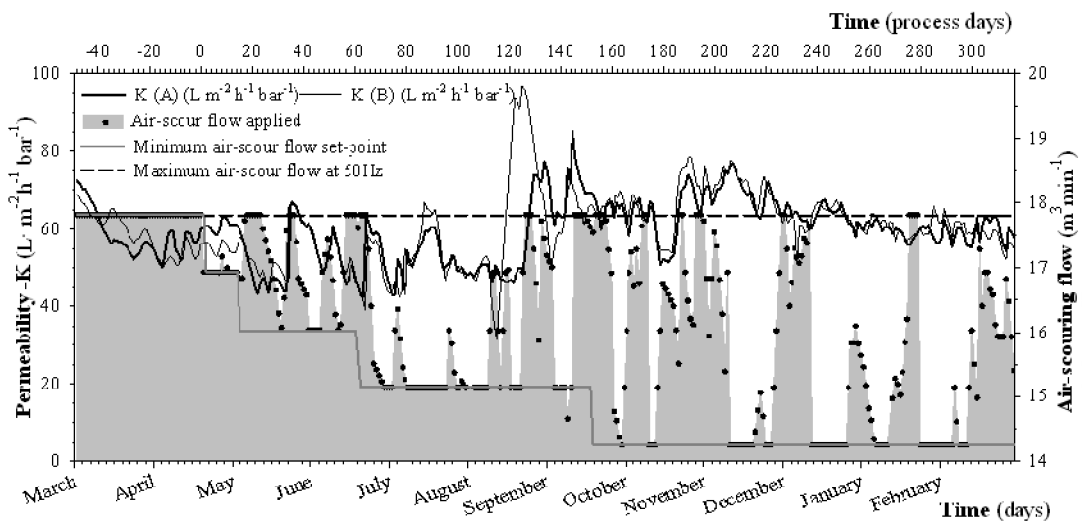


Figure 8.6 | Fouling evolution in the La Bisbal d'Empordà WWTP: K(A) with Smart Air MBR and K(B) without Smart Air MBR.

A final maximum reduction in the air scour flow rate of 20% was applied from day 160 to day 320. The behaviors of both profiles were very similar: the average permeability was 63.5 ± 5.0 LMH·bar⁻¹ for line A and 63.7 ± 5.93 LMH·bar⁻¹ for line B. Moreover, the filtration time was similar for both lines (17.9 ± 2.4 working hours/day for line A and 17.8 ± 2.8 working hours/day for line B), and the number of maintenance CEB cleanings was also very similar (90 for line A and 92 for line B). Therefore, no significant differences between filtration lines A and B were detected.

Note that the control system decreased the air scour flow rate when the fouling was reduced, usually after a CEB was performed (e.g., days 37 and 64 in Figure 8.6). However, when the fouling tendency was bigger, the control system increased the air scour flow rate in an attempt to recover the previous permeability tendency (e.g., days 52, 142 and 220 in Figure 8.7).

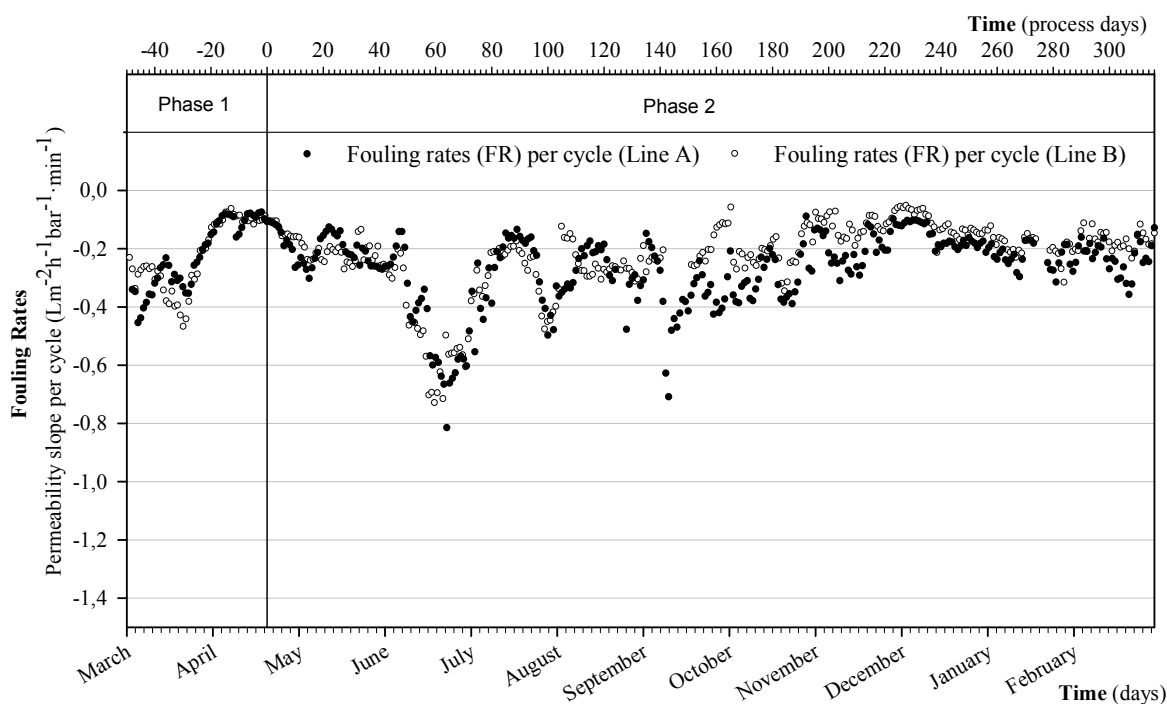


Figure 8.7 | Permeability slope per each permeate cycle: MBR-A with Smart Air MBR and MBR-B without Smart Air MBR.

A deeper examination of the fouling behavior revealed that the modifications of the air-scouring flow rates in line A did not affect significantly its fouling rate (FR) compared to line B (Figure 8.7). Before the closed-loop operation (from day -50 to day 0), the averaged FRs were -0.21 ± 0.1

LMH·bar⁻¹·min⁻¹ for line A and -0.22 ± 0.1 LMH·bar⁻¹·min⁻¹ for line B. During the first two months of closed-loop operation (from day 0 to day 65), the FRs decreased equally for both lines up to -0.81 LMH·bar⁻¹·min⁻¹ for line A and -0.72 LMH·bar⁻¹·min⁻¹ for line B at day 65. The FRs then increased because of the CEB that was performed in the WWTP, resulting in an average value of -0.29 ± 0.15 for line A and -0.30 ± 0.15 for line B just before the recovery chemical cleaning (days 115-130). After the recovery chemical cleaning (from day 130 onwards), the FRs fluctuated, reaching values of -0.19 LMH·bar⁻¹·min⁻¹ for line A and -0.16 LMH·bar⁻¹·min⁻¹ for line B at the end of the validation period. Throughout the validation period (330 days of operation), the average FR was -0.28 ± 0.16 LMH·bar⁻¹·min⁻¹ for line A and -0.28 ± 0.17 LMH·bar⁻¹·min⁻¹ for line B.

Considering the permeability values achieved (Figure 8.6) together with the FR values (Figure 8.7) at the end of Phase 2, the permeability in filtration line A decreased by 0.30% in each cycle, whereas the permeability for line B decreased by 0.25%. These results show that the air scour control system did not affect the fouling behavior in line A compared to line B.

The effect of the closed-loop air scour control system on the biological processes was evaluated by comparing the sludge properties and the biological nutrient removal efficiencies over the last 3 years (Table 8.3). The sludge concentration, filterability (which was measured as the capillarity suction time (CST)) and the sludge settleability (which was measured as sludge volumetric index (SVI)) did not exhibit any differences before and after the implementation. Similarly, the biological nutrient removal efficiencies remained constant over the last 3 years, except for the nitrogen removal efficiencies, which decreased in 2011 because of the implementation of a control system for biological aeration to reduce energy requirements in the oxidation ditch.

Table 8.3 | Activated sludge properties and biological nutrient removal over the last three years.

| Category | Parameter | Units | 2010 | 2011 | 2012 |
|-----------------------------|-------------------------------|--------------------|---------------|---------------|---------------|
| Sludge properties | Mixed Liquor Suspended solids | g·L ⁻¹ | 5.7 ± 1.4 | 6.3 ± 1.5 | 5.7 ± 1.2 |
| | SVI | mL·g ⁻¹ | 307 ± 93 | 227 ± 74 | 257 ± 80 |
| | CST | seconds | -- | 54 ± 10 | 50 ± 9 |
| Biological Nutrient Removal | Chemical oxygen demand | | 96 ± 4 | 95 ± 3 | 95 ± 2 |
| | Biochemical oxygen demand | % | 97 ± 2 | 97 ± 3 | 97 ± 2 |
| | Total nitrogen | | 93 ± 10 | 86 ± 13 | 85 ± 7 |
| | Phosphorous | | 81 ± 15 | 77 ± 19 | 80 ± 10 |

ENERGY CONSUMPTION

During the validation phase (Phase 2), 32% of the control actions applied corresponded to moderate or low variations in the air scour flow rate (case 1, case 2 with $ST \geq LT$, case 3 with $ST < LT$ and case 4), whereas 43% of the control actions corresponded to high variations in the air scour flow rate (case 3 with $ST \geq LT$): the air scour flow rate was incremented by the control system in only 25% of the cases (case 2 with $ST < LT$). The average reduction in the air scour flow rate was 13% over the 1-year validation period.

Before the operation of the air scour control system in a closed-loop regime, the energy consumption for the aeration demand of each filtration line was 289.5 kWh·day⁻¹ for a design air scour flow rate of 17.8 m³·min⁻¹ (at 50 Hz) (Figure 8.8).

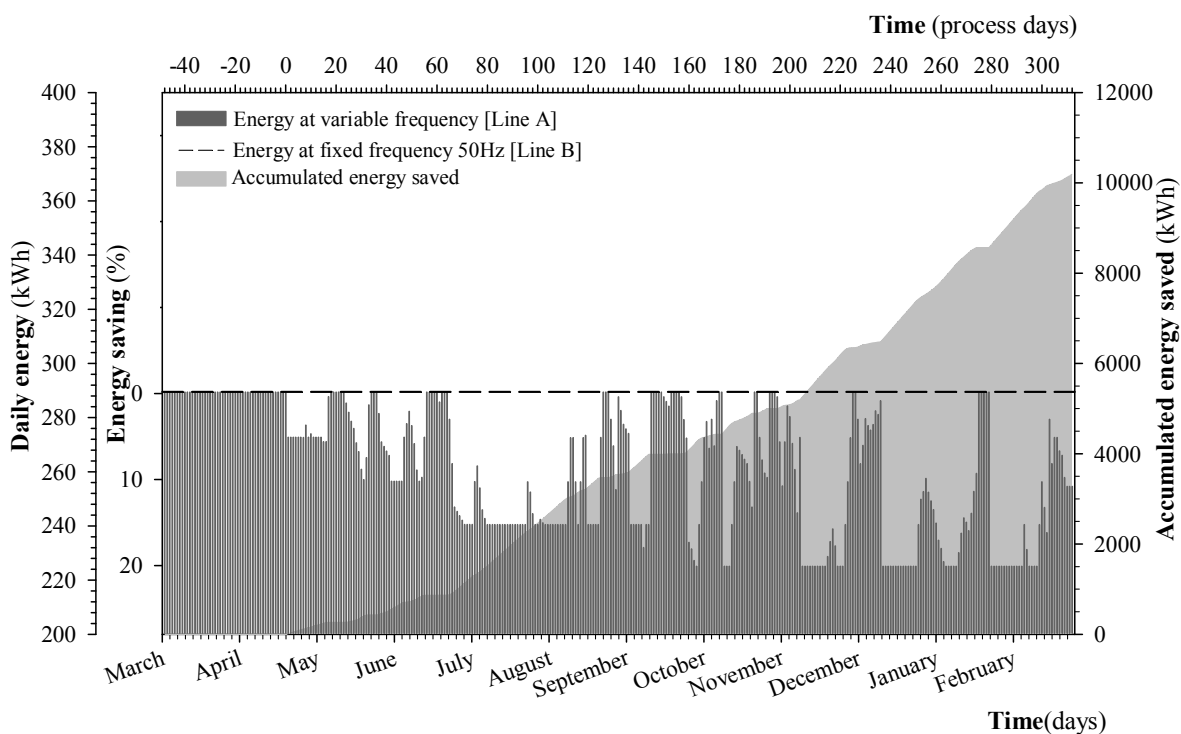


Figure 8.8 | Energy consumption evolution with Smart Air MBR.

The energy savings for filtration line A were estimated relative to its energy consumption for a maximum air scour flow of 17.8 m³·min⁻¹. The energy savings for filtration line A was 10500 kWh after 320 days (see Figure 8.8). The average energy savings in this line was 14%, reaching a maximum of 22%. Taking into account the average permeate flow rate (1600 m³·day⁻¹), the

energy saving ratio during this validation phase averaged $0.025 \text{ kWh}\cdot\text{m}^{-3}$ for a maximum value of $0.04 \text{ kWh}\cdot\text{m}^{-3}$.

Finally, the payback of the air scour control system was calculated considering that the system was installed for both filtration lines and for a fixed maximum reduction in the air scour flow rate reduction of 20%. For investment costs of the required equipment of 2950€ per filtration line, the payback of the control system was estimated at 1.8 years (based on the Spanish electricity cost).

8.4 CONCLUSIONS

The full-scale air-scouring control system was successfully validated, displaying a 13% average reduction in the air-scouring flow rate and a maximum reduction of 20%. This reduction in air-scouring flow rate caused the energy consumption during membrane aeration to decrease by an average of 14% and a maximum of 22%. The energy savings ratio was estimated as $0.025 \text{ kWh}\cdot\text{m}^{-3}$, with $0.04 \text{ kWh}\cdot\text{m}^{-3}$ as the maximum ratio. Permeability and fouling rate trends were not affected by the control system; they presented very similar patterns for both filtration lines throughout the experimental evaluation period of more than 320 days. The energy savings in the MBR, which normally operates very conservatively, is important for increasing the competitiveness of this technology.

DISCUSSION

The high demand for water and its shortage in arid or semi-arid regions make MBR a competitive technology thanks to the high quality effluent it produces. However, understanding and optimising a system as complex as that of MBRs, is difficult and time consuming. Between the different processes there are a high number of complex interactions which range from nutrient removal to hydrodynamic aspects, from activated sludge characteristics to filtration processes. It is imperative to take into consideration the characteristics of the sludge as this plays an important role in MBRs. MBRs are systems with high retention times and specific operating modes (i.e. permeate/backwashing, high shear), which directly affect the specifics of the sludge, such as EPS or SMP production, bacterial communities or particle size. Above all, what still remains as an inevitable phenomenon is the increase in TMP as a result of the fouling phenomena. Unless all the relationships are better understood, fouling phenomena will continued to be mitigated rather than prevented, and thus operational costs will increase.

This thesis aims to provide insights into the integrated operation of MBRs, which involve optimizing biological nutrient removal, minimizing fouling and, whenever possible, implementing cost saving strategies. Modelling and experimental studies have been carried out on both pilot-scale and full-scale systems to achieve this goal.

GENERAL DISCUSSION

Most MBR studies have been focused on single targets, for instance, optimizing BNR (Dvořák et al. 2013, Monclús et al. 2010a), studying the fouling phenomena (Arabi and Nakhla 2009, Drews et al. 2009) or examining the effects of sludge characteristics (Beltrán et al. 2009, Gao et al. 2011, Lee et al. 2003, Menniti et al. 2009, Sabia et al. 2013). Due to the high number of interactions among these previously mentioned phenomena, it is essential not to ignore any of the relevant aspects, but rather to consider them in an integrated way. First, the most relevant operational parameters for BNR are identified through deterministic modelling in **Chapter 4**. This chapter may focus on biological nutrient removal, some sludge properties and fouling phenomena have also been taken into account, although the filtration model presented some limitations regarding air scouring efficiency on fouling recovery. Complemented with expert knowledge, it has been possible to develop a decision tree to identify best set-point values for biological nutrient removal optimization. Nevertheless, the pilot plant did not allow an adequate degree of freedom

so as to explore optimization of hydrodynamics. **Chapter 5** explores hydrodynamics in a full-scale hybrid MBR. It illustrates a model-based optimization of the system with respect to effluent quality and operational costs depending on the treatment of wastewater flux through membranes, secondary settler or through a combination of both. It also details the opportunity to better model the hydraulics of the oxidation ditch using several tanks in-series and dividing each tank into two horizontal layers. This better hydraulic description led to a better calibrated model. Operation using membranes normally implies higher energy costs due to membrane aeration; therefore membrane aeration could be used to save some energy in the aerobic compartment. However, we demonstrate the capacity of coarse-bubble aeration to finish the nitrification step in the membrane tank. On the other hand, the operation of the plant with a secondary settler presented higher anoxic times, resulting in lower nitrates in the effluent along with lower associated costs. This, however, increased the risk of the rising sludge phenomena (because of possible denitrification in the settler), and also decreased the effluent quality (in comparison with membrane treatment) due to solid concentrations in the effluent.

Furthermore, the fouling phenomenon was not entirely explained by the models used in **Chapters 4 or 5**. Thus, other types of models to better describe TMP evolution were explored. **Chapter 6** illustrates the comparison of the description of TMP by means of a deterministic model and a data-driven one as well. We demonstrated that they complement each other since the deterministic models were able to assemble the TMP profile under stable operating conditions, whereas the higher dynamics in TMP and permeability were better fitted by the data-driven model. Deterministic models should always be complemented with experimental fouling indicators (i.e. CST, filterability, etc). However, the use of deterministic models to describe biological treatment processes through the world-wide accepted ASM family is the state-of-the-art practice (Henze et al. 2000). Data-driven models present the benefit of learning from the system by using empirical data. The use of available on-line data from sensor measurements monitoring the filtration enabled a reliable model tree for the TMP description to be developed. Similarly, other data-driven studies can help to assess the fouling and filterability behaviour (Maere et al. 2012, Van den Broeck et al. 2011). As the ASM-type model is so well accepted, data-driven models for BNR description are not common. Besides, usually amount of online data for influent nutrient concentrations is scarce due to a lack of nutrient sensors in most plants.

When models are not able to describe certain situations or relationships due to a lack of knowledge, the need for experimental studies arises. In this sense, **Chapter 7** outlines how biological and membrane aeration affect filtration performance, sludge properties and biological nutrient removal efficiency. Several studies have focused on the effect of the membrane air-scouring on TMP performance and sludge characteristics (Braak et al. 2011, Brannock et al. 2010, Choi et al. 2009, Germain et al. 2007, Hong et al. 2007, Ji and Zhou 2006), however, few of them paid attention to BNR evolution as they considered the membrane tank unsuitable for nutrient removal (Fenu et al. 2010b). Results in **Chapters 5 and 7** demonstrate the ability of the membrane aeration to nitrify. However, biological aeration (aeration in the aerobic compartment) reduction also affected filtration performance. The reduction of the aerobic set-point to values lower than $0.5 \text{ mg O}_2 \cdot \text{L}^{-1}$ led to significant changes in sludge properties, influencing the filtration with an increase in the TMP and fouling rate. **Chapter 7** focuses on energy efficiency, showing how energy savings can be achieved by increasing anoxic zones to the detriment of the biological aeration. In addition, a reduction of up to 20% of membrane air-scouring was accomplished without affecting the integrated process, and this was the major contributor to cost savings.

The results from **Chapter 7** validate the modification of the membrane air-scouring flow rates through an automatic control system in one of the two membrane lines of the full-scale facility (**Chapter 8**). The control actions to regulate the air-scouring flow rate were based on the evolution of the permeability (Ferrero et al. 2011a), and served as an indicator of the membrane performance and sludge characteristics. This full scale validation resulted in a cost savings of 15%, all the while maintaining good filtration performance, adequate BNR efficiency and satisfactory sludge properties in the system. Cost reduction was already noticeable in an MBR plant treating $3225 \text{ m}^3 \cdot \text{d}^{-1}$, but of course its extrapolation to bigger MBR plants could result in greater savings, thus contributing to convert MBR systems into more economically feasible technology. Although the reduction of the aerobic set-point in the biological part of the full scale system has not been described in this thesis (as this was done in the pilot plant -see **Chapter 7**), an automatic control system reducing the aerobic aeration and based on electric rates is currently being applied.

INTEGRATED OPERATION

The knowledge acquired from all of the studies during this thesis will be useful in the development of a knowledge-based supervision module, in other words the top echelon of a decision support system (DSS) for MBR operation. The supervision level is located hierarchically at the top of the automatic control and data acquisition levels (Figure 9.1). Data acquisition and signal processing is carried out to identify outliers, missing data and validate all data required for the control and supervision levels. Consequently, the validated data is used for the real-time automatic control. Data acquisition and control systems for biological aeration are normally available in most MBRs. However, although Comas et al. (2010) have already reported on the potential benefits of a knowledge-based approach, most of the real MBR systems still do not incorporate a closed loop control for air-scouring, rather preferring to use the open loop control, typically suggested by manufactures for conservative operation. None of them incorporate a set of knowledge-based rules able to supervise both biological, hydrodynamic and filtration processes in an integrated way, i.e. current MBR systems do not regulate, if needed, the set-points for aerobic DO, optimal LMH and maximum air-scour reduction in an integrated way.

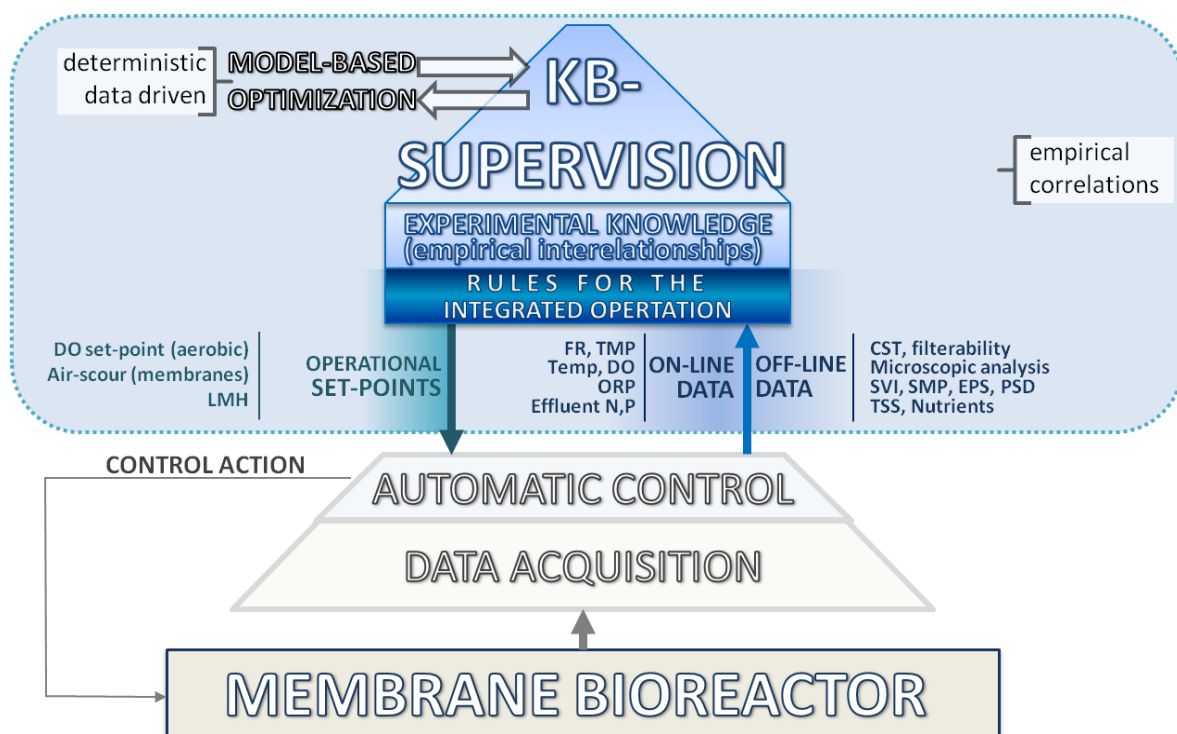


Figure 9.1 | A knowledge-based DSS for the integrated operation of MBR.

The knowledge collected from all empirical and modelling studies has allowed a table relating the modifications of operational parameters and the biological, filtration and costs issues to be developed (Figure 9.2). Some of the operational parameters are the controlled or manipulated variables of automatic control systems, others involve manual modifications. Therefore, this table forms the basis for the development of a set of rules for the integrated operation of MBRs and which will then become the knowledge base for the supervision module (Figure 9.1). These rules combined with on-line data (TMP, temperature, FR, DO, etc.) and off-line data (i.e. sludge characteristics, influent and effluent nutrient concentrations, TSS) will allow the proper operational set-points for the automatic control level along with some operational ranges that are restricted to be determined.

As demonstrated in Chapters 4, 5 and 6, as well as in other studies (Insel et al. 2011, Mannina and Cosenza 2013, Verrecht et al. 2010a), model-based studies can be useful to test and optimise operating set-points defined by the supervision level. All the rules for the integrated operation will have to be experimentally verified in full-scale systems. An initial example was the validation of a KB-supervision for a closed-loop air-scouring control system, which supervised the maximum air-scouring reduction allowed, while maintaining good filtration together with efficient BNR and good sludge quality (Chapter 8). In current practices in MBR systems the aerobic DO set-point is regulated just enough to fulfil the legal discharge limits for nutrient concentrations, but disregards filtration performances and changes in sludge properties. This validation of the automatic air-scouring control system and its knowledge-based supervision in a full-scale MBR is evidence of the usefulness of the DSS.

RELATIONSHIPS FOR THE INTEGRATED OPERATION

A summary of the relationships between the operating parameters and the biological, filtration, sludge characteristics and costs issues in an MBR are presented in Figure 9.2. These relationships are based on the results presented in this thesis and complemented by findings in the literature. It is necessary to point out that most of the work done in MBR does not relate the operational parameters to the processes previously mentioned. For instance, how filtration performance is affected by specific sludge properties is well studied. So too is the use of statistics to find the interactions between fouling phenomena and effluent characteristics or sludge properties.

However, these studies are not related to operational parameter changes, thus, they are not included in the table. In addition, there are some works related to the nutrient effect of the operational parameters, to the biological nutrient removal or to sludge properties which can fill the gaps, but as they were not carried out in MBR systems this knowledge has not been included in Figure 9.2.

From Figure 9.2, the exact effect of recirculation on the filtration performance has not been demonstrated clearly. However, optimization of BNR through recirculation changes, similar to CAS systems, has been identified. Gao et al. (2011) indicated the affect of the external recirculation on the denitrification processes, when high amounts of DO from the membrane tank are recirculated affecting the anoxic conditions.

The effects of the biological aeration increase are well known in the BNR, but little attention has been paid to its affect on sludge characterization and the filtration process. How the increase of the biological aeration decreased the production of bound EPS, SMP and PSD, and improved the filterability with no affect on sludge hydrophobicity has been demonstrated. In Chapter 7, there is an extended discussion about these effects. The results from Chapter 7 identify how the decrease in biological aeration, and the subsequent changes to the sludge properties, led to a decrease in the efficiency of the filtration process.

On the other hand, the increase in membrane aeration propitiates better filtration performances and increases the efficiency of the physical cleanings. Biological nutrient removal can also be achieved in the membrane compartment (Chapter 7). With regards to sludge properties, higher air-scouring provoke a decrease in the bound EPS, SMP and PSD (Chapter 7 and references therein). However, too much air-scouring creates high shear. The excess of shear in the system can also provoke floc breakage, leading to smaller particles, blocking membrane pores and increasing fouling (as identified in Chapter 6). High shear can also stress microorganism behaviour, with higher excretion of SMP or bound EPS (Germain et al., 2007).

On the subject of the permeate flux, no modification of flux properties related to nutrient removal were found. On the other hand, the increase in the flux is related to higher bound EPS and SMP production, higher PSD and lower filterability. Higher flux and closer to the critical flux are reported as negatively influencing the filtration process.

With regards to influent characteristics, higher F/M ratios were demonstrated to propitiate the production of bound EPS and SMP and decrease filterability. Thus, the higher F/M ratios are related to the increase in TMP values.

The effects of temperature on the BNR have not been studied specifically in MBR systems. Nevertheless, temperature plays an important role on sludge viscosity and it directly affects sludge properties and filtration performance. As was demonstrated in Chapter 6, the affect of the temperature led to a better TMP performance and decreased filterability values.

A step towards the integrated operation of MBRs has been presented in this thesis. However, further research is still needed to convert all of these relationships into rules and then implement them in the supervision module to validate them experimentally. In doing so, energy costs and the complexity associated with MBR operation will be significantly reduced, and will help to convert MBR systems into a more competitive technology, one to be considered seriously when facing water shortage problems.

| Operating parameters | | Nutrient removal | | | | Sludge Characteristics | | | | | | Filtration efficiency | |
|----------------------|------------------------|----------------------|--|--|---|------------------------|-------------------------|------------|------------------------------|-------------|----------------|-----------------------|-------------------|
| | | [COD] _{out} | [N-NH ₄ ⁺] _{out} | [N-NO ₃ ⁻] _{out} | [P-PO ₄ ³⁻] _{out} | Bound-EPS | SMP | PSD | CST Filterability DFCm | Filaments | Hydrophobicity | TMP, FR | K |
| ↑ | Aerobic recirculation | | ↓ C4, 1 | ↑ C4,1 | ↑ C4,1 | | | | | | | | |
| ↑ | Anoxic recirculation | | ↑ C4, 1,2 | ↓ C4,1,2 | ↓ C4,1,2 | | | | | | | | |
| ↑ | External recirculation | | ↑ 3 | ↓ 3 | ↓ 3 | | | | | | | | |
| ↑ | Biological aeration | ↓ C4, C7, 1 | ↓ C4, C7, 1 | ↑ C4, C7, 1 | ↑ C4, C7, 1 | ↓ 4, 5 | ↓ C7, 4, 5 | ↓ C7 | ↑ C7, 21 | ↓ 11, 13 | = C7 | ↓ C7 | ↑ C7 |
| ↑ | Membrane aeration | ↓ C4, C7, 3, | ↓ C7, C7, 3 | ↑ C4, C7, 3 | ↑ C4, C7, 3 | ↓ 6, 7, 8, 9, 10 | ↓ C7, 6, 7, 8, 9, 10 | ↓, ↑ 15 | ↑ C7, 21 | ↓ 11 | ↑ C7, 5, 12 | ↓ 13, 14,15,16 | ↑ 13, 14,15,16 |
| ↑ | Permeate flux | | | | | ↑ 18 | ↑ 18 | ↑ 15,19 | ↓ 21 | | | ↑ C4, C6, 20 | ↓ C4, C6, 20 |
| ↑ | Purge | | | | | ↑ 27 | ↑ 27 | | ↓ 22, 23, 24, 28 | ↓ 11 | | ↑ 28 | ↓ 22, 23, 24 |
| ↑ | F/M | | | | | ↑ 26 | ↑ 26 | | ↓ 26 | ↑ 11 | | ↑ 26, 29 | |
| ↑ | Temperature | | | | | | | | ↓ 30 | | | ↓ C6 | ↑ C6 |

Figure 9.2 | Effects of operating conditions on filtration performance, sludge and biological processes. The numbers in superscript indicate the literature references reaffirming the statement. In addition, C4 stands for Chapter 4, C5 Chapter 5, C 6 Chapter 6, C7 Chapter 7 and C8 means Chapter 8. Concretely, each literature reference are detailed below: ¹ (Tchobanoglous et al. 2003), ² (Bekir Ersu et al. 2008), ³ (Tan and Ng 2008), ⁴ (Gao et al. 2011), ⁵ (Arabi and Nakhla 2009), ⁶ (Menniti et al. 2009), ⁷ (Drews et al. 2006a), ⁸ (Drews et al. 2007), ⁹ (Wang et al. 2009), ¹⁰ (Menniti and Morgenroth 2010a), ¹¹ Jenkins, ¹² (Van den Broeck et al. 2011), ¹³ (Ma et al. 2013), ¹⁴ (Ferrero et al. 2011d), ¹⁵ (Germain and Stephenson 2005), ¹⁶ (Ji and Zhou 2006), ¹⁷ (De La Torre et al. 2008), ¹⁸ (Kimura et al. 2008), ¹⁹ (Germain et al. 2007), ²⁰ (Stricot et al. 2010), ²¹ (Sabia et al. 2013), ²² Nuengjamnong et al 2005, ²³ (Trussell et al. 2006), ²⁴ (Jiang 2008), ²⁵ (Kimura et al. 2005), ²⁶ (Huyskens et al. 2008), ²⁷ (Drews 2010), ²⁸ (Van den Broeck et al. 2012), ²⁹ (Lyko et al. 2008), ³⁰ (Gil et al. 2011).

CONCLUSIONS

This thesis presented a step towards the integrated operation of MBRs through experimental and model-based studies. The most important conclusions arising from the present work are summarized below:

- i. A model-based approach and sensitivity analysis enabled the identification of the most sensitive parameters for the integrated operation of nutrient removal and filtration processes.
- ii. The decision tree based on simulation studies and expert knowledge enabled the use of the optimal operating parameters for nutrient removal by MBRs, thus minimizing energy and costs.
- iii. An integrated model for the full-scale hybrid MBR has been used to optimise the hydrodynamics of the plant, treating the effluent by membranes or secondary settler. This model used the deterministic biological model (ASM2d), involving a two layer hydraulic model for oxidation ditch description, a qualitative model to estimate the risk of the activated sludge solid separation, a coarse bubble model for membrane aeration and a 1-D Bürger model for a proper description of the settler.
- iv. The optimisation of the hydraulic management resulted in significant savings by reducing membrane filtration in favour of gravitational settling, whilst still meeting legal discharge requirements.
- v. MBR fouling is better described by a deterministic model when operating above 20 °C, constant MLSS, DO and pH, subcritical filtration conditions or with permeate fluctuations; whereas it is better described by data driven-model when operating below 20 °C, low pH, under critical filtration conditions and in periods with relevant variations in other operating parameters, such as pH or DO in the aerobic reactor.
- vi. TMP description under steady state operation was demonstrated to be properly described by a deterministic model. However, under dynamic and changing operation the data-driven models can describe this behaviour better.

- vii. Experimental studies were necessary for the identification of the interrelationships between the biological and filtration processes.
- viii. A total flow reduction of 42% (75% energy reduction) has been achieved by managing biological and membrane aeration in MBRs to the optimal values ($0.5 \text{ mg O}_2 \cdot \text{L}^{-1}$ DO set-point and $1 \text{ m} \cdot \text{h}^{-1}$ SADm), while preserving filtration performance and sludge characteristics.
- ix. The air-scouring control system based on permeability trends was successfully validated at full scale for one year.
- x. The validation of the control system demonstrated an average air-scouring reduction of 13% (maximum reduction of 20%) leading to an average energy saving of 14% (maximum energy saving of 22%), without compromising permeability and fouling rate trends.

All results obtained as part of this thesis will form the knowledge base of the expert supervision module for the integrated operation of membrane bioreactors.

BIBLIOGRAPHY

Abusam, A., Keesman, K., Van Straten, G., Spanjers, H. and Meinema, K. (2001) Parameter estimation procedure for complex non-linear systems: calibration of ASM No. 1 for N-removal in a full-scale oxidation ditch. *Water Science & Technology* 43(7), 357-366.

Ahn, Y.T., Choi, Y.K., Jeong, H.S., Chae, S.R. and Shin, H.S. (2006) Modeling of extracellular polymeric substances and soluble microbial products production in a submerged membrane bioreactor at various SRTs. *Water Science and Technology* 53(7), 209-216.

Aimar, P., Howell, J.A. and Turner, M. (1989) Effects of concentration boundary layer development on the flux limitations in ultrafiltration. *Chemical Engineering Research and Design* 67(3), 255-261.

Al-Amri, A., Salim, M.R. and Aris, A. (2010) The effect of different temperatures and fluxes on the performance of membrane bioreactor treating synthetic-municipal wastewater. *Desalination*.

APHA (2005) *Standard Methods for the Examination of Water and Wastewater*, American Public Health Association. American Water Works Association (AWWA) & Water Environment Federation (WEF), Washington DC.

Arabi, S. and Nakhla, G. (2009) Characterization of foulants in conventional and simultaneous nitrification and denitrification membrane bioreactors. *Separation and Purification Technology* 69(2), 153-160.

Audenaert, W.T.M., Vermeersch, Y., Van Hulle, S.W.H., Dejans, P., Dumoulin, A. and Nopens, I. (2011) Application of a mechanistic UV/hydrogen peroxide model at full-scale: Sensitivity analysis, calibration and performance evaluation. *Chemical Engineering Journal* 171(1), 113-126.

Bacchin, P., Aimar, P. and Field, R.W. (2006) Critical and sustainable fluxes: Theory, experiments and applications. *Journal of Membrane Science* 281(1-2), 42-69.

Bekir Ersu, C., Ong, S.K., Arslankaya, E. and Brown, P. (2008) Comparison of recirculation configurations for biological nutrient removal in a membrane bioreactor. *Water Research* 42(6-7), 1651-1663.

Beltrán, S., Irizar, I., Monclus, H., Rodriguez-Roda, I. and Ayesa, E. (2009) On-line estimation of suspended solids in biological reactors of WWTPs using a Kalman observer. *Water Science and Technology* 60(3), 567-574.

Benedetti, L., Prat, P., Nopens, I., Poch, M., Turon, C., De Baets, B. and Comas, J. (2009) A new rule generation method to develop a decision support system for integrated management at river basin scale. *Water Science and Technology* 60(8), 2035-2040.

Bewtra, J.K., Nicholas, W.R. and Polkowski, L.B. (1970) Effect of temperature on oxygen transfer in water. *Water Research* 4(1), 115-123.

- Bixio, D., De Wilde, W., Nevo, V., Eliades, P., Lesjean, B. and Thoeys, C. (2008) Potential of innovative Dual CAS-MBR configurations in two very diverse market situations: Bulgaria and Cyprus. *Water Practice and Technology* 3(2).
- Bouhabila, E.H., Ben Aïm, R. and Buisson, H. (2001) Fouling characterisation in membrane bioreactors. *Separation and Purification Technology* 22-23, 123-132.
- Braak, E., Alliet, M., Schetrite, S. and Albasi, C. (2011) Aeration and hydrodynamics in submerged membrane bioreactors. *Journal of Membrane Science* 379(1-2), 1-18.
- Brannock, M., Wang, Y. and Leslie, G. (2010) Mixing characterisation of full-scale membrane bioreactors: CFD modelling with experimental validation. *Water Research* 44(10), 3181-3191.
- Brepols, C., Dorgeloh, E., Frechen, F.B., Fuchs, W., Haider, S., Joss, A., de Korte, K., Ruiken, C., Schier, W., van der Roest, H., Wett, M. and Wozniak, T. (2008) Upgrading and retrofitting of municipal wastewater treatment plants by means of membrane bioreactor (MBR) technology. *Desalination* 231(1-3), 20-26.
- Brepols, C., Schäfer, H. and Engelhardt, N. (2010) Considerations on the design and financial feasibility of full-scale membrane bioreactors for municipal applications. *Water Science and Technology* 61(10), 2461-2468.
- Bugge, T.V., Larsen, P., Saunders, A.M., Kragelund, C., Wybrandt, L., Keiding, K., Christensen, M.L. and Nielsen, P.H. (2013) Filtration properties of activated sludge in municipal MBR wastewater treatment plants are related to microbial community structure. *Water Research* 47(17), 6719-6730.
- Bürger, R., Diehl, S., Farås, S., Nopens, I. and Torfs, E. (2013) A consistent modelling methodology for secondary settling tanks: A reliable numerical method. *Water Science and Technology* 68(1), 192-208.
- Bürger, R., Diehl, S. and Nopens, I. (2011) A consistent modelling methodology for secondary settling tanks in wastewater treatment. *Water Research* 45(6), 2247-2260.
- Busch, J., Cruse, A. and Marquardt, W. (2007) Modeling submerged hollow-fiber membrane filtration for wastewater treatment. *Journal of Membrane Science* 288(1-2), 94-111.
- Busch, J. and Marquardt, W. (2009) Model-based control of MF/UF filtration processes: Pilot plant implementation and results. *Water Science and Technology* 59(9), 1713-1720.
- Chellam, S. (2005) Artificial neural network model for transient crossflow microfiltration of polydispersed suspensions. *Journal of Membrane Science* 258(1-2), 35-42.
- Choi, C., Kim, M., Lee, K. and Park, H. (2009) Oxidation reduction potential automatic control potential of intermittently aerated membrane bioreactor for nitrification and denitrification. *Water Science and Technology* 60(1), 167-173.

Comas, J., Meabe, E., Sancho, L., Ferrero, G., Sipma, J., Monclus, H. and Rodríguez-Roda, I. (2010) Knowledge-based system for automatic MBR control. *Water Science and Technology* 62(12), 2829–2836.

Comas, J., Rodríguez-Roda, I., Gernaey, K.V., Rosen, C., Jeppsson, U. and Poch, M. (2008) Risk assessment modelling of microbiology-related solids separation problems in activated sludge systems. *Environmental Modelling and Software* 23(10-11), 1250-1261.

Comas, J., Rodríguez-Roda, I., Sánchez-Marrè, M., Cortés, U., Freixó, A., Arráez, J. and Poch, M. (2003) A knowledge-based approach to the deflocculation problem: integrating on-line, off-line, and heuristic information. *Water Research* 37(10), 2377-2387.

Copp, J.B. (2002) *The COST Simulation Benchmark: Description and Simulator Manual*, Luxembourg.

Cosenza, A., Mannina, G., Neumann, M.B., Viviani, G. and Vanrolleghem, P.A. (2013) Biological nitrogen and phosphorus removal in membrane bioreactors: Model development and parameter estimation. *Bioprocess and Biosystems Engineering* 36(4), 499-514.

Dalmau, M., Rodríguez-Roda, I., Ayesa, E., Odriozola, J., Sancho, L. and Comas, J. (2013) Development of a decision tree for the integrated operation of nutrient removal MBRs based on simulation studies and expert knowledge. *Chemical Engineering Journal* 217, 174-184.

De Clercq, B., Coen, F., Vanderhaegen, B. and Vanrolleghem, P.A. (1999) Calibrating simple models for mixing and flow propagation in waste water treatment plants. *Water Science and Technology* 39(4), 61-69.

de Haas, D.W., Wentzel, M.C. and Ekama, G.A. (2000) The use of simultaneous chemical precipitation in modified activated sludge systems exhibiting biological excess phosphate removal Part 1: Literature review. *Water SA* 26, 439-452.

de la Torre, T., Iversen, V., Meng, F., Stüber, J., Drews, A., Lesjean, B. and Kraume, M. (2010) Searching for a universal fouling indicator for membrane bioreactors. *Desalination and Water Treatment* 18(1-3), 264-269.

De La Torre, T., Lesjean, B., Drews, A. and Kraume, M. (2008) Monitoring of transparent exopolymer particles (TEP) in a membrane bioreactor (MBR) and correlation with other fouling indicators *Water Science and Technology* 58(10), 1903-1909.

Delgrange, N., Cabassud, C., Cabassud, M., Durand-Bourlier, L. and Lainé, J.M. (1998) Neural networks for prediction of ultrafiltration transmembrane pressure – application to drinking water production. *Journal of Membrane Science* 150(1), 111-123.

Di Bella, G., Di Trapani, D., Torregrossa, M. and Viviani, G. (2013) Performance of a MBR pilot plant treating high strength wastewater subject to salinity increase: Analysis of biomass activity and fouling behaviour. *Bioresource Technology* 147, 614-618.

Di Bella, G., Mannina, G. and Viviani, G. (2008) An integrated model for physical-biological wastewater organic removal in a submerged membrane bioreactor: Model development and parameter estimation. *Journal of Membrane Science* 322(1), 1-12.

Drews, A. (2010) Membrane fouling in membrane bioreactors-Characterisation, contradictions, cause and cures. *Journal of Membrane Science* 363(1-2), 1-28.

Drews, A., Arellano-Garcia, H., Schöneberger, J., Schaller, J., Wozny, G. and Kraume, M. (2009) Model-based recognition of fouling mechanisms in membrane bioreactors. *Desalination* 236(1-3), 224-233.

Drews, A., Lee, C.H. and Kraume, M. (2006a) Membrane fouling - a review on the role of EPS. *Desalination* 200(1-3), 186-188.

Drews, A., Mante, J., Iversen, V., Vocks, M., Lesjean, B. and Kraume, M. (2007) Impact of ambient conditions on SMP elimination and rejection in MBRs. *Water Research* 41(17), 3850-3858.

Drews, A., Vocks, M., Iversen, V., Lesjean, B. and Kraume, M. (2006b) Influence of unsteady membrane bioreactor operation on EPS formation and filtration resistance. *Desalination* 192(1-3), 1-9.

Dubois, M., Gilles, K.A., Hamilton, J.K., Rebers, P.A. and Smith, F. (1956) Colorimetric method for determination of sugars and related substances. *Analytical Chemistry* 28(3), 350-356.

Dvořák, L., Svojitka, J., Wanner, J. and Wintgens, T. (2013) Nitrification performance in a membrane bioreactor treating industrial wastewater. *Water Research* 47(13), 4412-4421.

Eikelboom, D.H. (2000) *Process Control of Activated Sludge Plants by Microscopic Investigation.*, IWA Publishing, London.

Fang, F., Ni, B.J., Li, W.W., Sheng, G.P. and Yu, H.Q. (2011) A simulation-based integrated approach to optimize the biological nutrient removal process in a full-scale wastewater treatment plant. *Chemical Engineering Journal* 174(2-3), 635-643.

Fatone, F., Battistoni, P., Bolzonella, D., Pavan, P. and Cecchia, F. (2008) Long-term experience with an automatic process control for nitrogen removal in membrane bioreactors. *Desalination* 227(1-3), 72-84.

Fenu, A., Guglielmi, G., Jimenez, J., Spèrandio, M., Saroj, D., Lesjean, B., Brepols, C., Thoeve, C. and Nopens, I. (2010a) Activated sludge model (ASM) based modelling of membrane bioreactor (MBR) processes: A critical review with special regard to MBR specificities. *Water Research* 44(15), 4272-4294.

Fenu, A., Roels, J., Wambecq, T., de Gussem, K., Thoeye, C., de Gueldre, G. and van de Steene, B. (2010b) Energy audit of a full scale MBR system. *Desalination* 262(1-3), 121-128.

Fenu, A., Wambecq, T., Thoeye, C., De Gueldre, G. and Van de Steene, B. (2011) Modelling soluble microbial products (SMPs) in a dynamic environment. *Desalination and Water Treatment* 29(1-3), 210-217.

Ferrero, G. (2011) Development of an air-scour control system for membrane bioreactors, University of Girona, Girona, Spain.

Ferrero, G., Monclús, H., Buttiglieri, G., Comas, J. and Rodríguez-Roda, I. (2011a) Automatic control system for energy optimization in membrane bioreactors. *Desalination* 268(1-3), 276-280.

Ferrero, G., Monclus, H., Buttiglieri, G., Gabarron, S., Comas, J. and Rodríguez-Roda, I. (2011b) Development of a control algorithm for air-scour reduction in membrane bioreactors for wastewater treatment. *Journal of Chemical Technology and Biotechnology* 86(6), 784-789.

Ferrero, G., Monclus, H., Buttiglieri, G., Gabarron, S., Comas, J. and Rodríguez-Roda, I. (2011c) Development of a control algorithm for air-scour reduction in membrane bioreactors for wastewater treatment. *Journal of Chemical Technology and Biotechnology* 86(6), 784-789.

Ferrero, G., Monclús, H., Sancho, L., Garrido, J.M., Comas, J. and Rodríguez-Roda, I. (2011d) A knowledge-based control system for air-scour optimisation in membrane bioreactors. *Water Science and Technology* 63(9), 2025-2031.

Ferrero, G., Rodríguez-Roda, I. and Comas, J. (2012) Automatic control systems for submerged membrane bioreactors: A state-of-the-art review. *Water Research* 46(11), 3421-3433.

Field, R.W., Wu, D., Howell, J.A. and Gupta, B.B. (1995) Critical flux concept for microfiltration fouling. *Journal of Membrane Science* 100(3), 259-272.

Foster, C. (2003) *Wastewater treatment and technology*, Thomas Telford Publishing, London.

Frolund, B., Griebe, T. and Nielsen, P.H. (1995) Enzymatic activity in the activated-sludge floc matrix. *Applied Microbiology and Biotechnology* 43(4), 755-761.

Frølund, B., Palmgren, R., Keiding, K. and Nielsen, P.H. (1996) Extraction of extracellular polymers from activated sludge using a cation exchange resin. *Water Research* 30(8), 1749-1758.

Fu, Z., Yang, F., Zhou, F. and Xue, Y. (2008) Control of COD/N ratio for nutrient removal in a modified membrane bioreactor (MBR) treating high strength wastewater. *Bioresource Technology* 100(1), 136-141.

Gabarrón, S. (2014) Diagnosis, assessment and optimisation of the design and operation of municipal MBRs, University of Girona, Girona, Spain.

Gabarrón, S., Ferrero, G., Dalmau, M., Comas, J. and Rodriguez-Roda, I. (2014) Assessment of energy-saving strategies and operational costs in full-scale membrane bioreactors. *Journal of Environmental Management* 134(0), 8-14.

Galinha, C.F., Carvalho, G., Portugal, C.A.M., Guglielmi, G., Oliveira, R., Crespo, J.G. and Reis, M.A.M. (2011) Real-time monitoring of membrane bioreactors with 2D-fluorescence data and statistically based models. *Water Science and Technology* 63(7), 1381-1388.

Galinha, C.F., Carvalho, G., Portugal, C.A.M., Guglielmi, G., Reis, M.A.M. and Crespo, J.G. (2012) Multivariate statistically-based modelling of a membrane bioreactor for wastewater treatment using 2D fluorescence monitoring data. *Water Research* 46(11), 3623-3636.

Galinha, C.F., Guglielmi, G., Carvalho, G., Portugal, C.A.M., Crespo, J.G. and Reis, M.A.M. (2013) Development of a hybrid model strategy for monitoring membrane bioreactors. *Journal of Biotechnology* 164(3), 386-395.

Gao, D.W., Fu, Y., Tao, Y., Li, X.X., Xing, M., Gao, X.H. and Ren, N.Q. (2011) Linking microbial community structure to membrane biofouling associated with varying dissolved oxygen concentrations. *Bioresource Technology* 102(10), 5626-5633.

Germain, E., Nelles, F., Drews, A., Pearce, P., Kraume, M., Reid, E., Judd, S.J. and Stephenson, T. (2007) Biomass effects on oxygen transfer in membrane bioreactors. *Water Research* 41(5), 1038-1044.

Germain, E. and Stephenson, T. (2005) Biomass characteristics, aeration and oxygen transfer in membrane bioreactors: Their interrelations explained by a review of aerobic biological processes. *Reviews in Environmental Science and Biotechnology* 4(4), 223-233.

Gernaey, K.V. and Jørgensen, S.B. (2004) Benchmarking combined biological phosphorus and nitrogen removal wastewater treatment processes. *Control Engineering Practice* 12(3), 357-373.

Gil, J.A., Dorgeloh, E., van Lier, J.B., van der Graaf, J.H.J.M. and Prats, D. (2012) Start-up of decentralized MBRs: Part I: The influence of operational parameters. *Desalination* 285(0), 324-335.

Gil, J.A., Krzeminski, P., van Lier, J.B., van der Graaf, J.H.J.M., Wijffels, T. and Prats, D. (2011) Analysis of the filterability in industrial MBRs. Influence of activated sludge parameters and constituents on filterability. *Journal of Membrane Science* 385-386(0), 96-109.

Gillot, S., Ohtsuki, T., Rieger, L., Shaw, A., Takacs, I. and Winkler, S. (2009) Development of a unified protocol for good modelling practice in activated sludge modelling. *Influents* 4, 70-72.

Ginzburg, B., Peeters, J. and Pawloski, J. (2008) On-line fouling control for energy reduction in membrane bioreactors., Atlanta.

Grelier, P., Rosenberger, S. and Tazi-Pain, A. (2006) Influence of sludge retention time on membrane bioreactor hydraulic performance. *Desalination* 192(1-3), 10-17.

Guerrero, J., Guisasola, A., Comas, J., Rodriguez-Roda, I. and Baeza, J.A. (2012) Multi-criteria selection of optimum WWTP control setpoints based on microbiology-related failures, effluent quality and operating costs. *Chemical Engineering Journal* 188, 23-29.

Härtel, L. and Pöpel, H.J. (1992) A dynamic secondary clarifier model including processes of sludge thickening. *Water Science & Technology* 25(6), 267-284.

Hauduc, H., Neumann, M.B., Muschalla, D., Gamerith, V., Gillot, S. and Vanrolleghem, P.A. (2011) Towards quantitative quality criteria to evaluate simulation results in wastewater treatment – A critical review, p. 46, *Watermatex'11*, 8th IWA Symposium on Systems Analysis and Integrated Assessment. San Sebastian (Spain).

Henze, M., Gujer, W., Mino, T., Matsuo, T., Wentzel, M.C., Marais, G.V.R. and Van Loosdrecht, M.C.M. (1999) Activated Sludge Model No.2d, ASM2d. *Water Science and Technology* 39(1), 165-182.

Henze, M., Gujer, W., Mino, T. and Van Loosdrecht, M.C.M. (2000) Activated Sludge Models ASM1, ASM2, ASM2d and ASM3, IWA Publishing, London.

Henze, M., Loosdrecht, M.C.M.v., Ekama, G.A. and Brdjanovic, B. (2008) *Biological Wastewater Treatment: Principles, Modelling and Design*

Henze, M., Loosdrecht, M.C.M.v., Ekama, G.A. and Brdjanovic, D. (eds), IWA Publishing, London.

Hong, S.H., Lee, W.N., Oh, H.S., Yeon, K.M., Hwang, B.K., Lee, C.H., Chang, I.S. and Lee, S. (2007) The effects of intermittent aeration on the characteristics of bio-cake layers in a membrane bioreactor. *Environmental Science and Technology* 41(17), 6270-6276.

Hong, S.P., Bae, T.H., Tak, T.M., Hong, S. and Randall, A. (2002) Fouling control in activated sludge submerged hollow fiber membrane bioreactors. *Desalination* 143(3), 219-228.

Howell, J.A., Chua, H.C. and Arnot, T.C. (2004) In situ manipulation of critical flux in a submerged membrane bioreactor using variable aeration rates, and effects of membrane history. *Journal of Membrane Science* 242(1-2), 13-19.

Hulsbeek, J.J.W., Kruit, J., Roeleveld, P.J. and van Loosdrecht, M.C.M. (2002) A practical protocol for dynamic modelling of activated sludge systems. *Water Science and Technology* 45(6), 127-136.

Huyskens, C., Brauns, E., Van Hoof, E. and De Wever, H. (2008) A new method for the evaluation of the reversible and irreversible fouling propensity of MBR mixed liquor. *Journal of Membrane Science* 323(1), 185-192.

Insel, G., Hocaoglu, S.M., Cokgor, E.U. and Orhon, D. (2011) Modelling the effect of biomass induced oxygen transfer limitations on the nitrogen removal performance of membrane bioreactor. *Journal of Membrane Science* 368(1-2), 54-63.

Jeong, T.Y., Cha, G.C., Yoo, I.K. and Kim, D.J. (2007) Characteristics of bio-fouling in a submerged MBR. *Desalination* 207(1-3), 107-113.

Jeppsson, U. (2005) Aeration and mixing energy for BSM1, BSM1_LT and BSM2.

Ji, L. and Zhou, J. (2006) Influence of aeration on microbial polymers and membrane fouling in submerged membrane bioreactors. *Journal of Membrane Science* 276(1-2), 168-177.

Jiang, T. (2007) Characterization and modelling of Soluble Microbial Products in Membrane Bioreactors, Ghent University, Belgium.

Jiang, T. (2008) Characterization and Modelling of Soluble Microbial Products in Membrane Bioreactors, PhD Thesis, Ghent University.

Jiang, T., Myngheer, S., De Pauw, D.J.W., Spanjers, H., Nopens, I., Kennedy, M.D., Amy, G. and Vanrolleghem, P.A. (2008) Modelling the production and degradation of soluble microbial products (SMP) in membrane bioreactors (MBR). *Water Research* 42(20), 4955-4964.

Judd, S. (2008) The status of membrane bioreactor technology. *Trends in Biotechnology* 26(2), 109-116.

Judd, S. (2011) *The MBR Book. Principles and Applications of Membrane Bioreactors for water and wastewater treatment*, Elsevier, Oxford, UK.

Judd, S. and Judd, C. (2011) *The MBR book. Principles and Applications of Membrane Bioreactors for Water and Wastewater Treatment.* , Elsevier.

Kaneko, H. and Funatsu, K. (2013) A chemometric approach to prediction of transmembrane pressure in membrane bioreactors. *Chemometrics and Intelligent Laboratory Systems* 126, 30-37.

Khalili-Garakani, A., Mehrnia, M.R., Mostoufi, N. and Sarrafzadeh, M.H. (2011) Analyze and control fouling in an airlift membrane bioreactor: CFD simulation and experimental studies. *Process Biochemistry* 46(5), 1138-1145.

Kim, J.Y., Chang, I.S., Shin, D.H. and Park, H.H. (2008) Membrane fouling control through the change of the depth of a membrane module in a submerged membrane bioreactor for advanced wastewater treatment. *Desalination* 231(1-3), 35-43.

Kim, M.G. and Nakhla, G. (2009) The beneficial role of intermediate clarification in a novel MBR based process for biological nitrogen and phosphorus removal. *Journal of Chemical Technology and Biotechnology* 84(5), 637-642.

Kim, M.J., Sankararao, B. and Yoo, C.K. (2011) Determination of MBR fouling and chemical cleaning interval using statistical methods applied on dynamic index data. *Journal of Membrane Science* 375(1-2), 345-353.

Kimura, K., Miyoshi, T., Naruse, T., Yamato, N., Ogyu, R. and Watanabe, Y. (2008) The difference in characteristics of foulants in submerged MBRs caused by the difference in the membrane flux. *Desalination* 231(1-3), 268-275.

Kimura, K., Yamato, N., Yamamura, H. and Watanabe, Y. (2005) Membrane fouling in pilot-scale membrane bioreactors (MBRs) treating municipal wastewater. *Environmental Science and Technology* 39(16), 6293-6299.

Kraume, M. and Drews, A. (2010) Membrane bioreactors in waste water treatment - Status and trends. *Chemical Engineering and Technology* 33(8), 1251-1259.

Krzeminski, P., Iglesias-Obelleiro, A., Madebo, G., Garrido, J.M., van der Graaf, J.H.J.M. and van Lier, J.B. (2012a) Impact of temperature on raw wastewater composition and activated sludge filterability in full-scale MBR systems for municipal sewage treatment. *Journal of Membrane Science* 423-424, 348-361.

Krzeminski, P., Langhorst, W., Schyns, P., de Vente, D., Van den Broeck, R., Smets, I.Y., Van Impe, J.F.M., van der Graaf, J.H.J.M. and van Lier, J.B. (2012b) The optimal MBR configuration: Hybrid versus stand-alone - Comparison between three full-scale MBRs treating municipal wastewater. *Desalination* 284, 341-348.

Krzeminski, P., Van Der Graaf, J.H.J.M. and Van Lier, J.B. (2012c) Specific energy consumption of membrane bioreactor (MBR) for sewage treatment. *Water Science and Technology* 65(2), 380-392.

Kuba, T., Murnleitner, E., Van Loosdrecht, M.C.M. and Heijnen, J.J. (1996) A metabolic model for biological phosphorus removal by denitrifying organisms. *Biotechnology and Bioengineering* 52(6), 685-695.

Laspidou, C.S. and Rittmann, B.E. (2002a) Non-steady state modeling of extracellular polymeric substances, soluble microbial products, and active and inert biomass. *Water Research* 36(8), 1983-1992.

- Lapidou, C.S. and Rittmann, B.E. (2002b) A unified theory for extracellular polymeric substances, soluble microbial products, and active and inert biomass. *Water Research* 36(11), 2711-2720.
- Le-Clech, P., Chen, V. and Fane, T.A.G. (2006) Fouling in membrane bioreactors used in wastewater treatment. *Journal of Membrane Science* 284(1-2), 17-53.
- Le-Clech, P., Jefferson, B., Chang, I.S. and Judd, S.J. (2003) Critical flux determination by the flux-step method in a submerged membrane bioreactor. *Journal of Membrane Science* 227(1-2), 81-93.
- Lee, S.E., Koopman, B., Bode, H. and Jenkins, D. (1983) Evaluation of alternative sludge settleability indices. *Water Research* 17(10), 1421-1426.
- Lee, W., Kang, S. and Shin, H. (2003) Sludge characteristics and their contribution to microfiltration in submerged membrane bioreactors. *Journal of Membrane Science* 216(1-2), 217-227.
- Li, X.y. and Wang, X.m. (2006) Modelling of membrane fouling in a submerged membrane bioreactor. *Journal of Membrane Science* 278(1-2), 151-161.
- Liebig, T., Wagner, M., Bjerrum, L. and Denecke, M. (2001) Nitrification performance and nitrifier community composition of a chemostat and a membrane-assisted bioreactor for the nitrification of sludge reject water. *Bioprocess and Biosystems Engineering* 24(4), 203-210.
- Liu, Q.F., Kim, S.H. and Lee, S. (2009) Prediction of microfiltration membrane fouling using artificial neural network models. *Separation and Purification Technology* 70(1), 96-102.
- Lousada-Ferreira, M., Geilvoet, S., Moreau, A., Atasoy, E., Krzeminski, P., van Nieuwenhuijzen, A. and van der Graaf, J. (2010) MLSS concentration: Still a poorly understood parameter in MBR filterability. *Desalination* 250(2), 618-622.
- Lu, S.G., Imai, T., Ukita, M., Sekine, M., Higuchi, T. and Fukagawa, M. (2001) A model for membrane bioreactor process based on the concept of formation and degradation of soluble microbial products. *Water Research* 35(8), 2038-2048.
- Lyko, S., Wintgens, T. and Melin, T. (2008) Comparative Investigation on the impact of polymeric substances on membrane fouling during sub-critical and critical flux operation of a municipal membrane bioreactor, pp. 1849-1855.
- Ma, Z., Wen, X., Zhao, F., Xia, Y., Huang, X., Waite, D. and Guan, J. (2013) Effect of temperature variation on membrane fouling and microbial community structure in membrane bioreactor. *Bioresource Technology* 133(0), 462-468.
- Maere, T., Benedetti, L., Janssen, M., Weijers, S. and Nopens, I. (2008) Use of an automated calibration methodology and scenario analysis for WWTP optimisation: the Haaren case-study, Florence, Italy.

Maere, T., Verrecht, B., Moerenhout, S., Judd, S. and Nopens, I. (2011) BSM-MBR: A benchmark simulation model to compare control and operational strategies for membrane bioreactors. *Water Research* 45(6), 2181-2190.

Maere, T., Villez, K., Marsili-Libelli, S., Naessens, W. and Nopens, I. (2012) Membrane bioreactor fouling behaviour assessment through principal component analysis and fuzzy clustering. *Water Research* 46(18), 6132-6142.

Mannina, G. and Cosenza, A. (2013) The fouling phenomenon in membrane bioreactors: Assessment of different strategies for energy saving. *Journal of Membrane Science* 444, 332-344.

Mannina, G., Di Bella, G. and Viviani, G. (2011) An integrated model for biological and physical process simulation in membrane bioreactors (MBRs). *Journal of Membrane Science* 376(1-2), 56-69.

Marti, E., Monclus, H., Jofre, J., Rodriguez-Roda, I., Comas, J. and Balcazar, J.L. (2011) Removal of microbial indicators from municipal wastewater by a membrane bioreactor (MBR). *Bioresource Technology* 102(8), 5004-5009.

Martin-Garcia, I., Monsalvo, V., Pidou, M., Le-Clech, P., Judd, S.J., McAdam, E.J. and Jefferson, B. (2011) Impact of membrane configuration on fouling in anaerobic membrane bioreactors. *Journal of Membrane Science* 382(1-2), 41-49.

Meng, F., Chae, S.R., Drews, A., Kraume, M., Shin, H.S. and Yang, F. (2009) Recent advances in membrane bioreactors (MBRs): Membrane fouling and membrane material. *Water Research* 43(6), 1489-1512.

Menniti, A., Kang, S., Elimelech, M. and Morgenroth, E. (2009) Influence of shear on the production of extracellular polymeric substances in membrane bioreactors. *Water Research* 43(17), 4305-4315.

Menniti, A. and Morgenroth, E. (2010a) The influence of aeration intensity on predation and EPS production in membrane bioreactors. *Water Research* 44(8), 2541-2553.

Menniti, A. and Morgenroth, E. (2010b) Mechanisms of SMP production in membrane bioreactors: Choosing an appropriate mathematical model structure. *Water Research* 44(18), 5240-5251.

Metzger, U., Le-Clech, P., Stuetz, R.M., Frimmel, F.H. and Chen, V. (2007) Characterisation of polymeric fouling in membrane bioreactors and the effect of different filtration modes. *Journal of Membrane Science* 301(1-2), 180-189.

Monclús, H. (2011) Development of a decision support system for the integrated control of membrane bioreactors, University of Girona, Girona, Spain.

Monclús, H., Buttiglieri, G., Ferrero, G., Rodriguez-Roda, I. and Comas, J. (2012) Knowledge-based control module for start-up of flat sheet MBRs. *Bioresource Technology* 106, 50-54.

Monclús, H., Ferrero, G., Buttiglieri, G., Comas, J. and Rodriguez-Roda, I. (2011) Online monitoring of membrane fouling in submerged MBR. *Desalination* 277(1-3), 414-419.

Monclús, H., Sipma, J., Ferrero, G., Rodriguez-Roda, I. and Comas, J. (2010a) Biological nutrient removal in an MBR treating municipal wastewater with special focus on biological phosphorus removal. *Bioresource Technology* 101(11), 3984-3991.

Monclús, H., Zacharias, S., Santos, A., Pidou, M. and Judd, S. (2010b) Criticality of flux and aeration for a hollow fiber membrane bioreactor. *Separation Science and Technology* 45(7), 956-961.

Monti, A., Hall, E.R., Dawson, R.N., Husain, H. and Kelly, H.G. (2006) Comparative study of biological nutrient removal (BNR) processes with sedimentation and membrane-based separation. *Biotechnology and Bioengineering* 94(4), 740-752.

Naessens, W., Maere, T. and Nopens, I. (2012a) Critical review of membrane bioreactor models - Part 1: Biokinetic and filtration models. *Bioresource Technology* 122, 95-106.

Naessens, W., Maere, T., Ratkovich, N., Vedantam, S. and Nopens, I. (2012b) Critical review of membrane bioreactor models – Part 2: Hydrodynamic and integrated models. *Bioresource Technology* 122(0), 107-118.

Ndinisa, N.V., Fane, A.G. and Wiley, D.E. (2006a) Fouling control in a submerged flat sheet membrane system: Part I - Bubbling and hydrodynamic effects. *Separation Science and Technology* 41(7), 1383-1409.

Ndinisa, N.V., Fane, A.G., Wiley, D.E. and Fletcher, D.F. (2006b) Fouling control in a submerged flat sheet membrane system: Part II - Two-phase flow characterization and CFD simulations. *Separation Science and Technology* 41(7), 1411-1445.

Ng, T.C.A. and Ng, H.Y. (2010) Characterisation of initial fouling in aerobic submerged membrane bioreactors in relation to physico-chemical characteristics under different flux conditions. *Water Research* 44(7), 2336-2348.

Nopens, I., Benedetti, L., Jeppsson, U., Pons, M.N., Alex, J., Copp, J.B., Gernaey, K.V., Rosen, C., Steyer, J.P. and Vanrolleghem, P.A. (2010) Benchmark Simulation Model No 2: finalisation of plant layout and default control strategy. *Water Science and Technology* 62(9), 1967-1974.

Odriozola, J., Beltrán, S., Sancho, L., Dalmau, M., Comas, J., Rodriguez-Roda, I. and Ayesa, E. (2013) Model-based optimisation of MBR plants for C and N removal, Narbonne, France.

Oehmen, A., Lemos, P.C., Carvalho, G., Yuan, Z., Keller, J., Blackall, L.L. and Reis, M.A.M. (2007) Advances in enhanced biological phosphorus removal: From micro to macro scale. *Water Research* 41(11), 2271-2300.

Pendashteh, A.R., Fakhru'l-Razi, A., Chaibakhsh, N., Abdullah, L.C., Madaeni, S.S. and Abidin, Z.Z. (2011) Modeling of membrane bioreactor treating hypersaline oily wastewater by artificial neural network. *Journal of Hazardous Materials* 192(2), 568-575.

Philippe, N., Stricker, A.E., Racault, Y., Husson, A., Sperandio, M. and Vanrolleghem, P. (2013) Modelling the long-term evolution of permeability in a full-scale MBR: Statistical approaches. *Desalination* 325, 7-15.

Quinlan, J.R. (1992) Learning with continuous classes. Adams & Sterlings, E. (ed), pp. 343-348, Singapore.

Rieger, L., Gillot, S., Langergraber, G., Ohtsuki, T., Shaw, A., Tákacs, I. and Winkler, S. (2012) Guidelines for Using Activated Sludge Models, IWA Publishing London.

Rivas, A., Irizar, I. and Ayesa, E. (2008) Model-based optimisation of Wastewater Treatment Plants design. *Environmental Modelling & Software* 23(4), 435-450.

Robles, A., Ruano, M.V., Ribes, J. and Ferrer, J. (2012) Sub-critical long-term operation of industrial scale hollow-fibre membranes in a submerged anaerobic MBR (HF-SAnMBR) system. *Separation and Purification Technology* 100, 88-96.

Rodriguez-Roda, I., Comas, J., Poch, M., Ferrero, G., Sipma, J., Clara, P., Canals, J., Rovira, S. and Monclús, H. (2011) PATENTE-Procedimiento automatizado de control en tiempo real de un bioreactor de membranas y su sistema de control correspondiente. University of Girona and Ambiente-INIMA, O.M. (eds), Spain.

Roeleveld, P.J. and Van Loosdrecht, M.C.M. (2002) Experience with guidelines for wastewater characterisation in The Netherlands. *Water Science and Technology* 45, 77-87.

Rosenberg, M., Gutnick, D. and Rosenberg, E. (1980) Adherence of bacteria to hydrocarbons: A simple method for measuring cell-surface hydrophobicity. *FEMS Microbiology Letters* 9(1), 29-33.

Rosso, D., Larson, L.E. and Stenstrom, M.K. (2008) Aeration of large-scale municipal wastewater treatment plants: State of the art. *Water Science and Technology* 57, 973-978.

Sabia, G., Ferraris, M. and Spagni, A. (2013) Effect of solid retention time on sludge filterability and biomass activity: Long-term experiment on a pilot-scale membrane bioreactor treating municipal wastewater. *Chemical Engineering Journal* 221, 176-184.

Saltelli, A., Tarantola, S., Campolongo, F. and Ratto, M. (2004) Sensitivity Analysis in Practice: A Guide to Assessing Scientific Models. (2004). .

- Sarioglu, M., Insel, G., Artan, N. and Orhon, D. (2008) Modelling of long-term simultaneous nitrification and denitrification (SNDN) performance of a pilot scale membrane bioreactor. *Water Science and Technology* 57(11), 1825-1833.
- Sarioglu, M., Insel, G., Artan, N. and Orhon, D. (2009) Model evaluation of simultaneous nitrification and denitrification in a membrane bioreactor operated without an anoxic reactor. *Journal of Membrane Science* 337(1-2), 17-27.
- Scholz, M. (2005) Review of recent trends in Capillary Suction Time (CST) dewaterability testing research. *Industrial and Engineering Chemistry Research* 44(22), 8157-8163.
- Soleimani, R., Shoushtari, N.A., Mirza, B. and Salahi, A. (2013) Experimental investigation, modeling and optimization of membrane separation using artificial neural network and multi-objective optimization using genetic algorithm. *Chemical Engineering Research and Design* 91(5), 883-903.
- Stricot, M., Filali, A., Lesage, N., Spérandio, M. and Cabassud, C. (2010) Side-stream membrane bioreactors: Influence of stress generated by hydrodynamics on floc structure, supernatant quality and fouling propensity. *Water Research* 44(7), 2113-2124.
- Takács, I., Patry, G.G. and Nolasco, D. (1991) A dynamic model of the clarification-thickening process. *Water Research* 25(10), 1263-1271.
- Tan, T.W. and Ng, H.Y. (2008) Influence of mixed liquor recycle ratio and dissolved oxygen on performance of pre-denitrification submerged membrane bioreactors. *Water Research* 42(4-5), 1122-1132.
- Tchobanoglous, G., Burton, F.L. and Stensel, H.D. (2003) *Wastewater Engineering: Treatment and Reuse*, McGraw-Hill, New York.
- Tian, Y., Chen, L. and Jiang, T. (2011a) Characterization and modeling of the soluble microbial products in membrane bioreactor. *Separation and Purification Technology* 76(3), 316-324.
- Tian, Y., Chen, L., Zhang, S. and Zhang, S. (2011b) A systematic study of soluble microbial products and their fouling impacts in membrane bioreactors. *Chemical Engineering Journal* 168(3), 1093-1102.
- Tiranuntakul, M., Schneider, P.A. and Jegatheesan, V. (2011) Assessments of critical flux in a pilot-scale membrane bioreactor. *Bioresource Technology* 102(9), 5370-5374.
- Torfs, E., Vlasschaert, P., Amerlinck, Y., Bürger, R., Diehl, S. and Farås, S. (2013) Towards improved 1-D settler modelling: calibration of the Bürger model and case study, Chicago, IL, USA.
- Trussell, R.S., Merlo, R.P., Hermanowicz, S.W. and Jenkins, D. (2006) The effect of organic loading on process performance and membrane fouling in a submerged membrane bioreactor treating municipal wastewater. *Water Research* 40(14), 2675-2683.

van den Brink, P., Satpradit, O.-A., van Bentem, A., Zwijnenburg, A., Temmink, H. and van Loosdrecht, M. (2011) Effect of temperature shocks on membrane fouling in membrane bioreactors. *Water Research* 45(15), 4491-4500.

Van den Broeck, R., Krzeminski, P., Van Dierdonck, J., Gins, G., Lousada-Ferreira, M., Van Impe, J.F.M., van der Graaf, J.H.J.M., Smets, I.Y. and van Lier, J.B. (2011) Activated sludge characteristics affecting sludge filterability in municipal and industrial MBRs: Unraveling correlations using multi-component regression analysis. *Journal of Membrane Science* 378(1-2), 330-338.

Van den Broeck, R., Van Dierdonck, J., Caerts, B., Bisson, I., Kregersman, B., Nijskens, P., Dotremont, C., Van Impe, J.F. and Smets, I.Y. (2010) The impact of deflocculation-reflocculation on fouling in membrane bioreactors. *Separation and Purification Technology* 71(3), 279-284.

Van den Broeck, R., Van Dierdonck, J., Nijskens, P., Dotremont, C., Krzeminski, P., van der Graaf, J.H.J.M., van Lier, J.B., Van Impe, J.F.M. and Smets, I.Y. (2012) The influence of solids retention time on activated sludge bioflocculation and membrane fouling in a membrane bioreactor (MBR). *Journal of Membrane Science* 401–402(0), 48-55.

Vanhooren, H., Meirlaen, J., Amerlink, Y., Claeys, F., Vangheluwe, H. and Vanrolleghem, P.A. (2003) WEST: modelling biological wastewater treatment. *Journal of Hydroinformatics* 5(1), 27-50.

Verrecht, B., Judd, S., Guglielmi, G., Brepols, C. and Mulder, J.W. (2008) An aeration energy model for an immersed membrane bioreactor. *Water Research* 42(19), 4761-4770.

Verrecht, B., Maere, T., Benedetti, L., Nopens, I. and Judd, S. (2010a) Model-based energy optimisation of a small-scale decentralised membrane bioreactor for urban reuse. *Water Research* 44(14), 4047-4056.

Verrecht, B., Maere, T., Nopens, I., Brepols, C. and Judd, S. (2010b) The cost of a large-scale hollow fibre MBR. *Water Research* 44(18), 5274-5283.

Vesilind, P.A. (1968) Design of prototype thickeners from batch settling tests. *Water Sewage Works* 115(7), 302-307.

Wang, Z., Wu, Z. and Tang, S. (2009) Extracellular polymeric substances (EPS) properties and their effects on membrane fouling in a submerged membrane bioreactor. *Water Research* 43(9), 2504-2512.

Wilén, B.M. and Balmér, P. (1999) The effect of dissolved oxygen concentration on the structure, size and size distribution of activated sludge flocs. *Water Research* 33(2), 391-400.

Witten, I.H., Frank, E. and Hall, M.A. (2011) *Data mining: Practical machine learning tools and techniques*, Morgan Kaufmann

Wu, J., He, C. and Zhang, Y. (2012) Modeling membrane fouling in a submerged membrane bioreactor by considering the role of solid, colloidal and soluble components. *Journal of Membrane Science* 397–398(0), 102-111.

Wu, J.L., Le-Clech, P., Stuetz, R.M., Fane, A.G. and Chen, V. (2008) Effects of relaxation and backwashing conditions on fouling in membrane bioreactor. *Journal of Membrane Science* 324(1-2), 26-32.

Zarragoitia-González, A., Schetrite, S., Alliet, M., Jáuregui-Haza, U. and Albasi, C. (2008) Modelling of submerged membrane bioreactor: Conceptual study about link between activated sludge biokinetics, aeration and fouling process. *Journal of Membrane Science* 325(2), 612-624.

Zsirai, T., Aerts, P. and Judd, S. (2013) Reproducibility and applicability of the flux step test for a hollow fibre membrane bioreactor. *Separation and Purification Technology* 107, 144-149.

Zuthi, M.F.R., Ngo, H.H. and Guo, W.S. (2012) Modelling bioprocesses and membrane fouling in membrane bioreactor (MBR): A review towards finding an integrated model framework. *Bioresource Technology* 122(0), 119-129.

Zuthi, M.F.R., Ngo, H.H., Guo, W.S., Li, J.X., Xia, S.Q. and Zhang, Z.Q. (2013) New proposed conceptual mathematical models for biomass viability and membrane fouling of membrane bioreactor. *Bioresource Technology* 142, 737-740.